Università degli Studi di Palermo

AREA QUALITÀ, PROGRAMMAZIONE E SUPPORTO STRATEGICO
SETTORE STRATEGIA PER LA RICERCA
U. O. DOTTORATI

PhD School of Biomedicine, Neurosciences and Advanced Diagnostics
Department of Biomedicine, Neurosciences and Advanced Diagnostics (Bi.N.D.)
SSD BIO/10 - Biochemistry

BIO-WASTE PRODUCTS OF *MANGIFERA INDICA* L. REDUCE ADIPOGENESIS AND COUNTERACT HYPERTROPHY IN 3T3-L1 MODEL

DOCTOR
GIOVANNI PRATELLI

COORDINATOR
Prof. FABIO BUCCHIERI

TUTOR
Prof. MARIANNA LAURICELLA

CO-TUTOR
Prof. DANIELA CARLISI

XXXV CYCLE
YEAR OF TITLE ACHIEVEMENT 2023

SUMMARY

INTRODUCTION

1. ADIPOSE TISSUE

1.1 Adipose Tissue Types and Functions

In the course of evolution, the mechanism of energy storage in organic molecules as lipids has been highly preserved in unicellular as well as multicellular organisms. While multicellular organisms evolved the ability to store energy in a specific tissue with the development of specialized tissues, prokaryotes and single cell eukaryote only store lipids within intracellular organelles (*Driskell et al., 2014*). Adipose tissue (AT) is considered as connective tissue organized to form a large organ with moderate anatomy, particular vascular and nerve components, complex cytology, and high physiological plasticity. Several adipose tissue depots are located in two compartments of the body in particular, below the skin and in the trunk, defined subcutaneous and visceral depots respectively. Therefore, AT can be considered a multi-depot organ contributing to many survival processes as fuel for metabolism, immune responses and thermogenesis consists mainly of parenchymal cells called adipocytes in addition, in AT are present endothelial cells, blood cells, fibroblasts, pericytes, preadipocytes, macrophages, and several types of immune cells. Two main types of adipose tissues are morphologically distinguishable (Figure 1) called white (WAT) and brown (BAT) adipose tissue (*Cinti, 2012; Zwick et al., 2018*).

There is a longstanding belief that WAT is derived from the mesoderm germ layer, but some studies indicate that adipose depots originate from neural crest cells which derived from the ectoderm (*Berry et al., 2013*) while, BAT develops embryonically, derived from Myf5- and Pax7- expressing myogenic precursor cells in the mesoderm that also give rise to skeletal muscle cells and a portion of white adipocytes (*Wang and Seale, 2016*). White adipocytes are spherical cells with ~90% of their volume comprising a single cytoplasmic lipid droplet and a pressed nucleus, whereas brown adipocytes are polygonal cells with a roundish nucleus and several multilocular lipid droplets (LDs) moreover, brown adipocytes are also characterized by large amount of mitochondria (*Cinti, 2012*). Mitochondria in brown adipocytes are marked by the expression of uncoupling protein 1 (UCP1), a unique protein located in the inner membrane of the mitochondria that uncouples oxidative phosphorylation from ATP synthesis, resulting in the production of heat. Through this process, called thermogenesis, BAT is specialized in utilizing the energy derived from lipids (*Kwok et al., 2016*). In particular, stimulation by norepinephrine triggers a signaling cascade that activates UCP1, which uncouples aerobic respiration by dissipating the inter-membrane proton-motive force and generating heat instead of ATP. Compared with WAT, the high number of mitochondria and the large amount of vessels confer to BAT its characteristic brown colour (*Pilkington, 2021*).

WAT represents the largest proportion of whole-body AT and can be found subcutaneously, around major organs and blood vessels in the abdominal cavity. For this reason, the accumulation of WAT due to store excess of triglycerides, especially in visceral depots, is the main risk factor for cardiometabolic disorders, hypertension and cardiovascular diseases development. In contrast, BAT represents approximately only a small percentage of all AT in adult humans and can be found in cervical, supraclavicular, axillary, paraspinal, mediastinal and abdominal depots. Moreover, newborns possess interscapular BAT that reduces in size over time and is no longer observable in adults. In animals, especially in rodents, BAT protects from hypothermia by dissipating energy as heat and more recently has been found to also have anti-obesity and anti-diabetes properties, as well as to confer cardiometabolic health benefits (*Scheele and Wolfrum, 2020; Koenen et al., 2021*).

Recently a third type of AT (Figure 1), known as 'Beige' or 'Brite' has been identified (*Harms and Seale, 2013*). Beige AT is a subpopulation of WAT that adopts, upon the stimulation by low temperatures, characteristics of both brown and white adipocytes including increased UCP1 expression, mitochondrion density and vascularization in a process known as adaptive thermogenesis, or 'browning' (*Kwok et al., 2016; Rui, 2017; Zwick et al., 2018*). Beige AT development is mediated by distinct mechanisms, within subcutaneous WAT from a distinct subset of preadipocytes or by *de novo* beige adipogenesis or by white-to-brown adipocyte transdifferentiating of existing white adipocytes (*Rui, 2017)*. Several studies have shown that physical activity, various diet, pre-and probiotics, pharmaceutical agents as well as numerous bioactive compounds derived from plants, and adipokines can also induce browning of WAT (*Pilkington, 2021*).

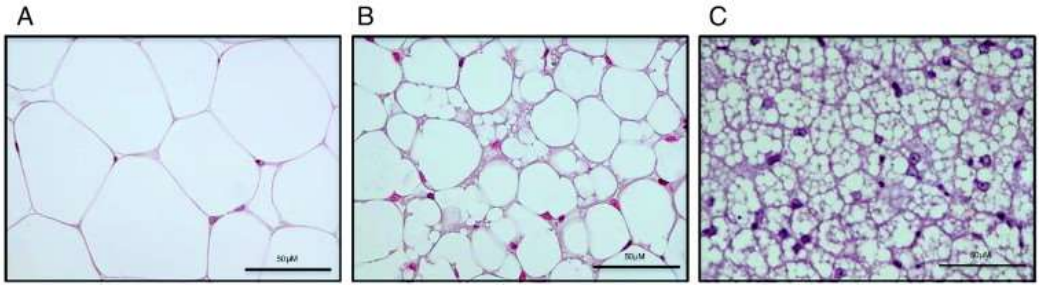

Figure 1. Morphology of the three main different types of adipocytes. Hematoxylin and eosin staining of (A) white, (B) brite/beige and (C) brown adipocytes. Scale bars 50 μm (*Keipert and Jastroch, 2014*).

In recent years, other two types of AT have been identified and defined pink and yellow AT. Pink adipocyte was observed for the first time in 2014 in the subcutaneous WAT during female mice pregnancy and throughout lactation time. Pink adipocytes seems to originate from white adipocytes which take on epithelial-like characteristics to train milk-secreting alveolar structures (*Giordano et*

al.,2014). Pink adipocytes contain LDs, cytoplasmatic projections and are rich of organelles such as peroxisomes, rough endoplasmic reticulum and mitochondria, all typical characteristics of epithelial cells. While in mice pink adipocytes seem to origin by a reversible transdifferentiation from WAT adipocytes and disappeared following the pregnancy, lactation, and post-lactation periods, it is not clear whether this type of adipocytes is also present in humans (*Cinti, 2018*).

Yellow AT is located in bone marrow (MAT) and, in a healthy and lean person, represents over 10% of total fat mass. Adipocyte of the bone morrow are like the white adipocyte for its unilocular morphology, but display a distinct lipid profile, metabolism as well gene expression, e.g., seem to be resistant to calorie restriction-induced hydrolysis of stored triglycerides (*Zinngrebe, 2020*). All AT phenotypes and their related functions are summarized in Figure 2.

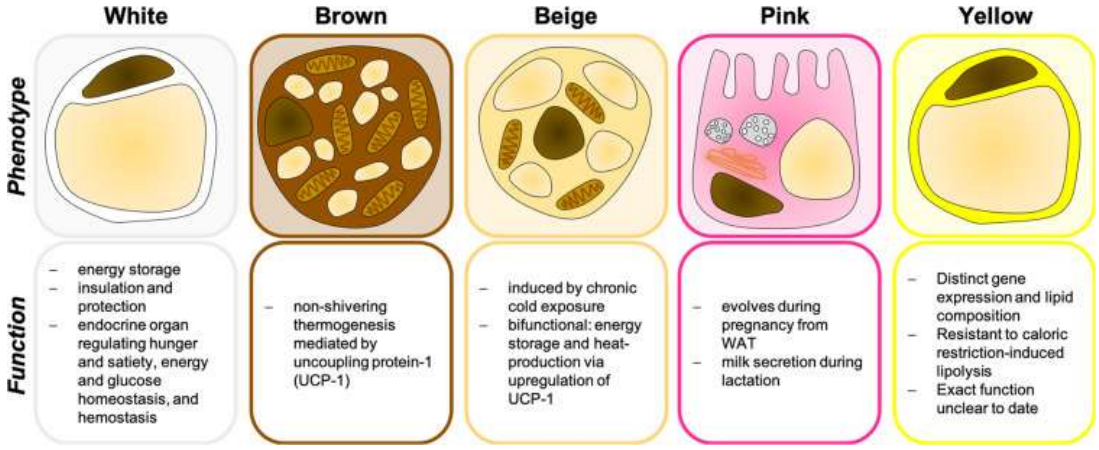

Figure 2. The typical phenotypic appearance of white, brown, beige, pink, and yellow adipocytes is depicted with the distinct functions of the respective adipose tissue (*Zinngrebe et al., 2020*).

Although AT is a connective tissue and the primary site for energy storage of lipid, studies in the last years have demonstrated that AT plays an essential role as a metabolically active organ in systemic health. Indeed, AT is an endocrine organ producing and secreting adipokines, adipose-tissue-specific hormones, lipids and proteins as well as pro- and ant-inflammatory cytokines that contribute to its endocrine activity. AT also responds to a variety of circulating metabolites and hormones, such as catecholamines, insulin, cortisol, lipids, growth hormone and many others. In this scenario AT, together with liver and skeletal muscle, is a major metabolic organ to maintaining correct glucose homeostasis. Failure in primary AT functions such as lipid storage, endocrine function and responsiveness to insulin, can have great influence on comprehensive human health. Indeed e.g., obesity is a major risk factor for the development of several disease such as

cardiovascular disease (CVDs), type 2 diabetes mellitus (T2DM), hepatic steatosis and some forms of cancer (*Harvey et al., 2020*).

Adipogenesis: AT is considered as a dynamic organ and its role contributes to maintain physiological functions in the human body including lipid storage, energy homeostasis, as well as represents a major player in insulin and other hormonal signaling. Although AT is composed by different cells (blood cells, macrophages, endothelial cells, fibroblasts, and stem cells), mature adipocytes remain the main cell type. Adipogenesis is a cell process by which adipose-derived stem cells or preadipocytes differentiate into mature adipocytes. This process plays a critical role in AT development and systemic energy homeostasis (*Pant et al., 2020*).

Mesenchymal stem cells (MSCs) are non-hematopoietic multipotent adult stem cells which are capable of differentiate into mesodermal lineages including adipocytes, osteocytes, chondrocytes, but also ectodermal and endodermal lineages. Human MSCs are present in white adipose tissue, in the form of adipose-derived stem cells (ADSCs). MSCs are the precursors of adipocytes which differentiate into lipoblasts, then into preadipocytes, and finally, into mature adipocytes. When adipogenesis occurs, the fibroblast-like preadipocytes differentiate into adipocytes insulin-responsive. The differentiation process is a complex process in which many transcription factors are implicated including peroxisome proliferator-activated receptors (PPARs), CCAAT/enhancer-binding proteins (C/EBPs), Krüppel-like factors (KLFs), and proteins signal transducers and activators of transcription (STATs) (*Bahmad et al., 2020*).

White and brown adipocytes originate from MSCs however, the immediate precursor cells leading to the development of white and brown are different: Myf-5 negative adipogenic precursor cells induce white adipocytes, while Myf-5 positive myogenic precursor cells become brown adipocytes (Figure 3). The Myf-5 negative cells become white pre-adipocytes by expression of bone morphogenetic protein-2 and 4 (BMP2 and BMP4) and beige pre-adipocytes following exposure to β3-adrenergic activators or cold. Moreover, BMP2 promotes osteogenesis in human bone-marrow cells and white adipogenesis in mouse-derived 3T3-L1 and C3H10T1/2 cells by the induction of PPARγ expression while, BMP4 promotes MSCs into adipogenic lineage but also adipogenesis in mouse embryonic stem cells. On the other hand, the Myf-5 positive cells became brown pre-adipocytes by the expression of bone morphogenetic protein-7 (BMP7) and PRDM16. BMP7 induces brown adipogenesis by p38MAPK pathway activation which promotes the specific transcriptional factors expression of brown adipogenesis including UCP1, PPARγ, Peroxisome proliferator-activated receptor gamma coactivator 1-alpha, beta (PGC-1α,β) and C/EBPs while, PRDM16 is expressed both in precursor cells and adipocytes. Moreover, the action of PRDM16 and

C/EBPβ determines the BAT fate from myogenic lineage through the inducing of PGC-1α and PPARγ expression. In addition, it has been shown that Myf-5 positive precursor cells can also differentiate into white adipocytes; in fact, a white adipocytes subset derived from myf-5 positive progenitor cells has been identified. This subset of white adipocytes undergoes to the loss of phosphatase and tensin homologue (PTEN) (*Ahmad et al., 2020*).

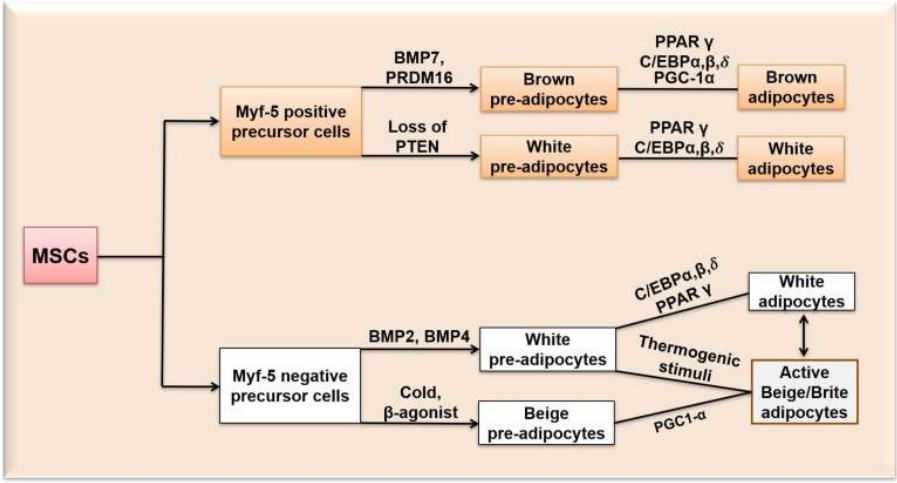

Figure 3. Differentiation of MSCs into white, beige/brite and brown adipocytes (*Ahmad et al., 2020*).

A variety of factors are involved in adipogenesis process. This complex process includes primarily two steps. The first step is the commitment from MSCs to preadipocytes which resides in the vesicular structure of AT positive for the molecular markers such as platelet-derived growth factor receptor α or/and β (PDGFRα, PDGFRβ). However, extensive multiple interplay pathways have been identified including MAPK, AMP-activated protein kinase (AMPK), transforming growth factor-β (TGF-β), Wnt, and Hedgehog pathways as well as previously mentioned BMPs. These factors are involved in multiple functions, such as stemness program, regulation of metabolic states and cell proliferation. For instance, Wnt signaling induces stemness and inhibits adipogenesis through the stabilization of β-catenin that represses the PPARγ-C/EBPα complex while, BMP2 and BMP4 promote adipogenic differentiation in mouse embryonic fibroblasts (MEFs) in part through SMAD4-mediated upregulation of PPARγ. The hedgehog signaling pathway opposes adipogenesis through interference of BMPs signaling while, other pathways, such as TGF-β, FGF, ERK/MAPK, p38/MAPK, and Notch signaling, can act as pro- or anti-adipogenic factors based on the experimental system, specific ligands, cell type as well as the developmental or differentiation stage. The second step in adipogenesis involves the differentiation of preadipocytes into mature adipocytes. This differentiation regulation network includes the involvement of two main

adipogenic transcription factors PPARγ and C/EBPα, which carry out the entire terminal differentiation process controlling the transcriptional activation of mature adipocytes markers including insulin receptor, adiponectin and FABP4. Other transcription factors promoting adipogenesis in the network, are C/EBPβ, RXRα/β, and STAT5. Moreover, together with these transcription factors, multiple epigenetic regulators, histone modifiers and multiple microRNAs participate in the adipogenesis process (*Zhao et al., 2022; Nunn et al., 2022*).

In addition, ligands and hormones regulate adipogenesis process though modulating signaling pathways. Insulin by binding its receptor, activates the signaling cascade such as insulin receptor substrate (IRS), phosphoinositide 3-kinase (PI3K), AKT and the mechanistic target of rapamycin complex 1 (mTORC1), promoting glucose uptake into differentiating preadipocytes. On the other hand, glucocorticoids bind glucocorticoid receptor (GCR) stimulating transcription via C/EBPs and PPARγ, enhancing insulin signaling required for adipogenesis (*Nunn et al., 2022*).

1.2 White Adipose Tissue (WAT)

AT is an essential organ for the regulation of energy homeostasis and WAT is primarily tasked to store excess energy. The WAT is distributed throughout the body and is capable of expanding to accommodate excess energy in the form of accumulated lipids as triglycerides, characteristics distinguishing from other tissues. Anatomically, WAT comprises two major depots, subcutaneous WAT and visceral WAT around internal organs. Visceral WAT, which is concentrated in the abdominal cavity, is further subdivided into mesenteric, omental, perirenal, and peritoneal depots (*Choe et al., 2016*). The main localizations of AT types are summarized in following Figure 4.

WAT undergo hyperplasia to increase the number of adipocytes and hypertrophy to increase the size of adipocyte, allowing adipose tissue to expand in times of nutrient excess. As needed, i.e., during fasting and exercise, triglycerides stored in adipose tissue are mobilized to provide fatty acids (FAs) for energy utilization by the rest of the body. Stored triglycerides are therefore in a constant state of flux, whereby energy storage and energy mobilization are determined largely by hormonal fluctuations. Thus, adipose tissue functions as an energy balance “hub” that integrates and services the energy requirements of diverse organ systems, such as the liver, skeletal and heart muscle, pancreas, and brain (*Chait and den Hartigh, 2020*).

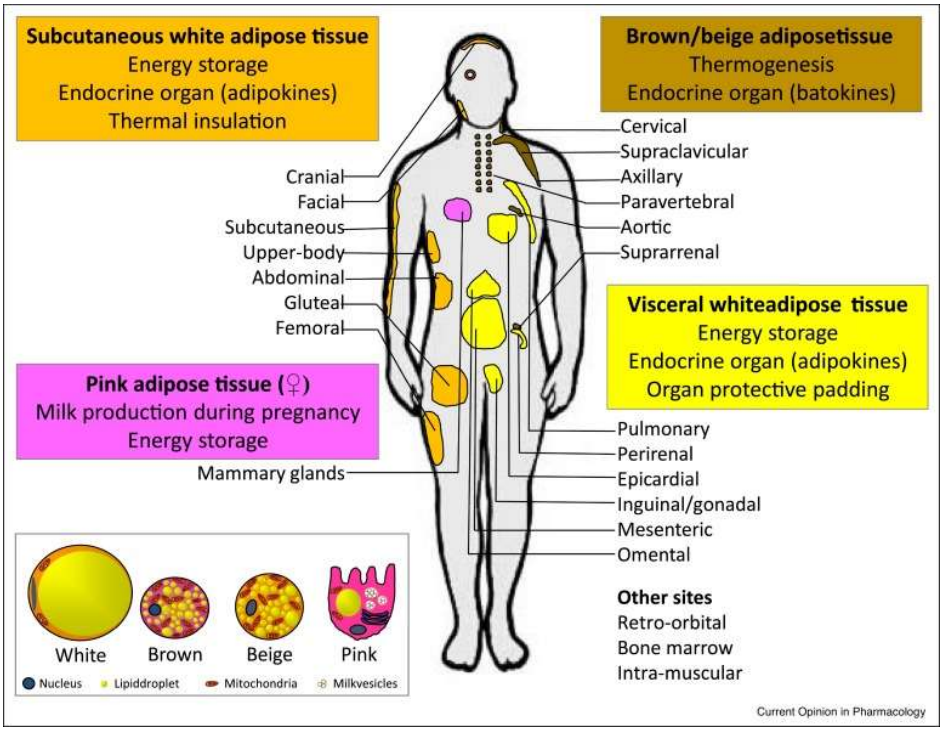

Figure 4. Schematic representation of AT types depots in human body (*Rodríguez et al., 2020*).

In healthy lean individuals, the majority of adipose tissue resides in subcutaneous depots, where it serves a thermoregulatory function, and from which stored triglycerides can be readily mobilized when needed (*Schoettl et al., 2018*). Conditions that favour adipose tissue expansion, if endured chronically, will eventually exceed the storage capacity of defined adipose tissue depots, leading to the ectopic deposition of triglycerides in other tissues, including intra-abdominal depots. (*Chait and den Hartigh, 2020*).

WAT stores triglycerides during positive energy balance to prevent abnormal lipid deposition in different districts of the body, which would result in unfavourable metabolic complications occurring both in lipodystrophic individuals and murine models. In contrast, WAT releases lipids in the form of non-esterified fatty acids (NEFAs) during a demand of energy, acting in response to different energy states and hormonal signals. In WAT, lipoprotein lipases (LPLs) are the main enzymes that mediate the uptake of triglycerides introduced with the diet. The active sites of these enzymes are located at the blood vessels luminal surface and hydrolyze triglycerides carried by very-low-density lipoprotein (VLDL) and chylomicrons transported through the bloodstream. With these, FAs and monoacylglycerols are carried inside the cells, to be used or stored, by passive diffusion or by fatty-acid transport proteins (FATPs), fatty-acid translocase/CD36, fatty-acid binding proteins (FABPs) or caveolin-1 (*Kwok et al., 2016*). Within the cell, these

monoacylglycerols are acylated by acyl coenzyme A synthase (ACS) and then, diacylglycerol acetyltransferase (DGAT) promotes the synthesis of triglycerides (*Yen et al., 2008*).

Energy homeostasis is maintained by balancing between the uptake and the release of lipids, but also via stimulatory and inhibitory signals induced by sympathetic nervous and hormonal systems. Indeed, a low state of energy signalled by catecholamines, such as epinephrine and norepinephrine, promotes lipolysis in WAT with consequent release of NEFAs into circulation. The transduction of these signals, via cyclic AMP, activate protein kinase A (PKA) which phosphorylates on LDs surface in adipocytes, perilipin A and hormone-sensitive lipase (HSL) promoting lipolysis. On the other hand, insulin, a signal for high state of energy, reduces cyclic AMP levels and PKA activity with subsequent inhibition of HSL (*Zechner et al., 2012*).

1.3 Adipose Tissue Metabolism

AT stores triacylglycerols (TAGs) during energy surplus conditions while release FAs during high energy demand to other tissues. By nutritional and hormonal cues, AT balances lipid storage and breakdown within the fat cell. For this reason, AT is central to the regulation of systemic lipid metabolism through two main processes such as lipogenesis and lipolysis.

Lipogenesis: Adipocytes accumulate lipid via two processes. In the first process, under normal food intake conditions, adipocytes take up lipids from the circulation in the form of FFAs liberated from circulating TAGs via the action of LPL secreted by adipocytes. LPL is transported to the adjacent capillary lumen to catalyse the hydrolysis of FFAs to from circulating TAGs containing lipoproteins such as chylomicrons produced in the small intestine and VLDL synthesized by the liver. On the other hand, adipocytes also take up glucose, converted to glycerol and used as base structure for the sequential esterification of FAs for form TAGs. The final step is the TAGs synthesis by re-esterification of circulating FFAs mediated by DGAT. (*Richard et al., 2020*).

The second process is *de novo* lipogenesis (DNL), by this process adipocytes are capable of synthesizing new lipids from circulating carbohydrates (Figure 5). Lipogenesis comprises both *de novo* synthesis of FAs from acetyl-coenzyme A (acetyl-CoA) and the esterification of these FAs to a glycerol backbone producing TAGs. DNL relies on two key enzymes that are abundant in adipocytes: acetyl-CoA carboxylase (ACC) and fatty acid synthase (FAS) to convert acetyl-CoA to palmitate, which can then be elongated and desaturated to form other fatty acid species. Those enzymes are transcriptionally regulated by sterol response element binding protein 1c (SREBP1c) and carbohydrate response element binding protein (ChREBP) (*Chouchani and Kajimura, 2019*).

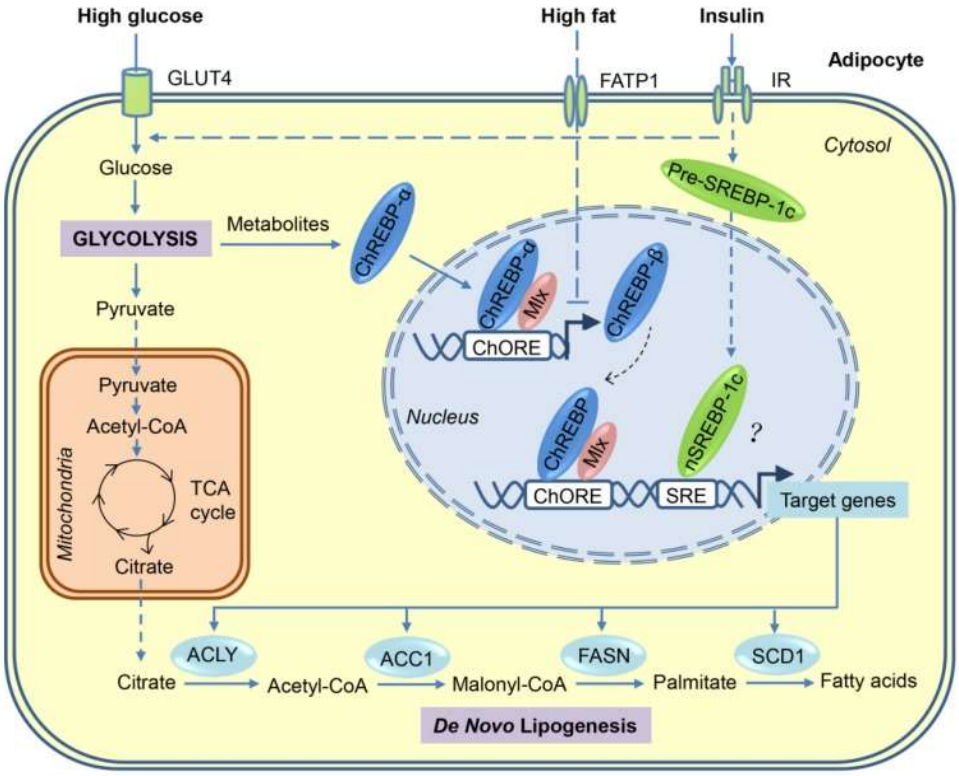

Figure 5. Transcriptional activation of *de novo* lipogenesis in adipocytes in response to high-sugar or high-fat diets (*Song et al., 2018*).

It was reported that mice lacking AT ChREBP have decreased DNL and insulin resistance (IR) in contrast, mice with whole body knockout of SREBP1c do not display decreased lipogenic gene expression in AT supporting ChREBP as the primary lipogenic transcription factor driving AT DNL. However, an inducible mouse model overexpressing insulin-induced gene 1 (Insig1), that inhibits SREBP1c activation and its transcriptional activity, showed that some acute and chronic white adipocyte-specific compensatory mechanisms are activated to restore adipocyte DNL. In this context, a decrease of SREBP1c activity result in decreased lipogenic gene expression, impaired whole body glucose tolerance and high lipid clearance suggesting that both SREBP1c and ChREBP play important roles in adipocyte DNL (*Crewe et al., 2019*).

Although hepatic DNL activity exceeds that of AT and contributes mainly to generation of circulating lipids, in humans fed high-carbohydrate diets hepatic DNL generates only a small part of total *de novo* fat biosynthesis. This aspect suggest that AT contributes strongly to whole body DNL during a state of carbohydrate excess. In this condition, adipocyte DNL is generally low but has

been report to be important for whole body substrate metabolism while the inhibition of WAT DNL is associated with IR (*Richard et al., 2020*).

Compared with lipid accumulation following a high fat diet, DNL is energetically costly. The adipocyte uses two pathways of glucose metabolism to make DNL. A part of the circulating glucose, following the consume of carbohydrates, is taken by adipocytes through insulin-stimulated GLUT4. Through glycolysis, glucose in the cytosol is converted to pyruvate, transported into mitochondria and then oxidated in tricarboxylic acid (TCA) cycle. The oxidation of glucose generates mitochondrial acetyl-CoA to fuel mitochondrial citrate synthesis (*Song et al.,2018*). Furthermore, mitochondrial citrate is exported to the cytosol, where adenosine triphosphate (ATP)-citrate lyase and Acetyl-CoA Carboxylase (ACC) lead to malonyl-CoA production. In parallel, glucose-6-phosphate is also shunted to the pentose phosphate pathway to generate NADPH used to fatty acid synthesis reactions that utilize malonyl-CoA to generate long-chain fatty acids (LFAs) for TAGs synthesis. FAS converts malonyl-CoA into palmitate, which is the first fatty acid product in DNL. Moreover, the metabolic intermediates of DNL regulate the fatty acid utilization in the adipocyte. In fact, cytoplasmic malonyl-CoA inhibits carnitine palmitoyl transferase 1 (CPT1) with subsequent mitochondrial β-oxidation while citrate allosterically activates ACC to stimulate malonyl-CoA formation. In addition, the NADPH/NADP+ ratio likely plays a crucial role in controlling fatty acid utilization in the adipocyte. TAGs synthesis requires a series of acyltransferases that facilitate stepwise esterification of a glycerol molecule to three free fatty acid molecules. TAGs synthesis rates depend on both the levels of FFAs and glycerol-3-phosphate (G3P). G3P acts as the precursor for the TAGs glycerol backbone and can be generated by the shunt glucose (*Chouchani and Kajimura, 2019*).

DNL is highly regulated by nutritional status and hormones. DNL during fasting is maintained low due to the increase of cellular cAMP levels and blood glucagon. Those factors inhibit DNL trough AMP-activated protein kinase (AMPK) and cAMP-dependent protein kinase (PKA). On the other hand, a meal rich in carbohydrates increases the levels of insulin and blood glucose which stimulate DNL by increasing lipogenic enzymes activity and lipogenic gene expression. Thus, DNL is extremely important in the integration of glucose and lipid homeostasis. DNL dysregulations promotes many metabolic problematic conditions such as IR, hyperglycemia, T2DM, CVDs, non-alcoholic fatty liver disease (NAFLD) and hyperlipidemia (*Song et al., 2018*).

Lipolysis: When metabolic fuels are low and/or energy demand is high such as fasting, exercise, and cold exposure TAGs stores in adipocytes are mobilized by catabolic process known as lipolysis to supply at peripheral tissues new energy (*Braun et al., 2018*). Although FFAs have an essential

role, high concentrations are toxic. This is due to their limited solubility and amphipathic but also to their active transformation into cytotoxic lipid species highly bioactive. Overall, these critical and devastating effects of FFAs are defined “lipotoxicity” and can lead to cellular alterations and also cell death. Aberrant lipolysis in adipocyte is involved in various metabolic diseases such as IR, T2DM and cancer cachexia (*Li et al., 2022*).

In adipocytes, three major neutral lipases regulate the canonical pathway of lipolysis (Figure 6): adipose triglyceride lipase (ATGL) also known as Desnutrin, hormone-sensitive lipase (HSL), and monoglyceride lipase (MGL). These lipases act sequentially in a controlled manner together with numerous cofactors to degrade TAGs stored in LDs. ATGL catalyses the first step hydrolysing TAGs to diglycerides (DAGs) then, DAGs are degraded by HSL into monoglycerides (MAGs) releasing FFAs in each step. MGL completes the process hydrolysing the last ester bond in monoglycerides, with the generation of one last FFA and a glycerol backbone. However, lipolysis may not be linear because as many of the protein involved in lipolysis are multifunctional enzymes which catalyse reactions in both directions, allowing the FFAs re-esterification and recycle (*Yang and Mottillo, 2020; Grabner et al., 2021*).

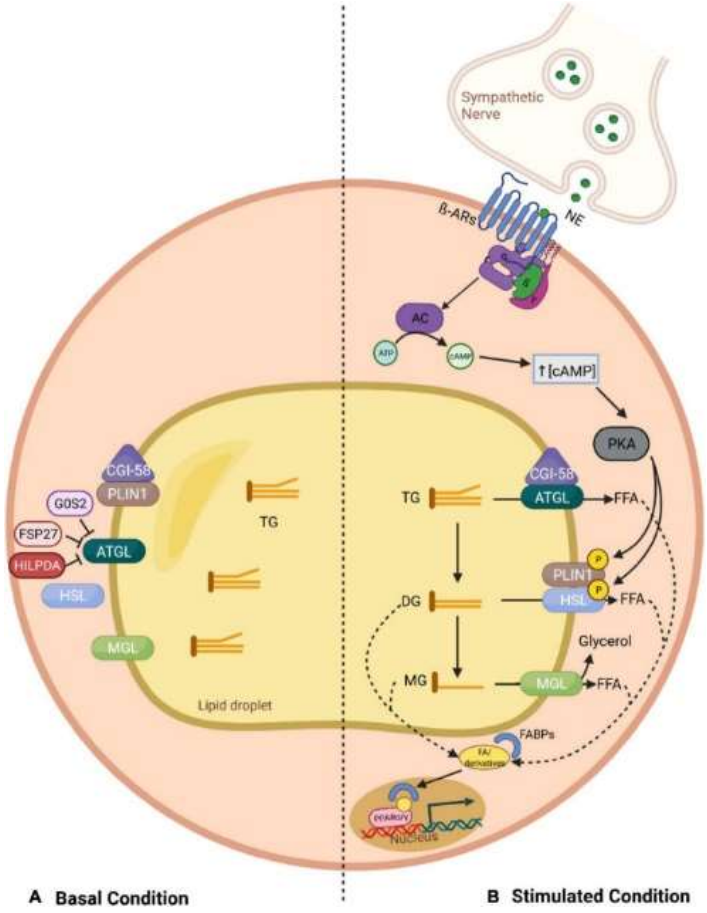

Figure 6. Overview of the canonical lipolysis pathway in adipocytes in the basal (A) and stimulated (B) status (*Li et al., 2022*).

Several studies on these enzymes regulation, revealed a complex system of interactions with protein partners which modulate ATGL, HSL, and MGL enzyme activity but also their localization, stability, or affinity to other proteins. Dysregulations of these proteins can be led to critical alterations in neutral lipid metabolism and associated processes. These protein partners including FABPs (especially FABP4/A-FABP), PLINs, LC3, a-b Hydrolase domain-containing protein 5

(ABHD5), G0/G1 Switch Gene 2 (G0S2), Hypoxia-Inducible LD-Associated Protein (HILPDA), Fat-Specific Protein-27 (FSP-27), Pigment Epithelium-Derived Factor (PEDF), Ubiquitin Regulatory X Domain-Containing Protein 8 (UBXD8), Golgi Brefeldin a Resistance Factor 1 (GBF1), 14-3-3 proteins, Peroxisome Biogenesis Factor 5 (PEX5), Vimentin (VIM), Cavin-1, and ChREBP (*Hofer et al., 2020*).

Lipolysis is strictly regulated by endocrine, paracrine, autocrine and sympathetic nervous system (SNS); these systems modulate the activity of lipases by regulating their intracellular locations but also modulating their interaction with regulatory factors. Under basal conditions, such as feeding, ATGL can be found on the surface of LDs but also in the cytoplasm, while HSL primarily remains in the cytoplasm while, Perilipin1 (PLIN1) sequesters ABHD5, the co-activator of ATGL, limiting its function. Moreover, other additional proteins can ulteriorly inhibit ATGL activity by their direct interaction with ATGL. As a result, the rate of TG hydrolysis within the basal state is low (*Li et al., 2022*).

On the other hand, during periods of high energy demand, lipolysis is activated principally by action of catecholamines. Sympathetic nerve fibers innervating AT, after stimulation, release norepinephrine, which binds to β-adrenergic receptors (β-ARs) on the plasma membrane of adipocytes. Hormonal binding leads a stimulatory G protein (Gs)-mediated cascade with consequent high intracellular production of cyclic AMP (cAMP) by the adenylyl cyclase activity (AC). Then, cAMP accumulation in the cytoplasm promotes protein kinase A (PKA) activation, which in turn modulates lipolysis (*Heeren and Scheja, 2018*).

Moreover, non-adrenergic lipolytic stimuli include melanocortins, glucocorticoids, natriuretic peptides, parathyroid hormone (PTH), bile acids, secretin, and growth hormones (Figure 7). Generally, these hormones are less potent lipolytic inducers than β-adrenergic stimulation however, some of these hormones clearly utilize different pathways than β-adrenergic signaling with additive or synergistic affects to increase lipolysis (*Braun et al., 2018*).

After a meal, the levels of circulating insulin rapidly increase suppressing lipolysis through decrease cAMP levels. In particular, insulin binds the insulin receptor (IR) and through the docking protein insulin receptor substrate 1 (IRS1) and IRS2, activates the lipid kinase phosphatidylinositol 3-kinase (PI3-K) increasing production of PIP3 which stimulates the serine threonine kinase AKT/Protein kinase B. Then, AKT phosphorylate several proteins such as phosphodiesterase 3 B (PDE3B), which leads to the hydrolysis of cAMP and attenuate catabolic signals that promote lipolysis such as inactivation of PKA, and consecutive downregulation of HSL and perilipin phosphorylation. In contrast, during fasting state, insulin levels are reduced and norepinephrine is

released promoting lipolysis. The differential insulin effects between glucose uptake and lipolysis can be explained by selective insulin signaling/resistance that occurs in adipocytes (*Yang and Mottillo, 2020*).

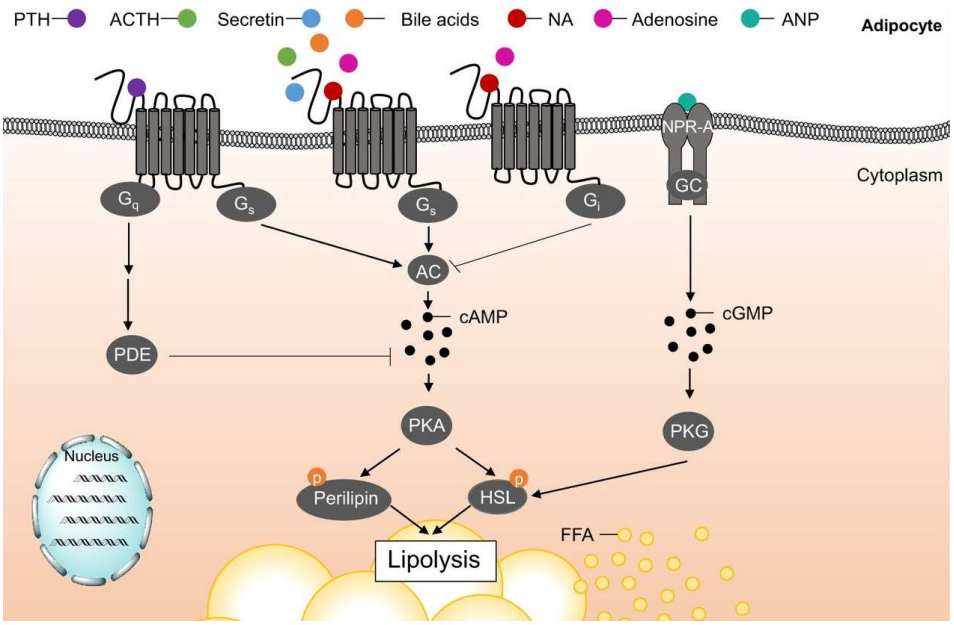

Figure 7. Non-adrenergic lipolytic stimuli (*Braun et al., 2018*).

In patients with diabetes and also in patients with obesity, AT can become insulin resistant. In this condition, insulin lose the ability to inhibit lipolysis and reduce FFAs and glycerol levels in serum. Therefore, high lipolysis leads to increased FFAs levels not only in fasted but also in fed state. Consequently, this constant exposure to high FFA levels promotes the uptake and ectopic storage of lipids in some tissues as liver and muscle. Ectopic lipids lead to impair insulin signaling in adipocyte and, for this reason, increased lipolysis may be a major contributor to whole body IR (*Czech, 2020*).

In summary, lipogenesis is a process by which carbohydrates are converted into FAs as well as promotes the TAGs biosynthesis and LDs in adipocytes. Lipolysis, in contrast, breaks down TAGs to free fatty acids (FFAs) and glycerol to be either oxidized or released. A main pathways of lipid mobilization occurs through the uptake of circulating FFAs by liver, muscle and other tissues. Lipogenesis and lipolysis are sensitive processes to nutrition but also to hormones signaling such as insulin, norepinephrine and glucagon. For this reason, both processes are highly regulated for maintenance of systemic energy homeostasis and insulin sensitivity (*Luo and Liu, 2016*).

The main steps of lipogenesis and lipolysis processes are shown in Figure 8.

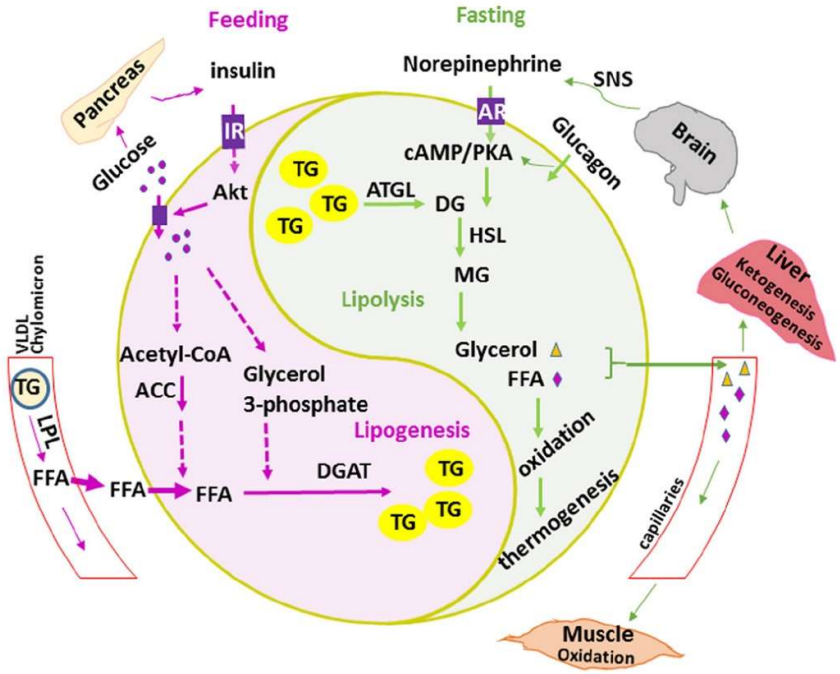

Figure 8. Lipid metabolism and mobilization controlled by adipose tissue (*Luo and Liu, 2016*).

1.4 White Adipose Tissue as Endocrine Organ

Initially, AT was classified as a simple energy storage organ, but now is known to be a major endocrine system secreting adipokines, chemokines, growth factors, and cytokines. The adipokines secretion seems to be different by AT depot and depends on the AT energy status, this leads to variable paracrine/autocrine effects of this mediators within particular depots. In fact, adipokines are important mediators of several metabolic processes including fatty acid oxidation, DNL, insulin signaling, cell growth, inflammation, angiogenesis, gluconeogenesis, glucose uptake, as well energy expenditure in various metabolically active tissues such as the liver, pancreas, heart, skeletal muscle, and brain (*Chait and den Hartigh, 2020*).

Cytokines are secreted directly from AT, but also can be released from other cell populations in AT such as preadipocytes, fibroblasts and immune cells. Moreover, cytokines are involved in cell signaling playing a main role in immune regulation and usually not acting as growth factors for non-immune cell populations. Beyond increases in depot size, diet-induced obesity alters AT leading to dysregulation in adipocytes biology and function moreover, increases in adipocytes number enhances circulating adipokines concentration. Inflammation in AT is linked to obesity and its related metabolic diseases. In this context hypoxia, which occurs in response to adipocytes with less vascularity, improves adipokine release from adipocytes. In fact, hypoxia is suggested to

initiate obesity-induced inflammation and together with increased release of adipokines is crucial in the IR with consequent high increases in glucose concentration. Thus, increased adipokines release following excessive adipose deposition, causes hypoxia in AT leading to increase in cytokines release and recruitment of immune cells (*Booth et al., 2016*).

Leptin: is a small (16 kDa) peptide prevalently secreted from AT which seems to be the major source for circulating leptin. Studies involving genetically obese (*ob/ob*) and diabetic (*db/db*) mice confirmed the presence of this circulating factor. Conversely to the *ob/ob* mouse which lacks leptin, circulating levels of leptin increase with weight gain and decrease with weight loss, according to role of leptin as a signal of AT stores (*Galic et al., 2010*).

In fact, the deletion of the *Ob (Lep)* gene exclusively in AT, determines non-quantifiable circulating levels of leptin. However, other tissues such as skeletal muscle, heart, mammary glands, gastric mucosa, brain, and placenta, produce small amounts of leptin under specific conditions. The circulating levels of leptin are highly proportional to the amount of AT. Female subjects with general larger fat mass show higher circulating levels of leptin compared with male subjects of similar body weight. This is partly due to inhibition by androgens, stimulation by estrogen and depot-related differences in leptin expression. Leptin, as a pleiotropic hormone, regulates several physiological processes, such as food intake, neuroendocrine and immune function, non-shivering thermogenesis, reproduction, haemostasis, angiogenesis. To carry out its function, leptin binds its receptor LepRb, which is especially abundant in the hypothalamic region and to a lower measure in peripheral tissues and macrophages. However, it is not yet clear the exact leptin-sensing mechanism by which the CNS communicates to the peripheral tissues, and vice versa, in response to leptin (*Zhao et al., 2021*).

Leptin is considered as a pre-inflammatory cytokine that shows structural and functional properties that belong to the IL-6 family of cytokines. Leptin is an anorexigenic peptide, it is involved in the energy expenditure increase and is principally removed from plasma by glomerular filtration following proteolytic degradation. Because leptin concentrations in the AT and plasma are dependent on the amount of energy stored as fat, leptin levels are higher in obese subjects and increase with overfeeding, while lean subjects have lower circulating levels of leptin. Partially, insulin mediates the leptin regulation in fact, in response to low insulin levels leptin decreases while, increases in response to insulin stimulation or with feeding. Moreover, leptin levels increase also by glucocorticoids, acute infection and proinflammatory cytokines. Conversely, other agents such as growth hormone (GH), adrenergic stimulation, thyroid hormone, cold exposure, but also

smoking and thiazolidinediones decrease leptin levels. Leptin is produced in greater amount in subcutaneous compared with visceral AT. In fact, the higher concentration of circulating leptin in females is due, partly, to a higher rate of subcutaneous fat. In addition, leptin has been involved in other roles, such as glucose metabolism, lipid oxidation, modulation of food reward, and adipocyte apoptosis (*Coelho et al., 2013*).

Adiponectin: encoded by *AdipoQ* gene, represents the highest circulating adipokine which blood levels result ~40-fold higher than circulating levels of leptin. Moreover, adiponectin levels are usually higher in women compared to men and have an inverse correlation with weight status for both genders in fact, unlike most adipokines, lower blood levels of adiponectin are associated with higher body mass index (BMI). Adiponectin is correlated to some metabolic processes such as lipid trafficking and glucose homeostasis playing also a role in the pathogenesis of IR and diabetes (*Booth et al., 2016*).

Adiponectin, is released by adipocytes as endocrine hormone and have anti-inflammatory effects. Moreover, it can enhance insulin sensitivity in tissues such as skeletal muscle and liver. Adiponectin binds two G protein-coupled receptors, AdipoR1 and AdipoR2, most expressed in muscle, liver and heart. Conversely to leptin, circulating levels of adiponectin are lower in subjects with obesity and type 2 diabetes. Anti-diabetic effects of adiponectin are exploited primarily by suppression of hepatic gluconeogenesis but also trough the increase of glucose uptake in skeletal muscle *in vitro*. Adiponectin also acts in an autocrine manner, increasing insulin-independent and insulin-stimulated glucose uptake and regulating lipid accumulation (*Harvey et al., 2020*).

Adiponectin improves whole-body insulin sensitivity and this is shown in genetic and diet-induced obesity models. In muscle cells *in vitro*, insulin sensitivity improvement through adiponectin is dependent on the AMPK activation and subsequent mTOR/S6 kinase activity reduction which results in IRS1 inhibitory phosphorylation reduction. Moreover, stimulation of fatty acid oxidation and glucose uptake in both skeletal muscle and AT by adiponectin are dependent on AMPK signaling. In particular, AMPK signaling activation employees from the AdipoR1 while the AdipoR2 seem to be main for regulating PPARα gene expression, with subsequent increase in mitochondrial biogenesis and fatty acid oxidation. Finally, adiponectin stimulates appetite and reduces energy expenditure, those effects are deleted following the removal of AdipoR1 or AMPK signaling. In addition, leptin sensitivity is strongly increased in adipo −/− mice suggesting that the adiponectin and leptin actions have reciprocal functions on homeostatic mechanism to maintain fat levels/energy stores stimulating or suppressing appetite and energy expenditure (*Galic et al., 2010*).

Resistin: is a small peptide (12.5 kDa) and its structure is strikingly similar to that of adiponectin. It is secreted by adipocytes and also by other cell types in particular, immunocompetent cells. Circulating levels of resistin are increased in obese mouse models and in obese humans. Moreover, its levels decreased by rosiglitazone, an anti-diabetic drug, while increased in genetic or diet-induced forms of obesity. Resistin is implicated in diabetes and in its related complications. In addition, *in vitro* studies shown that macrophage stimulation with pro-inflammatory cytokines or with lipopolysaccharide (LPS), markedly induces an increase in resistin production. Resistin release seems stimulated by inflammation but also by hyperglycemia, growth and gonadal hormones; on the other hand, its release within the AT on adipocytes themselves leads to IR. The regulation, as well the neutralization of resistin in glucose tolerance in tissues shows that resistin negatively modulates the insulin signaling, increasing glucose uptake; in addition, it increases hepatic gluconeogenesis promoting IR. Furthermore, compared to mature adipocytes, resistin expression is higher in pre-adipocytes indicating its potential role in adipogenesis regulation (*Coelho et al., 2013*).

Some evidences suggest that VAT is the major contributor to circulating levels of resistin, supporting the correlation between IR and resistin. Moreover, resistin has an active role in the promotion of inflammatory responses; in fact, it can upregulate inflammatory cytokines release in monocytes and macrophages, such as Tumor Necrosis Factor-α (TNFα) and IL-6, by NF-kB pathway activation. In addition, resistin is positively associated with circulating C-reactive protein (CRP) (*Chait and den Hartigh, 2020*).

Although resistin is an adipokine that in some cases is associated with unfavourable health conditions such as IR and obesity, a clear role for resistin is still under investigation. There is also evidence that resistin is important in the fasting blood glucose regulation. Therefore, resistin could be necessary for glycaemic control, further showing the importance of adipocyte endocrine function in supporting metabolic health. It is well referring that resistin is prevalently secreted from adipocytes in rodents, while macrophages are the main resistin source in humans. However, across species the function of resistin remains the same (*Harvey et al., 2020*).

Thus, AT not only responds to afferent signals from traditional hormone systems and the CNS but also expresses and secretes factors with important endocrine functions. In addition to leptin, adiponectin, resistin, TNFα and IL-6, other several cytokines and component are secreted from AT, including Macrophages and Monocyte Chemoattractant Protein-1 (MCP-1) (*Kershaw and Flier, 2004; Chait and den Hartigh, 2020*), Plasminogen Activator Inhibitor-1 (PAI-1), proteins of the Renin Angiotensin System (RAS), Adipsin and Acylation Stimulating Protein (ASP) (*Kershaw and*

Flier, 2004; Coelho et al., 2013), Visfatin, (*Coelho et al., 2013; Booth et al., 2016*), Apelin, Vaspin, Adipolin, Wnt 1 Inducible Signaling pathway Protein-1 (WISP-1), Subfatin (*Booth et al., 2016*), Omentin (*Booth et al., 2016; Chait and den Hartigh, 2020*), Retinol Binding Protein-4 (RBP-4) (*Galic et al., 2010; Booth et al., 2016*), Fibroblast Growth Factor 21 (FGF21) (*Chait and den Hartigh, 2020*), and enzymes involved in the metabolism of steroid hormones (*Kershaw and Flier, 2004*).

1.5 Adipose Tissue Hypertrophy and Inflammation

In the last years, several studies aimed at evaluating how the excess of energy is stored in AT by hyperplasia or hypertrophy process. Physiologically, adipocytes proliferate or expand to store more energy as form of TAGs. In obesity, adipocytes expand overly their diameter and are defined as hypertrophic adipocytes, up to critical size. Alteration in adipocyte size could lead to the development of T2DM and NAFLD, as well as triggers low-grade chronic inflammation, excessive collagen deposition, and insufficient angiogenesis (Figure 9), with consequent abnormal adipokines release and alteration in glucose metabolism. The adipocyte hypertrophy effects on metabolic dysfunction varied in different adipose depots.

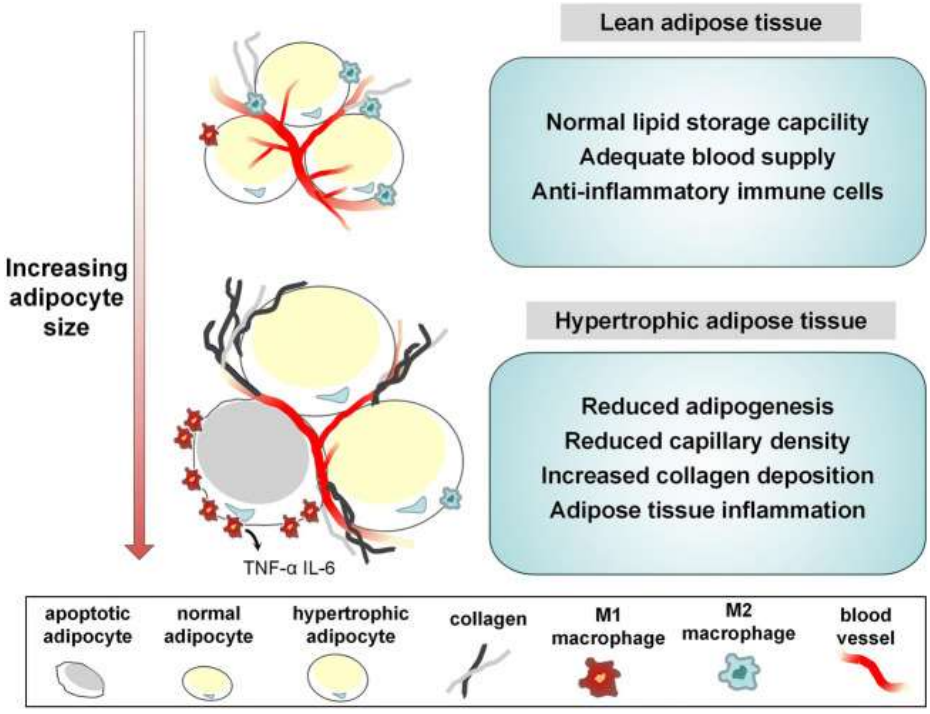

Figure 9. Adipocyte hypertrophy-induced and metabolic dysregulations (*Liu et al., 2020*).

In particular, VAT contains more large adipocytes and fewer preadipocytes, while SAT contains more small adipocytes. Mean adipocytes size is larger in VAT than in SAT however, these two depots have no difference in the proportion of small adipocytes. Moreover, cell differentiation markers expressions is greater in SAT, while VAT shows greater inflammatory genes expression. In light of this, VAT tends to be less involved in TAGs deposition but rather is more related to adipose inflammation in comparison to SAT. In addition, adipocyte hypertrophy in VAT markedly influences the total plasma content of cholesterol, apolipoprotein B, low-density lipoprotein (LDL), and TAGs while, SAT shows higher blood glucose level, plasma insulin level, and IR. This difference could be described by different blood support in VAT and SAT depots (*Liu et al., 2020*).

An excess of nutrient, especially in lipids content, can lead to lipotoxicity in various body tissues. Adipocyte hypertrophy can be considered an adaptive response to maintenance of AT nutrient buffering capacity protecting from lipotoxicity. Adipocyte hypertrophy and metabolic disease are correlated in context-dependent manner. In fact, in some obese patients the hypertrophic threshold may be overcome as a result of adipocyte buffering capacity excess, leading to ectopic fat deposition in peripheral tissues. In contrast, lean humans with smaller adipocytes show a poorer metabolic response to overfeeding, suggesting that increased adipocyte size may be beneficial and resulting as a metric for nutrient buffering capacity. In line with this, severe adipocyte hypertrophy in obesity is directly linked to BMI and metabolic disease in humans as well in mice. Moreover, hypertrophy has also pleiotropic effects on adipocytes function. For instance, hypoxia may occurs with adipocytes expansion and oxygen diffusion in the tissues distance, induces hypoxic-response genes, metabolic dysfunction, ER and oxidative stress as well inflammation. In addition, several studies demonstrate a negative correlation between adipocyte hypertrophy and fibrosis, due to an excess extracellular matrix (ECM) deposition, feature of obese AT. Although it has been shown that ECM content in AT is increased in human and murine obesity, the relationship between fibrosis and metabolic disease is not yet well-defined, especially in humans. However, the relationship between fibrosis and metabolic disease seems to be BMI-dependent: lean subjects show increased fibrosis and elevated diabetes risk, suggesting a maladaptive role, while in obese subjects the fibrotic changes may be adaptive when hypertrophic threshold is overcome (*Muir et al., 2016*).

It has been highly demonstrated that excess of lipid accumulation in ectopic tissues can induce local inflammation and IR. For example, the ectopic fat accumulation in pancreas can result in a major β-cell dysfunction. Although IR has different potential pathogenic mechanisms, according to its association with obesity, it is likely that AT dysfunction becomes the greater contributor to subsequent related complications in obese patients. In a model to track adipogenic footpath *in vivo*

and using stable isotope methodology to measure SAT and VAT adipogenesis, Kim et al. confirmed the positive association between adipocyte turnover and insulin sensitivity, identifying adipocyte hypertrophy as the major mechanism of adult fat mass expansion and supporting the concept that the failure of AT plasticity results in IR and metabolic disease. However, similar findings have also been reported in human study. Moreover, other studies revealed that metabolically obese normal-weight (MONW) individuals are characterized by increase of visceral adiposity levels, IR, higher susceptibility to T2DM and CVDs. These data indicate that both visceral and subcutaneous regional depositions of AT as well hypertrophy and hyperplasia can contribute to an increased risk of IR (*Longo et al., 2019*).

Hypertrophic adipocytes show distinguishing features. In the obese AT, hypertrophic adipocytes exhibit necrotic-like abnormalities which are increased in HSL-deficient mice as well as in diet-induced obesity (DIO) mouse models. In obesity, the increase of dead adipocytes amount leads to AT function and induces inflammation. Adipocyte hypertrophy also induces local AT hypoxia due to a relative less vasculature. In fact, during AT hypoxia, several angiogenic factors and inflammatory response-associated genes are upregulated, such as activation of hypoxia-inducible factor-1α (HIF-1α) which is a key transcription factor mediating hypoxic responses, promoting fibrosis in AT. Another hypertrophic adipocyte feature is the increased expression and secretion of several pro-inflammatory cytokines, including TNFα, IL-6, IL-1β, and monocyte chemoattractant protein-1 (MCP-1). This high production and secretion of proinflammatory cytokines leads to phosphorylation of IRS-1 resulting in the development of IR. Moreover, proinflammatory cytokines also promote AT inflammation by recruiting various immune cells, such as macrophages and T cells (*Choe et al., 2016*).

On the base of its anatomic location and morphological structure, WAT develops diverse and unique inflammatory phenotypes. According to this, it is known that obesity triggers a more intense inflammatory reaction in VAT than in SAT. Indeed, VAT contains more macrophages compared with SAT both in obese mice and humans as well as also a higher degree of hypertrophy. Infiltration of bone marrow-derived inflammatory cells is a key feature of the WAT inflammation and it is known that inflammatory cells infiltration in expanding WAT induces adipocyte and metabolic dysfunctions (*Kawai et al., 2021*).

Adipose tissue macrophages (ATMs) are key players in obesity associated inflammation. Two different phenotypic classes of macrophages are distinguishable: M1, which release pro-inflammatory cytokines and M2, anti-inflammatory, which contribute to repair and remodeling. M1 macrophage phenotype and inflammatory pathways are predominant in obesity. During cellular

hypoxia states, one response of activated proinflammatory macrophages is the formation of crown like structures (CLS) that surround necrotic adipocytes. *In vitro* studies demonstrate that LPS or interferon-γ (IFN-γ) stimulation of these macrophages increases macrophages M1 phenotype and subsequent its activation in AT. In addition, macrophages are capable of secreting chemotactic molecules such as TNF-α potent mediator that recruits cytokines including IL-6, IL-1β, and MCP-1. In contrast, the action of IL-4 and IL-13 (TH2 cytokines), promotes an alternative activation state M2 and producing IL-10, an anti-inflammatory cytokine that also enhances insulin sensitivity. IL-4, which mediates this alternative/anti-inflammatory activation, is highly expressed in lean AT. (*Menendez et al., 2022*).

The major feature of WAT from patients with metabolic disfunctions, such as T2DM, is adipocyte hypertrophy with severe proinflammatory macrophages infiltration. In the context of low-grade inflammation, these metabolically-activated proinflammatory ATMs, seem to be different when compared with classically activated M1 macrophages involved in the context of a full-fledged inflammatory reaction. In fact, M1 macrophages involved in acute inflammatory reactions express high levels of CD274, CD38, and CD319 on their cell surface, while the ATMs in obese organism do not. These obese ATMs show rather a different gene expression profile with subsequent less inflammatory phenotype and lower pro-inflammatory cytokines release, when compared to classically activated M1 macrophages. These observations are in line with the presence of low-grade inflammation in obesity however, is not fully understood how this lower immune cell activation degree is obtained and maintained (*Kawai et al., 2021*).

2. OBESITY

Obesity is a complex, multifactorial and chronic disease characterized by excessive body fat accumulation increasing the risk of developing various comorbidities, such as CVDs, T2DM, hypertension, and some form of cancer. Obesity results from a combination of genetic, environmental and behavioural factors. The prevalence of obesity has reached epidemic proportions worldwide, affecting individuals of all ages, ethnicities, and socioeconomic backgrounds. The genetic component of obesity is not yet fully understood, but several genes have been identified that play a role in regulating energy balance and body weight, whose genetic variants associated with an increased risk of obesity. For instance, mutations in the Melanocortin-4-receptor (MC4R) gene have been associated with severe obesity, while common variants in the fat mass and obesity-associated (FTO) gene have been linked to a modest increase in BMI as well as TMEM18, a hypothalamic gene that has recently been linked to obesity and BMI (*Bluher, 2019; Loos and Yeo, 2022*).

Environmental and behavioural factors are the primary drivers of the obesity epidemic and have a greater impact on obesity prevalence than genetic factors. Changes in the food environment, including the widespread availability of highly processed, calorie-dense foods, have contributed to the increased prevalence of obesity. In addition, the prevalence of physical inactivity has increased, with sedentary lifestyles becoming the norm in many societies but also other behavioural factors, such as stress, sleep deprivation, and smoking cessation, may also contribute to the development of obesity (*Apovian, 2016; Afshin et al., 2019*).

Diagnosis of obesity using BMI is straightforward, inexpensive, and widely available. However, BMI is not a perfect measure of adiposity, and some individuals with a high BMI may have a low body fat percentage, while others with a normal BMI may have excess body fat. Therefore, other measures, such as waist circumference and imaging techniques, may be more accurate in some cases (*Moltrer et al., 2022*). Diagnosing obesity is typically based on measuring BMI, which is a calculation of a person's weight in kilograms divided by their height in meters squared (kg/m^2). As show in Table 1, BMI of 25-29.9 is considered overweight, while a BMI of 30 or higher is classified as obese (*Apovian, 2016*). However, BMI may not accurately reflect body composition or differentiate between fat mass and muscle mass, particularly in athletes or individuals with a high muscle mass.

WHO CLASSIFICATION OF WEIGHT STATUS	
WEIGHT STATUS	**BODY MASS INDEX (BMI), kg/m^2**
Underweight	<18.5
Normal range	18.5 – 24.9
Overweight	25.0 – 29.9
Obese	≥ 30
Obese class I	30.0 – 34.9
Obese class II	35.0 – 39.9
Obese class III	≥ 40

Table 1. BMI chart with obesity classifications adopted from the WHO 1998 report. Contributed by the World Health Organization - "Report of a WHO consultation on obesity. Obesity Preventing and Managing a Global Epidemic" (Iqbal and Rehman, 2023).

Therefore, other measures such as waist circumference, body fat percentage, and imaging studies such as dual-energy X-ray absorptiometry (DEXA) or magnetic resonance imaging (MRI) may be used in conjunction with BMI to diagnose obesity (*Apovian, 2016; Bluher, 2019*). In addition to these physical measurements, healthcare providers may also perform laboratory tests to evaluate for obesity-related comorbidities such as IR, dyslipidaemia, and inflammation. These tests may include fasting glucose, haemoglobin A1C, lipid panel, and liver function tests. Overall, a comprehensive evaluation of a patient's medical history, physical examination, and laboratory tests can help diagnose obesity and assess the risk of developing obesity-related comorbidities (*Ghesmaty et al., 2018; van der Valk et al., 2019*).

Obesity is associated with a range of health consequences, including CVD, T2DM, certain types of cancer, obstructive sleep apnoea, and asthma. The exact mechanisms linking obesity to these diseases are not fully understood, but excess body fat is known to contribute to chronic inflammation, and oxidative stress, all of which are involved in the pathogenesis of these diseases (*Kim et al., 2020*).

Moreover, obesity leads to metabolic abnormalities, such as hyperinsulinemia and dyslipidaemia. Hyperinsulinemia is a state of elevated insulin secretion caused by IR, while dyslipidaemia refers to abnormal levels of lipids in the blood, such as high TAGs and LDL, and low levels of high-density lipoprotein (HDL). On the other hand, low-grade of inflammation is a common feature of obesity and is associated with the development of IR, dyslipidaemia, and CVD. T2DM is another significant health consequence of obesity, with approximately 90% of individuals with T2DM being overweight or obese. Excess body fat has been linked to IR, which is a precursor to T2DM. IR occurs when the body's cells become less responsive to insulin, a hormone that helps regulate blood sugar levels. As a result, blood sugar levels rise, leading to type obesity, as well as changes in lung function and airway mechanics (*Hotamisligil, 2017; Piché et al., 2020*).

Obesity is a major risk factor for CVD, the leading cause of death worldwide. Obesity increases the risk of developing hypertension, atherosclerosis, coronary artery disease, heart failure, and stroke. Hypertension occurs when the force of blood against the walls of the arteries is too high, leading to damage to the arterial walls and an increased risk of atherosclerosis. Atherosclerosis is the build-up of plaque in the arteries, which can lead to coronary artery disease, heart failure, and stroke. In particular, abdominal obesity, characterized by excess fat accumulation in the abdominal cavity, is a strong predictor of CVD (*Piché et al., 2020*).

Moreover, obesity leads to changes in the hormonal order, which can have far-reaching effects on health. Obesity is associated not only with increased levels of insulin bat also with increased levels of leptin, and cortisol, which can contribute further to the development of IR, dyslipidaemia, and hypertension. Obesity is also associated with decreased levels of adiponectin, a hormone that has anti-inflammatory and insulin-sensitizing properties (*Bluher, 2019; Rohm et al., 2022*). In addition, NAFLD is associated with obesity and has become the most common cause of chronic liver disease. In the next decade, it could become the main cause of liver transplantation (*Sarwar et al., 2018*).

Obesity is also correlated with an increased risk of several types of cancer, including breast, colon, and prostate cancer. The exact mechanisms underlying the relationship between obesity and cancer are not fully understood but are thought to be related to the metabolic and hormonal changes associated with obesity (*Gallagher and LeRoith, 2015*).

Prevention and treatment of obesity involves a multi-disciplinary approach, including dietary changes, physical activity, behavioural modifications, and, in some cases, medication or surgery. However, long-term weight loss maintenance remains a challenge, with only a small percentage of individuals able to achieve and maintain significant weight loss through lifestyle modifications alone (*Batsis et al., 2015*). While there is no single solution for obesity, early intervention and management can improve outcomes and reduce the risk of developing obesity-related comorbidities (*Colquitt et al., 2014; Yanovski and Yanovski, 2014*).

Thus, early diagnosis and treatment are crucial for reducing the health burden of obesity, but long-term weight loss maintenance remains a challenge. A better understanding of the underlying mechanisms linking obesity to these diseases is needed to develop effective prevention and treatment strategies. In conclusion, obesity is a major public health problem that has significant health and economic consequences. The prevalence of obesity continues to increase worldwide, and effective prevention and management strategies are urgently needed to address this global problem. Advances in genetics, epigenetics, and metabolomics have shed light on the complex aetiology of obesity and its associated pathologies. This knowledge can be used to develop personalized treatment strategies that target the underlying causes of obesity and improve patient outcomes.

3. ANTI-OBESITY THERAPIES

Obesity has a great impact on health, quality of life, and society; for this reason, its management interventions are of great importance. Several and different therapeutic approaches for the management, control and treatment of obesity are used based on different factors including the severity of obesity, age, sex, underlying causes, psychosocial factors, familiarity, and obesity-related complications. Behavioural and dietary changes and the increase in physical exercise are considered the first-line treatment in obese patients, thanks to less side effects of these treatments. However, when these lifestyle interventions alone are not sufficiently, drug therapy is recommended especially for those patients for whom bariatric surgery is no possible. Nowadays, the role of drugs in obesity treatment is controversial due their limited effectiveness in fact, the drug therapy may have different effects in different people (*Salari et al., 2021*).

Drug therapy is applied as adjunct to lifestyle changes in subjects who fail to reach their treatment finish line and have a BMI $\geq$ 30 kg/m^2 or lower in some patients which BMI may not reflect accurately the degree of obesity, as well as patients with a BMI $\geq$ 27 kg/m^2 in the presence of obesity-related comorbidities such as dyslipidaemia, hypertension, obstructive sleep apnoea, and

T2DM. On the other hand, bariatric surgery is indicated in patients which have more severe forms of obesity with a BMI ≥ 40 kg/m^2 or BMI ≥ 35 kg/m^2 in the presence of comorbidities, and also for patients with a BMI between 30 and 35 kg/m^2 which have uncontrollable T2DM or metabolic syndrome. The pharm therapy approved in USA for obesity treatment includes the use of short-term individually or in combination drugs such as phentermine, orlistat, liraglutide, semaglutide, a combination of phentermine/topiramate, and a combination of naltrexone/bupropion. However, in Europe, only orlistat, liraglutide, and naltrexone/bupropion are approved. Furthermore, also metformin and sodium-glucose cotransporter-2 inhibitors are applied in the clinic. Instead, Lorcaserin, a selective agonist of the 5-hydroxytryptamine serotonin 2C receptor (5-HT$_{2C}$), was recently retired from the US market due to increase of cancer incidence, even if a certain causal relationship had not been defined (*Angelidi et al., 2022*).

The use of pharmacotherapy to control obesity is to improve patient take part to lifestyle changes also overcoming the biological adaptations following the weight loss. Several and increased evidences have shown that behavioural changes interventions together anti-obesity medication can provide greater weight loss compared to care conditions only. However, the efficacy of anti-obesity drugs is often restricted to a reduction of 5-10% of body weight over a 1-year and weight loss usually does not exceed 6-8 months. Five weight loss medications, lorcaserin, liraglutide, orlistat, naltrexone/bupropion, and phentermine/topiramate, were compared in relation to weight loss efficacy, grouped in a systematic review and network meta-analysis including 28 randomized controlled trials and 29,018 patients in total. These studies have shown that participants in the placebo group had a statistically significant lower odds ratio for achieving 5% weight loss after one year compared with participants taking medications (*Wiechert and Holzapfel, 2021*).

Orlistat: (Xenical®) is approved for adult and adolescent obesity treatment, it promotes weight loss by inhibiting gastrointestinal lipases and reducing the fat gastrointestinal absorption. Usually, 120 mg of orlistat ingested three times a day reduces the absorption of fat by 30%. Moreover, orlistat seems to be more efficient in inhibiting the fat digestion in solid foods, compared to liquids. Numerous trials support orlistat's efficacy not only for weight loss but also for maintenance. In fact, compared to subjects taking placebo, those receiving orlistat lose more weight during the first year of treatment and reduce the weight recovery in the second year of treatment. However, they have lower serum levels of vitamins D, E, and β-carotene but which can easily be reintegrated with oral multivitamin supplementation. In addition, trials in Europe demonstrated similar results over a 2-year. In addition to promoting weight loss and maintaining lost weight, orlistat has been shown to improve insulin sensitivity and lower serum glucose levels. In study conducted in Sweden, the

subjects receiving orlistat, showed a risk reduction in development of T2DM, compared to placebo plus diet and lifestyle group. In patients with obesity and T2DM with or without insulin treatment, orlistat resulted in improved glycemic control, determined by serum blood glucose and glycate haemoglobin A1c levels (HbA1c) measurements, and reduced total cholesterol, LDL, TAGs, and apolipoprotein B levels. Similar results were found in subjects with obesity and T2DM, hypercholesterolemia, or hypertension (*Tchang et al., 2021*).

The most common adverse effects of orlistat are abdominal or stomach pain, diarrhoea, and steatorrhea, while only a few cases of severe liver and acute renal injury are reported. The major contraindications reported about orlistat using are linked to pregnancy, malabsorption syndrome, and cholestasis. The medication is distributed in 120 mg capsules and is suggested the administration of three times a day (*Kakouri et al., 2021*).

Liraglutide: (Victoza®) is a glucagon-like peptide 1 (GLP-1) agonist that was approved for the treatment of T2DM. GLP-1 is secreted after meals and it has multiple effects as an incretin hormone. It regulates blood glucose trough the inhibition of glucagon secretion and increasing the insulin secretion in a glucose-dependent manner. Moreover, GLP-1 slows gastric emptying, induces postprandial satiety, as well as reduces appetite through effects on the CNS. The liraglutide pharmacodynamics is very complex, acting at various levels to keep glucose homeostasis by regulating insulin secretion and eating behavior. In addition, liraglutide is more stable in plasma than the human endogenous GLP-1, highly binding to the plasma proteins. As side effects, nausea, vomiting, diarrhoea, constipation, and dyspepsia were frequently reported, but which were tolerated by most patients over time. The recommended dose is subcutaneous administration of 1.8 mg day to day (*Tak and Lee, 2021*).

A 20-week trial in subjects with obesity shown that treatment with liraglutide led to a dose-dependent weight loss of up to 4.4 kg, compared with 3.0 kg for placebo. Moreover, in patients with prediabetes monitored after 3 years, the treatment with liraglutide was linked with higher weight loss than placebo and the time-to-onset of T2DM was essentially protracted with liraglutide treatment. In addition, overweight patients without diabetes and after weight loss by energy-restricted dieting, were randomized either to liraglutide or to placebo, with the aim of compare weight maintenance. In the course of this maintenance period, the weight loss with liraglutide was 6.2% than with placebo 0.2% (*Aaseth et al., 2021*).

Naltrexone/Bupropion: The combination of naltrexone/bupropion leverages the complementary effects of 2 separate agents. Bupropion is a dopaminergic and noradrenergic medication used as an antidepressant and a smoking cessation aid by acting on the central perception of reward. It affects

the arcuate hypothalamic nucleus (ARC), an important region involved in the integration of hunger and satiety signaling, stimulating the secretion of proopiomelanocortin (POMC) and subsequent, release of α-melanocyte stimulating hormone (α-MSH). Successively, it acts on melanocortin MC4R, leads to an increase of energy expenditure and satiety. On the other hand, naltrexone is an opioid antagonist which principally acts on the μ-opioid receptor. POMC also stimulates the release of β-endorphin which, attaching to the μ-opioid receptor on POMC neurons, completes an autoinhibitory loop reducing the production of POMC. Naltrexone blocks this loop enhancing the secretion of POMC produced by bupropion treatment. Some trials demonstrated that the optimal dosage of the combination is 32 mg naltrexone/360 mg bupropion daily. Other important studies in subjects with obesity and T2DM shown a higher percentage of weight loss compared to placebo but also a moderate reduction in HbA1c. Successfully, the addition of the drug combination to an intensive behavioural changes program, leads to a greater weight loss, compared to participants taking placebo (*Angelidi et al., 2022*).

Adverse effects related to naltrexone/bupropion treatment including nausea, vomiting, dizziness, constipation, and dry mouth. The use of naltrexone is contraindicated in patients that assume opioid analgesics, while bupropion is not recommended in combination with medications that lower seizure threshold and inhibitors of monoamine oxidase. Likewise to other drug therapy approved by FDA, naltrexone/bupropion can be prescribed for its effects on weight loss and metabolic profile. However, it should not be administered in patients with uncontrolled hypertension, as a consequence of its sympathomimetic effects. For this reason, more studies need to carry to evaluate the long-term safety and benefits associated to cardiovascular and metabolic health (*Idrees et al., 2022*).

4. *MANGIFERA INDICA* L. (MANGO)

Nowadays, there is a great interest in the use of medicinal plants and bioactive compounds, such as polyphenols contained in them. Polyphenols possess numerous biological properties including radical scavenging, ant-inflammatory and anti-cancer actions. Vegetables and fruits contain several different bioactive phytocompounds, such as polyphenols, carotenoids, anthocyanins, as well as vitamins. For this reason, several studies have greatly demonstrated that a diet rich in fruits and vegetables significantly provides health benefits reducing the chronic diseases insurgency, such as CVD, diabetes, and cancer (*Rodriguez-Casado, 2016; van Breda and de Kok, 2018*).

Mangifera indica L. (mango) belongs to genus *Mangifera*, in the *Anacardiaceae* family and it is native to India and Southeast Asia however, currently mango is grown in other parts of the world and since few years also in Europe (*Rodríguez Pleguezuelo et al., 2012*).

About eight hundred varieties of mango fruit are available worldwide but not all are produced and commercialized. In the south of Italy, particularly in Sicily, can be found different mango cultivars mainly in the provinces of Palermo, Messina, and Catania, such as Kensington Pride, Osteen, Tommy Atkins, Keitt, Kent, Maya, Glenn, and Irwin varieties (*Gentile et al., 2019; Fratianni et al., 2020; Polizzi et al., 2022*).

Although the local mango spread can be compromised by pathogenic agents (*Ismail et al., 2013*), this new agricultural revival met the farmer's optimism to recover abandoned soils making an added value at the consumption of the fruit which, besides having qualitative and nutraceutical properties comparable to those imported by tropical areas, have also the advantage of ripening on the tree offering and be eaten fresh. The mango tree is a vigorous evergreen, fast-growing, and long-lived with leaves perennial, pointed, and shiny. The inflorescence appears as panicles containing yellowish-green or whitish-red flowers. The trees can be up to 30-40 m in tropical regions, while in subtropical areas is very reduced. Each mango fruit varieties possesses its own particular taste and size which are between 5-15 cm long, 4-10 cm in diameter and 150-750 g in weight (*Lauricella et al., 2017*).

Mango fruit is anatomically is classified as a deliquescent drupe (Figure 10). It consists of a thick, smooth, and glandular exocarp (peel/skin), green when unripe and yellow-orange-red at full ripeness. The edible part consists of a fibrous, juicy mesocarp orange-yellow (flesh/pulp), and a lignified endocarp (pit/husk) which cover the seed (kernel). Peel, pulp, and kernel of mango constitute the 15-20%, 45-65%, and 20-45%, respectively, of the whole fruit fresh weight however, this depends primarily on genotype. Indeed, genotype has relevant impact on characterization of several compounds within pulp, peels, and kernel of mango fruit whose promote health moreover, variability is also further enhanced by a lot of factors such as climatic conditions, ripening stage at harvest, cultivation techniques, and pre- postharvest treatments (*Lenucci et al., 2022*).

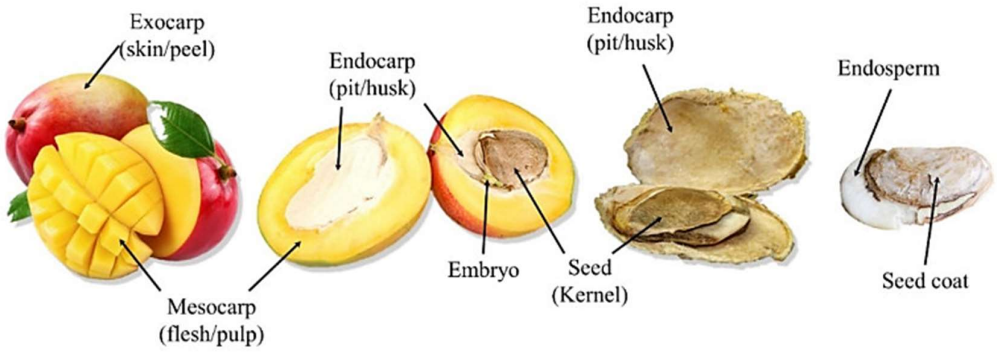

Figure 10. Anatomy of a typical mango fruit (*Mangifera indica* L.) (*Lenucci et al., 2022*).

Several studies shown that mango possesses relevant nutritional, anti-inflammatory, antioxidant, metabolic, and immunomodulatory functions to human health. It contains carbohydrates, lipid, organic acids, proteins, dietary fiber, chlorophylls, and large amounts of bioactive compounds, such as flavonoids, carotenoids, polyphenols, phytosterols, and volatile compounds. Polyphenols identified in mango pulp include mangiferin, gallotannins, quercetin, isoquercetin, ellagic acid, β-glucogallin, and gallic acid which represents the most phenol compound in this fraction. In addition, mango fruits are rich in monosaccharides whose levels differ depending on the cultivars and ripening stages. The energy value for 100 g of the pulp ranges from 60 to 190 kcal (Table 2) (*Maldonado-Celis et al., 2019*).

Parameter	Content (g per 100 g of fruit dry weight basis)
Water	78.9–82.8
Ashes	0.34–0.52
Total lipid	0.30–0.53
Total protein	0.36–0.40
Total carbohydrate	16.20–17.18
Total dietary fiber	0.85–1.06
Energy (kcal)	62.1–190

Table 2. *Proximal composition analysis of mature mango fruit (Mangifera indica* L.) (*Maldonado-Celis et al., 2019*).

Mango fruit processing generates peel and kernel as the two main by-products, wholly discarded as waste. The use of mango by-products as resource of high-value functional ingredients for food supplementation and formulation of pharmaceutical, cosmeceutical, nutraceutical products, is

greatly increased, thanks to their biochemical profiles. This is become an important point in the management of bio-waste to improve agri-food production sustainability. For instance, mango peel flour has been used to increase same aliments nutritional and antioxidant properties including pasta, bread, and biscuits. Furthermore, the mango kernel fats physicochemical characteristics are very comparable to those of other fruits such as cocoa and karitè seed butters, making it an alternate option for applications in cosmetics. In addition, it has a subtle and rich in with vitamins A and E, other antioxidants, and essential FAs, making it an optimal choice for pharmaceutical and food ends (*Lenucci et al., 2022*).

The mango peel consists of various valuable phytochemicals, including carotenoids, polyphenols, other bioactive compounds and dietary fiber, which possesses antioxidant and free-radical-scavenging properties. Two more important phytochemicals, quercetin 3-Ogalactoside and mangiferin, are also present in the peel. The mango peel composition greatly depends on level of ripeness, locality, cultivars, and climatic conditions in its region of production. In addition, mango peel contains a macronutrients variety such as carbohydrates (20–30%), protein, lipids, amino acids, organic acids, and micronutrients. The content of vitamins C and E varies widely in different cultivars and resulting higher in ripened than in raw mango peel. In addition, the mango peel contains significantly higher levels than pulp of the following minerals: Ca, K, Mg, Na, Fe, Mn, Zn and Cu (*Maldonado-Celis et al., 2019; Lebaka et al., 2021*).

On the other hand, the nutritional composition of mango seed varies mostly on the basis of cultivar and geographical differences. Similarly to mango pulp, the seed is rich in nutrients, and is used for the development of numerous value-added products. It contains high amounts of carbohydrates, lipids protein, and several minerals. Although the protein amount is low, it is nutritious protein thank to its essential amino acid composition which is higher than the standard proteins. Mango seed, contains also oil and its fat characteristics are similar with other vegetable butter, with a main content of stearic and oleic acids; moreover, in some varieties, the content of unsaturated fatty acid is up to three times higher than that content of saturated fatty acids (SFAs). The mango seed contains abundant minerals levels, particularly K, Ca, P, and Mg. It also contains vitamins C and E and other essential vitamins, including K and B-vitamins. Finally, similar to the pulp and the peel, it is also a great source of polyphenols with potent antioxidant activity including tannins, gallic acid, coumarins, caffeic acid, vanillin, mangiferin, ferulic acid, cinnamic acid, and considering its antioxidant properties greater than that of other fruit seeds (*Mwaurah et al., 2020; Lebaka et al., 2021*).

Several studies have reported the antioxidant properties of mango demonstrating that the mango peel have a considerable metabolite content and antioxidant activity and suggesting its possible use as functional additive in the production of juices, nectars, and other mango-based products (*Morales et al., 2020; Lebaka et al., 2021*). Arshad et al. performed a study to explore *in vivo* the antioxidant potential of mango peels against dyslipidemia and oxidative stress in overweight subjects. The results showed that upon consumption of mango peel powder, LDL, cholesterol, TAGs, urea, and creatinine levels were decreased while, HDL was increased as well as ROS produced in the body were reduced, suggesting that mango peels have a strong management potential against oxidative stress and dyslipidemia in obese subjects (*Arshad et al., 2021*). In another study, was evaluated the biological properties of extract obtained from *Mangifera indica* L. leaves in preclinical *in vitro* models finding that the extract was rich in polyphenols and owned high antioxidant, anti-inflammatory, and antifibrotic activities (*Sferrazzo et al., 2022*).

Recent studies showed that phytochemicals contained in mango perform an anti-inflammatory role in different chronic pathological disorders associated with inflammatory responses. Mohan et al. evaluated and demonstrated *in vitro* conditions, by DPPH radical scavenging activity and lipoxygenase inhibition assay, the anti-oxidant and anti-inflammatory activities of the leaf extracts and fractions of *Mangifera indica* L. (*Mohan et al., 2013*). Another study determined the effect of Ubá mango juice with and without peel extract on the adiposity and inflammation modulation in high-fat diet-induced obese Wistar rats. The results shown the antioxidant and anti-inflammatory effects of Ubá mango by increasing HDL, PPAR-γ, LPL, and decreasing blood glucose, total cholesterol, alanine aminotransferase, FAS and TNF-α (*Gomes Natal et al., 2016*). Recent research has shown the importance of mango polyphenols to intestinal health and in the prevention of chronic inflammatory diseases including inflammatory bowel diseases. These patients produce high amount of pro-inflammatory cytokines, such as IL-1, IL-6, IL-12, and TNF-α which induce the expression of enzymes related with inflammation, such as iNOS and COX-2. The anti-inflammatory effect of mango has been demonstrated to prevent or mitigate inflammation and other symptoms associated with chronic intestinal diseases, via the suppression of pro-inflammatory cytokines, as well as improve intestinal health (*Kim et al., 2021*). Moreover, phytochemical compounds of mango have been also reported to exert anti-diabetic effects. Mango peel extracts are able to ameliorate diabetes resulting in a blood glucose levels reduction, an increased plasma insulin level, and decreased levels of fructosamine and glycated haemoglobin (*Gondi and Prasada, 2015*).

Mangifera indica L. exhibits a great anticancer therapeutic potential, thanks to bioactive phytochemicals contained in its different parts which have shown antiproliferative and anticancer

activity in different cancer cell lines (*Mirza et al., 2021*). In a recent study, Lauricella et al. have demonstrated that mango peel extracts impact cell viability and inhibit the colony formation of tumor cells. Mango peel induces ROS production, JNK and ERK1/2 activation, and Nrf2 and MnSOD increase. These events lead to DNA damage response by phosphorylation of γH2AX, phosphorylation of ATM kinase and upregulation of p53 (*Lauricella et al., 2019*). In another study, it was analysed the involvement of mitochondria in cell death induced by mango peel extracts in colon cancer cell lines. Mango peel extracts affect the cell viability inducing an imbalance of cellular redox responses and nuclear genotoxic stress (*Lo Galbo et al., 2021*).

Moreover, natural bioactive compounds may be used in obese patients because of their ability to impact on various key mechanisms involved in the complex pathophysiological mechanisms. Mango extracts obtained by different plant and fruit are also used in traditional medicine for treating obesity. Taing et al. have demonstrated the effects of mango peel from three mango cultivars on a 3T3-L1 adipocyte cell line to inhibit adipogenesis, and that peel extracts from different cultivars show different effects on adipogenesis in the 3T3-L1 adipocyte (*Taing et al., 2013*). To assess the benefits of mango fruit powder on the early metabolic negative aspects of a high-fat diet, Sabater et al. analysed the effects of mango fruit powder on body composition, circulating parameters, and the gene expression related to fatty acid oxidation and insulin sensitivity in a high-fat diet mice fed. The results show that mango fruit powder exerts protective effects in the initial steps of IR and hepatic lipid accumulation induced by a high-fat diet. In addition, AMPK and SIRT1 appear as master regulators of these positive effects (*Sabater et al., 2017*). In a randomized human clinical study were evaluated the effects of daily supplementation of mango for 6 weeks on inflammation and metabolic functions in lean and obese subjects. The obtained results demonstrate that in obese participants HbA1c and PAI-1 were reduced as well as plasma concentrations of IL-8 and MCP-1 (*Fang et al., 2018*). Another study demonstrated the effect of a Mangifera indica L. leaf extracts on adipogenic differentiation of 3T3-L1 cells. *Mangifera indica* leaf extracts exert anti adipogenic effects reducing lipid content, oxidative stress, inflammation as well as expression of gene involved lipid metabolism such as FAS, PPARγ, DGAT1-2. In addition, leaf extracts induced significantly adiponectin production (*Sferrazzo et al., 2019*). Furthermore, it has been also shown that fresh mango consumption improves postprandial glucose and insulin responses in obese adults (*Pinneo et al., 2022*).

RESEARCH PROJECT AIMS

Some parts described in the following chapters have also been previously published in papers in which I am the first author and of which I hold the copyright together with the co-authors. These parts are merely descriptive and appropriately quoted.

Pratelli et al., Antioxidants (Basel). 2022, 11, 363. doi: 10.3390/antiox11020363.

Pratelli et al., Int J Mol Sci. 2023, 24, 5419. doi: 10.3390/ijms24065419.

In recent years, the incidence of obesity significantly increased worldwide representing a health problem (*Chooi et al., 2019*). The expansion of white adipose tissue (WAT) which characterize obese patients results from a combination of factors, including overnutrition, unhealthy diet, reduced physical activity and genetic predisposition (*Conway and Rene, 2004*). In a normal healthy person excess calories are stored as triacylglycerols (TAGs) in WAT. When energy intake exceeds energy expenditure, this leads to a hypertrophic expansion of WAT which has been correlated with lipotoxicity and alteration of adipose tissue functionality (*Longo et al., 2019; Engin, 2017*). The expansion of adipose tissue (AT) can be a consequence of two different events: accumulation of fat in existing adipocyte and differentiation of fibroblast such as pre-adipocytes in mature adipocyte by de novo adipogenesis. (*Berry et al., 2014*). Therefore, the regulation of adipogenesis is significant for obesity prevention and treatment. Several transcription factors regulating the expression of genes involved in adipocyte differentiation are activated during adipogenesis. Among them, C/EBP and PPARγ are master regulators (*Ambele et al., 2020*). They are involved in the stimulation of transcription factors and enzymes which promote lipid accumulation within adipocytes, such as SREBP-1c, ACC and FAS (*Choi et al., 2014*). AMPK is a nutrient sensor which is activated in response to cellular energy depletion. To restore cellular ATP levels, AMPK stimulates energy-produced processes such as glycolysis, lipolysis and fatty acid oxidation, while inhibits energy-consuming process such as lipogenesis. In adipocytes the activation of AMPK by phosphorylation of threonine 172 suppresses lipid biosynthesis. In particular AMPK phosphorylates and inactivates ACC, the enzyme involved in malonyl-CoA synthesis, as well as inhibits the expression of SREBP-1c, FABP4 and FAS (*Herzig and Shaw, 2018*). This results in the attenuation of lipid accumulation in mature adipocytes. Recently, several studies highlighted that AMPK is involved in adipocyte differentiation. Particularly, AMPK activation inhibits adipogenesis by reducing the expression of C/EBP and PPAR in 3T3-L1 cells (*Habinowski and Witters, 2001*).

Hypertrophic expansion of WAT represents an important risk factor for the development of several chronic diseases, including insulin resistance (IR), type 2 diabetes mellitus (T2DM), non-alcoholic fatty liver disease (NAFLD), cardiovascular diseases (CVD) and some forms of cancers (*Barnes, 2011; Sarwar et al., 2018; Avgerinos et al., 2019; Liu et al., 2022*). Excess dietary fat intake has been associated with overweight and fat deposition in mice and humans and represents a serious health risk (*Hill et al., 2000; Raatz et al., 2017; Hu et al., 2018*). However, the quality of dietary fats has been shown to induce differential lipid storage. In fact, evidence shows that a high intake of saturated long-chain fatty acids (SLFAs), such as palmitic acid (PA), is associated with obesity (*Palomer et al., 2018*), while a diet containing monounsaturated (MUFAs) and polyunsaturated fatty acids (PUFAs) or medium-chain fatty acids (MFAs) may have beneficial effects on body

weight and obesity (*Ibrahim et al., 2021*). PA induces hypertrophy by increasing lipid droplets (LDs) content, and causes DNA damage in adipocytes in vitro (*Ishaq et al., 2022*). Moreover, high consumption of PA increases the expression of pro-inflammatory cytokines in adipose tissue (*Fritsche, 2015*) as well as endoplasmic reticulum (ER) stress and reactive oxygen species (ROS) causing extensive oxidative damage to proteins, lipids and DNA, and promoting metabolic dysfunction and lipotoxicity in adipocytes (*Furukawa et al., 2004*).

Nowadays, several plants, due to the presence of bioactive compounds, have shown beneficial effects on the prevention and treatment of obesity by inhibiting adipogenesis, stimulating lipolysis in adipocytes (*Ojulari et al., 2019; Bu et al., 2019; Vinesh et al., 2020; Ansary et al., 2020; De Blasio et al., 2021*); in particular, polyphenols exhibit effectiveness against not only in obesity but also in its related chronic diseases (*De Blasio et al., 2021; D'Anneo et al., 2022*).

Mango (*Mangifera indica* L.) is a plant belonging to the *Anacardiaceae* family whose cultivation is widespread in tropical and subtropical areas of the world. In recent years, mango cultivation has also spread in different regions of Mediterranean area, including the South of Italy, which is characterized by a favourable subtropical climate and adapted soils for mango cultivation (*Lauricella et al., 2017*). Mango fruit is highly appreciated all over the world not only for its aroma and pleasant taste, but because it is rich in active ingredients with an undisputed nutritional and nutraceutical value (*Lauricella et al., 2017*). A vast literature highlights how different parts of the plant (leaves, flowers and bark) and of the fruit (peel, pulp and seed) contain phytochemicals capable of exerting anti-inflammatory, anti-oxidant and antitumoral effects (*García-Rivera et al., 2011; Mohan et al., 2013; Lauricella et al., 2017; Lauricella et al., 2019*). The edible part of the mango is only the pulp. Mango peel and seed are the main bio-wastes from mango processing, representing a consistent part of the fruit (35% to 60%).

In the present study, we characterized bioactive compounds present in peel and seed of mango cultivated in Sicily (Italy) and examined the ability of these mango extracts in inhibiting adipogenesis in 3T3-L1 cells. In particular, this study provides evidence that both mango peel extracts (MPE) and mango seed extracts (MSE) exert anti-adipogenic effects which seem to be mediated by downregulation of PPARγ and the activation of AMPK. In addition, our data highlight that MPE and MSE exert an anti-oxidant effect, counteracting ROS production during adipocyte differentiation.

Moreover, keeping in view the potent health benefits of these mango extracts, the present study was also designed to evaluate the ability of MPE and MSE to counteract lipotoxicity induced in adipocytes by saturated long chain fatty acids (SLFAs). To this end, we used an *in vitro* model in

which mature 3T3-L1 adipocytes were treated with high doses of PA, resulting in artificially hypertrophied mature adipocytes. In our model, we examined the effect of mango extracts on PA-induced hypertrophy and oxidative stress. Our data provide evidence that MPE and MSE reduced lipid accumulation and exerted anti-oxidant effects by reducing lipogenesis, inducing lipolysis and counteracting ER stress and ROS increase. The activation of the AMPK and Nrf2 pathways seems to suggest that MPE and MSE reduced lipotoxicity induced by PA in adipocytes.

MATERIALS AND METHODS

1. MANGO PEEL AND SEED EXTRACTS PREPARATION

Mango (*Mangifera Indica* L.) fruits grown in Sicily (Italy) were used in this study. Initially, the peel and seed were manually removed from the fruits, washed with distilled water, cut and lyophilized (Hetosicc Lyophilizer Heto CD 52-1). Next, the lyophilized products were powered using an electric blender, solubilized in ethanol-PBS 1:1 solution and kept overnight at 37° C in constant agitation. Final concentration of both Mango Peel Extracts (MPE) and Mango Seed Extracts (MSE) was 75 mg/mL. Subsequently, the extracts were centrifuged at 120x g for 10 min and the supernatants were subjected to a subsequent centrifugation at 15-500x g for 10 min. MPE and MSE were stored in the dark at -20° C until use. The working solutions of MPE and MSE were diluted to final concentration in the culture medium. The concentration of ethanol in the final solution did not exceed 0.06% of culture medium and was added as vehicle in control cells.

2. HPLC-ESI-MS ANALYSIS

The lyophilized sample of Mango peel and seed described above were solubilized as previously reported (*Sferrazzo et al., 2019*). The sample was subjected to ultrasound and vortex treatment, followed by filtration with 0.45 mm PTFE filters. The standard mangiferin calibration curve included 4 concentration points: 0.3, 0.45, 0.6 and 0.75 ppm. The standard gallic acid calibration curve included 4 concentration points: 1.5, 4.5, 7.5 and 15 ppm. All samples were analysed in LC-MS/MS using the instrumentation: Q-Exactive LCq/Orbitrap MS, interfaced with UHPLC Ultimate 3000 RS in ESI (Electrospray Ionization). All experiments were performed in negative mode. The analyses were carried out using 2 different HPLC methods as previously reported (*Lauricella et al., 2019*). MS total ion counts (TIC) was employed to monitor the eluate. Gallic acid and mangiferin standards were supplied by Sigma-Aldrich (St. Louis, MO, USA).

3. CELL CULTURE AND REAGENTS

Mouse 3T3-L1 cell line was obtained from the American Type Culture Collection (ATCC). 3T3-L1 cells were cultured in complete DMEM (Euroclone, Pero, Italy) supplemented with 10% (v/v) heat-inactivated fetal bovine serum (FBS; Euroclone, Pero, Italy), 2 mM L-glutamine (BioWest, Nuaillé, France), 1% Non-Essential Amino Acids (BioWest, Nuaillé, France), 100 U/mL penicillin and 50 µg/mL streptomycin (Euroclone, Pero, Italy). The cells were maintained as monolayer in flasks of 75 cm^2 at 37 C in a 5% CO_2 humidified incubator. When 3T3-L1 pre-adipocyte cells reached 80%

of confluence, were detached from tissue culture flask using trypsin-EDTA (0.5 mg/mL trypsin and 0.2 mg/mL EDTA) and seeded in accordance to the experimental conditions. All reagents and compounds, except where differently reported, were purchased from Sigma-Aldrich (Milan, Italy).

4. ADIPOCYTE DIFFERENTIATION AND TREATMENTS

To obtain mature adipocytes, 3T3-L1 pre-adipocyte cells (undifferentiated cells, Undif. cells) were seeded at 0.2 x 10^5/well in 24-well plate or 0.8 x 10^5/well in 6-well plate and maintained in this state two days post-confluence. Then, confluent pre-adipocytes were incubated for 3 days in differentiation medium (MDI) (DMEM supplemented with 10% (v/v) heat-inactivated fetal bovine serum, 2 mM L-glutamine, 1% Non-Essential Amino Acids, 100 U/mL penicillin and 50 g/mL streptomycin, containing the pro-differentiative agents 0.5 mM 3-isobutyl-1-methylxanthine (IBMX), 1 µM dexamethasone and 1 µg/mL insulin). Then, the culture medium was replaced and the cells were incubated for additional 5 days with maintenance medium (MM) (DMEM supplemented with 10% (v/v) heat-inactivated fetal bovine serum, 2 mM L-glutamine, 1% Non-Essential Amino Acids 100 U/mL penicillin and 50 µg/mL streptomycin containing 1 µg/mL insulin). To evaluate the effects of MPE and MSE, different doses (25, 50 and or 100 µg/mL) of each extract were added to MDI and MM until complete adipocytes differentiation. The culture medium and treatments were changed every two days and differentiation was completed at day 8. At this time the cells exhibited characteristic of mature adipocytes. Undifferentiated cells (Undif.) were grown in DMEM supplemented with 10% (v/v) heat-inactivated fetal bovine serum, 2mML-glutamine, 1% Non-Essential Amino Acids 100 U/mL penicillin and 50 µg/mL streptomycin. Adipocyte differentiation was evaluated based on the expression of adipogenic markers, LDs formation and TAGs accumulation. Control undifferentiated (Undif.) and differentiated adipocyte 3T3-L1 cells (Dif.) were treated with vehicle containing 0.06% ethanol. This concentration did not exert any toxic effects on the cells.

5. PALMITATE (PA) SOLUTION PREPARATION AND TREATMENTS

Palmitate (PA) was solubilized in an EtOH 10% solution (25mM) in a heated and stirred water bath at 65° C for 15 min. Once completely solubilized, a 500 µM working dilution was appropriately prepared in culture medium containing 5% BSA and incubated at 37° C for 1 h under constant shaking to ensure their conjugation before adding it to differentiated 3T3-L1 adipocytes. Vehicle containing 5% BSA was used as control (differentiated 3T3-L1 adipocytes, Diff). PA alone or in the

presence of 100 µg/mL MPE or MSE was added to differentiated 3T3-L1 adipocytes and kept for 48 h.

6. CELL VIABILITY ASSAY

To evaluate cell viability, cells were treated with MTT 3-(4,5-dimethylthiazol-2-yl)- 2,5-diphenyltetrazolium bromide which measures the activity of mitochondrial dehydrogenases as reported (*Maggio et al., 2016*). 3T3-L1 undifferentiated cells were plated in 96-well plate at a density of 8 x 10^3/well. After 24 h the cells were exposed to different concentrations of MPE or MSE (25, 50, 75, 100, 150 and 200 µg/mL) for 8 days. MTT reagent (11 mg/mL in PBS, 20 µL) was added to each well and incubated for another 2 h at 37° C. Then, the colored crystal of produced formazan was dissolved in 100 µL of lysis buffer (20% sodium dodecyl sulphate in 50% N,N-dimethylformamide, pH 4.0). The absorbance was measured by a microplate reader (OPSYS MR, Dynex Technologies, Chantilly, VA, USA) at 540 nm with a reference wavelength of 630 nm. Cell viability was measured as the percentage of the optical density (OD) values of treated cells compared with untreated cells as control.

On the other hand, undifferentiated 3T3-L1 cells were seeded in 96-well plates (8 x 10^3 cells/well) until complete differentiation. Then, differentiated 3T3-L1 adipocyte cells were exposed to different concentrations of PA alone or in the presence of 100 µg/mL MPE or MSE for 48 h. Cell viability was evaluated by MTT assay as above reported. The cytotoxic effects of PA on differentiated 3T3-L1 adipocyte cells were also evaluated by propidium iodide (PI) staining. Differentiated cells were treated with 500 µM PA alone or together with 100 µg/mL MSE or MPE. After 48 h of treatment, cells were washed and stained with PI. After a short incubation at the dark, the fluorochrome in excess was removed and the cells were analysed by fluorescence microscopy using excitation and emission wavelengths appropriate for PI fluorescence (λex = 488 nm and λem = 610/620nm).

7. ANTIOXIDANT ACTIVITY

Radical scavenging activity of MPE and MSE were determined by DPPH (1,1-diphenyl- 2-picrylhydrazyl) radical. Different concentrations of MPE and MSE (25, 50, 75, 100 and 200 µg/mL) were added to ethanol DPPH solution (100 µM) in a final volume of 1 mL. Each concentration of extracts (A1) was incubated for 30 min in the dark at room temperature; then the loss of absorbance was measured at 517 nm spectrophotometrically. DPPH radicals have a maximum absorption at 517

nm, the peak disappears with reduction by an antioxidant compound. In the same way the negative control (A0) was prepared with ethanol DPPH solution, whereas a blank sample (A2) containing ethanol was used as reference. Radical scavenging activity (% of DPPH radical inhibition) was calculated using the following equation:

$$\text{Inhibition (\%)} = 1 - (A1 - A2/A0 - A2) \times 100$$

8. WESTERN BLOT ANALYSIS

Protein levels were analysed by Western blotting. Differentiated and treated cells were lysed as previously reported (*Lauricella et al., 2016*). Protein concentration was evaluated by Bradford Protein Assay (Bio-Rad Laboratories S.r.l., Segrate, Milan, Italy). Next, 30 µg/sample of total proteins were resolved by sodium dodecyl sulfate (SDS)-polyacrylamide gel electrophoresis (PAGE) and blotted on a nitrocellulose membrane (Bio-Rad). For all immunodetection analyses were used specific primary antibodies against PPARγ (sc-7273), PPARα (sc-9000), FABP4/aP2 (sc-18661), Adipsin (sc-47683), GLUT4 (sc-53566), MnSOD (sc-133254), GRP78 (sc-166490), phosphorylated-JNK (sc-6254), CHOP (sc-793), and caspase-3 (sc-65487), purchased from Santa Cruz Biotechnology (Santa Cruz, CA, USA); PERK (ab65142) purchased from Abcam (Cambridge, UK); phosphorylated-ACC (#07-303) purchased from EMD Millipore Corporation (Temecula, CA, USA); AMPKα (#2532), Thr172-phosphorylated-AMPKα (#2535), and phosphorylated-HSL (#4126) purchased from Cell Signaling (Danvers, MA, USA); SREBP-1c (#bs-1402R) purchased from BioSS (Dundee, United Kingdom); Nrf2 (NBP1-32822) and Perilipin-2 (NB110-40877SS) purchased from Novus Biologicals (Bio-Techne SRL, Milan, Italy); HO-1, Heme Oxygenase 1 (orb5455) purchased from Biorbyt Ltd. (Cambridge, United Kingdom). Subsequently, filters were incubated with HPR-conjugated secondary antibodies (Amersham, GE Healthcare Life Science, Milan, Italy), immunoreactive signals were detected using enhanced chemiluminescence (ECL) reagents (Cyanagen, Bologna, Italy) and the signals obtained were performed with ChemiDoc XRS (Bio-Rad, Hercules, CA, USA). The intensity of the protein bands was quantified using Quantity One 1-D Analysis software (Bio-Rad) and β-actin (A5060) or γ-Tubulin (T3559) purchased from Sigma-Aldrich were used for bands normalization.

9. OIL RED O (ORO) STAINING

The effect of MPE and MSE on adipogenesis was evaluated through Oil Red O (ORO) staining (Sigma-Aldrich, St. Luois, MO, USA). Mature 3T3-L1 adipocytes, differentiated in a 24-well plate, were fixed with 10% formaldehyde for 1 h, washed with PBS and rinsed with 60% isopropanol for 5 min until completely dry. Next, the cells were stained with Oil Red O working solution (0.35 g in 100 mL isopropanol) for 10 min and then washed with dH_2O several times. The pictures were obtained by using Leica DM-IRB microscope and images were acquired on a Leica DC300F digital camera using Leica IM50 software, as representative images of the experimental conditions. In addition, the pictures were analysed in ImageJ, converted into high-contrast black and white images to visualize LDs and scored as the percentage area per field. Finally, Oil red O quantification was also performed by extracting the dye by 100% isopropanol for 10 min and the absorbance of the Oil Red O was measured at 490 nm; the percentage of the OD values of treated cells was compared with untreated cells as control.

10. DETECTION OF REACTIVE OXYGEN SPECIES (ROS) GENERATION

The cell-permeant 20,70-dichlorodihydrofluorescein diacetate (H_2DCFDA) (Molecular Probe, Life Technologies, Eugene, OR, USA) dye was used to quantify the production of reactive oxygen species (ROS) as previously reported (*Celesia et al., 2020*). For these experiments undifferentiated 3T3-L1 cells (0.2 x 10^5/well) were seeded in 24-well plates and grown until to complete differentiation in absence or presence of 100 µg/mL MPE or MSE, on the other hand differentiated 3T3-L1 adipocytes were treated with 500 µM PA in absence or presence of 100 µg/mL MPE or MSE for 48 h. At the end, the cells were washed with PBS and incubated with 10 µM H_2DCFDA dye for 30 min in the dark in an incubator with 5% CO_2 at 37 C. Then, fluorochrome was removed, cells were washed in PBS and analysed by fluorescence microscopy by using excitation and emission wavelengths that are appropriate for green fluorescence (FITC filter with λex = 485 nm and λem = 530 nm).

11. TRIACYLGLYCEROLS (TAGs) EVALUATION

3T3-L1 cells were differentiated for 8 days in the absence or presence of different concentrations of MPE or MSE (25, 50 or 100 µg/mL) or differentiated 3T3-L1 adipocytes were treated with 500 µM PA in absence or presence of 100 µg/mL MPE or MSE for 48 h. Then, cells were lysed with 5%

NP-40 and the triacylglycerols (TAGs) content of supernatants was quantified using a spectrophotometric commercial kit for triglyceride determination (SENTINEL CH. SpA, Milan, Italy). TAGs concentrations were calculated based upon a standard curve standard and normalized to total cellular protein content measured by Bradford assay as reported (*Roh and Jung, 2012*).

12. STATISTICAL ANALYSIS

Each experiment and all determinations were performed in triplicate. The data were represented as mean ± S.D. The statistical significance of the differences between groups were evaluated using Tukey's test following one-way ANOVA test. A p-value < 0.05 was considered the threshold for statistical significance. Where not specified, the data is not significant with respect to the related control.

RESULTS

1. HPLC-ESI-MS Analysis of Mango Peel (MPE) and Seed Extracts (MSE)

In collaboration with the colleagues of the Department of Biological, Chemical and Pharmaceutical Sciences and Technologies (STEBICEF), Section of Chemistry at the Palermo University, we have performed the comprehensive characterization of the phenolic fraction of Sicilian mango peel and seed by HPLC-ESI-MS to compare the composition in water-soluble phenolic compounds in the two different parts of the fruit and the influence on the activity. As reported in the literature, gallic acid and its derivatives were the largest family found in mango flesh, peel and seed kernel samples (*Lauricella et al., 2017*). Quantification of mangiferin and gallic acid was performed with the calibration curves of their own standards. According to previous studies, the gallates, gallotannins and maclurin derivatives were quantified using the calibration curve of gallic acid (*Gómez-Caravaca et al., 2016*). Table 3 and Table 4 show the quantification of free polar compounds in MPE and MSE, expressed as mg/100 g dry matter.

	Compound	RT (min)	ESI⁻ [M − H]⁻ (*m/z*)		Molecular Formula	mg/100 g
			Teor.	*Exp.*		
1	Disaccaride	6.22	341.1089 [M − H]⁻ 377.0856 [M + Cl]⁻ 387.1144 [M + FA]⁻	341.1090 [M − H]⁻ 377.0857 [M + Cl]⁻ 387.1145 [M + FA]⁻	$C_{12}H_{22}O_{11}$	ND [a]
2	Quinic acid	6.70	191.0561 [M − H]⁻	191.0562 [M − H]⁻	$C_7H_{12}O_6$	ND [a]
3	Glucosyl gallate	7.00	331.0671 [M − H]⁻	331.0673 [M − H]⁻	$C_{13}H_{16}O_{10}$	108.14
4	Gluconolactone	7.53	223.0459 [M + FA]⁻	223.0460 [M + FA]⁻	$C_6H_{10}O_6$	ND [a]
5	Lepidimoic Acid	7.70	965.2627 [3M − H]⁻	965.2614 [3M − H]⁻	$C_{36}H_{54}O_{30}$	ND [a]
6	Citric acid	8.39	191.0197 [M − H]⁻	191.0198 [M − H]⁻	$C_6H_8O_7$	ND [a]
7	Gallic acid	8.63	169.0142 [M − H]⁻	169.0141 [M − H]⁻	$C_7H_6O_5$	118.57
8	Maclurin mono-O-galloyl-glucoside	24.74	575.1042 [M − H]⁻	575.1041 [M − H]⁻	$C_{26}H_{24}O_{15}$	72.03
9	Mangiferin	25.01	421.0776 [M − H]⁻	421.0776 [M − H]⁻	$C_{19}H_{18}O_{11}$	2.81
10	Maclurin di-O-galloyl glucoside	25.34	727.1152 [M − H]⁻	727.1145 [M − H]⁻	$C_{33}H_{28}O_{19}$	20.21
11	Digallic acid	25.46	321.0252 [M − H]⁻	321.0255 [M − H]⁻	$C_{14}H_{10}O_9$	Trace
12	Maclurin tri-O-galloyl-glucoside	26.21	879.1262 [M − H]⁻	879.1253 [M − H]⁻	$C_{40}H_{32}O_{23}$	6.05
13	Tetragalloyl glucose	26.31	787.0999 [M − H]⁻	787.0998 [M − H]⁻	$C_{34}H_{28}O_{22}$	4.88
14	Methylgallate	26.36	183.0299 [M − H]⁻	183.0301 [M − H]⁻	$C_8H_8O_5$	225.87
15	Pentagalloyl glucose	26.73	939.1109 [M − H]⁻	939.1100 [M − H]⁻	$C_{41}H_{32}O_{26}$	17.89
16	Methyl-digallate ester	29.68	335.0409 [M − H]⁻	335.0411 [M − H]⁻	$C_{15}H_{12}O_9$	487.15

[a] Not determined.

Table 3. Polyphenols characterization of MPE.

HPLC-ESI-MS analysis of MPE presented free polar compounds usually observed for tropical fruits including phenolic acid derivatives, in particular the gallic acid derivatives. As evidenced in Table 3, methyl digallate (487.15mg/100 g), methyl gallate (225.87mg/100 g), gallic acid (118.57 mg/ 100 g) and glucosyl gallate (108.14 mg/100 g) were the principal phenolic compounds. Interestingly, the characterization of the polyphenolic profile of MPE provided evidence that different families such as organic acids, gallates and gallotannins, xanthones and benzophenone derivatives enrich this fruit and could be the main players in the analysed mechanism. In addition, differently from other previous studies, we demonstrate for the first time the presence of lepidimoic acid, a pectic disaccharide, in mango peel (*Lauricella et al., 2019*)

On the other hand, HPLC-ESI-MS analysis of MSE in Table 4 shows the presence of 8 polar compounds in MSE. Characterization of MSE evidenced higher concentration of polyphenols in MSE than MPE; in particular, methyl gallate was the major component (2520 mg/100 g) and methyldigallate ester isomer (1210 mg/100 g) the second most abundant compound.

	Compound	RT (min)	ESI [M − H] (m/z)		Molecular Formula	ppm	mg/100 g
			Teor.	Exp.			
1	Disaccaride	1.5	341.1089 $[M-H]^-$	341.1089 $[M-H]^-$	$C_{12}H_{22}O_{11}$	trace	trace
2	Quinic acid	1.5	191.0561 $[M-H]^-$	191.0561 $[M-H]^-$	$C_7H_{12}O_6$	trace	trace
3	Glucosyl gallate	4.6	331.0671 $[M-H]^-$	331.06707 $[M-H]^-$	$C_{13}H_{16}O_{10}$	2.80	280
4	Gallic acid	5.8	169.0142 $[M-H]^-$	169.01425 $[M-H]^-$	$C_7H_6O_5$	1.3	130
5	Methylgallate	15.3	183.0299 $[M-H]^-$	183.02990 $[M-H]^-$	$C_8H_8O_5$	25.2	2520
6	Mangiferin	20.9	421.0776 $[M-H]^-$	421.07763 $[M-H]^-$	$C_{19}H_{18}O_{11}$	0.5	50
7	Methyl-digallate ester isomer	22.6		335.04086 $[M-H]^-$		12.1	1210
8	Maclurin tri-O-galloyl-glucoside	29.0	879.1262 $[M-H]^-$	879.11651 $[M-H]^-$	$C_{40}H_{32}O_{23}$	trace	trace

Table 4. Polyphenols characterization of MPE.

2. MPE and MSE Possess ROS Scavenger Activities

To ascertain the antioxidant activity of MPE and MSE we performed DPPH• radical scavenging assay, as reported in Materials and Methods. Figure 11 shows the effect of different concentrations (25–200 µg/mL) of both the extracts. Our data demonstrated that both MPE and MSE possess an elevated radical scavenging activity. The inhibition of DPPH• free radical exerted by mango extracts was dose-dependent and resulted higher in MSE than MPE, in accordance with the higher concentrations of polyphenols in MPE. In fact, at a concentration of 100 µg/mL, the DPPH• inhibition exerted by MPE was only by 73%, respect to that of MSE that reached an inhibition value equal to 59%.

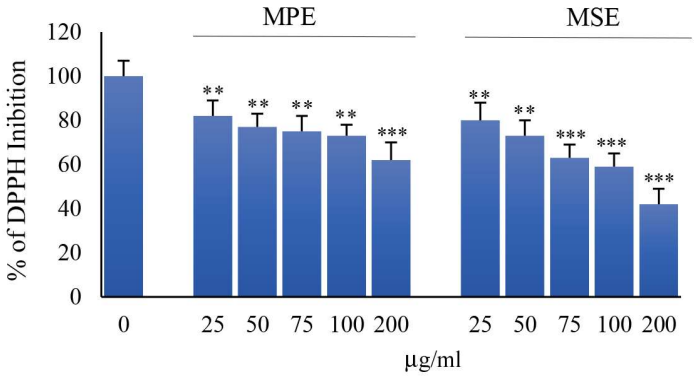

Figure 11. MPE and MSE possess radical scavenging activity. The antioxidant activity of MPE and MSE was evaluated by DPPH• (1,1-diphenyl-2-picrylhydrazyl) radical scavenging assay. Different concentrations of MPE and MSE (25–200 µg/mL) were added on ethanol DPPH solution and absorbance of each concentration was measured at 517 nm by spectrophotometer. The bar graphs represent the mean of three independent experiments ± SD. ** $p < 0.01$ and *** $p < 0.001$ with respect to the only vehicle control.

3. Effects of MPE and MSE on the Viability of 3T3-L1 Pre-Adipocytes

3T3-L1 cell line is one of the most widely used cell system for studying adipogenesis. In fact, these cells cultivated in the presence of a cocktail of pro-differentiative agents show the characteristics of mature adipocyte in metabolism and lipid accumulation (*Green and Meuth, 1974*). Preliminary studies were performed to determine the non-toxic concentrations of MPE and MSE on 3T3-L1 pre-adipocytes undifferentiated (Undif.) cells. To this end, we evaluated the effect of different doses (25–200 µg/mL) of both the extracts on the viability of 3T3-L1 cells using the MTT assay. The results shown in Figure 12 indicate that 200 µg/mL of MPE or MSE slightly decreased the cell viability when compared to control cells after 8 days of treatment. Differently, the viability of 3T3-L1 cells was not affected by 100 µg/mL of both the extracts.

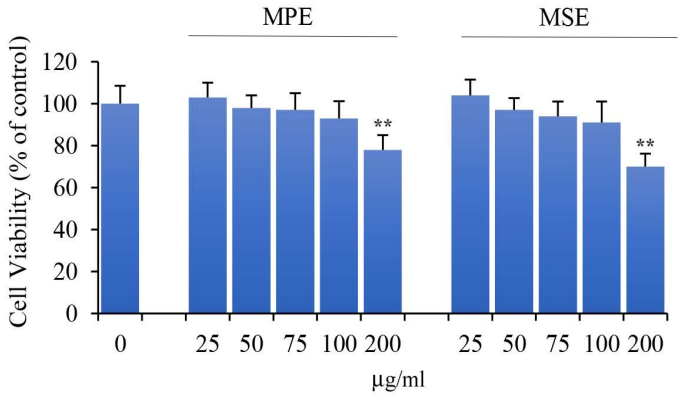

Figure 12. Effects of MPE and MSE on the viability of 3T3-L1 pre-adipocyte cells. 3T3-L1 cells (8 x 10^3/200 µL of culture medium) were exposed to different doses (25–200 µg/mL) of MPE or MSE for 8 days. Then, the percentage of viable cells was assessed by MTT assay. The values reported are the mean ± SD of three independent experiments. ** $p < 0.01$ with respect to control cells treated with vehicle only.

4. MPE and MSE Reduced Lipid Content during 3T3-L1 Adipocyte Differentiation

Then, we first evaluated the ability of MPE and MSE to counteract the differentiation of 3T3-L1 cells into adipocytes. To this end, 3T3-L1 pre-adipocytes were differentiated for 8 days in the presence or absence of different doses (25, 50 and 100 µg/mL MPE or MSE), as reported in Materials and Methods. Results demonstrated that 3T3-L1 cells incubated with adipogenic medium appeared enlarged with the cytoplasm enriched of numerous droplets of various size, as observed by phase contrast microscopy (not shown). These morphological changes were less evident in 3T3-L1 cells differentiated in the presence of MPE or MSE. The addition of MPE or MSE also at the highest dose of 100 µg/mL did not exert toxic effects on the cells (not shown). Then, Oil Red O staining was applied to investigate the intracellular lipid accumulation as lipid droplets (LDs). Microscopic examinations showed that differentiated 3T3-L1 cells increased Oil Red O staining compared with undifferentiated 3T3-L1 cells. Notably, MPE or MSE treatment markedly reduced the number and the size of LDs, compared to differentiated cells with a dose dependent effect (Figure 13A,B). Based on these results, 100 µg/mL of both MPE and MSE was chosen for further investigations. LDs production was quantified by measuring the absorbance of the solubilized Oil Red O-stained LDs at 490 nm. As shown in Figure 13C, both 100 µg/mL MPE and MSE reduced the absorbance of the stained cells by 31% and by 41%, respectively, compared to differentiated cells. These data suggest that MPE and MSE decreased the amount of lipids in 3T3-L1 adipocytes. Such a reduction in lipid accumulation was also sustained by measuring the triacylglycerols (TAGs) content. The results showed that the intracellular TAGs accumulation increased in differentiated cells by 200% relative to undifferentiated cells. Interestingly, we observed a significant dose-dependent decrease in TAGs content. In particular, the addition of 100 µg/mL MPE or MSE significantly decreased the TAGs content by 36% and 45%, respectively, compared to differentiated cells (Figure 13D).

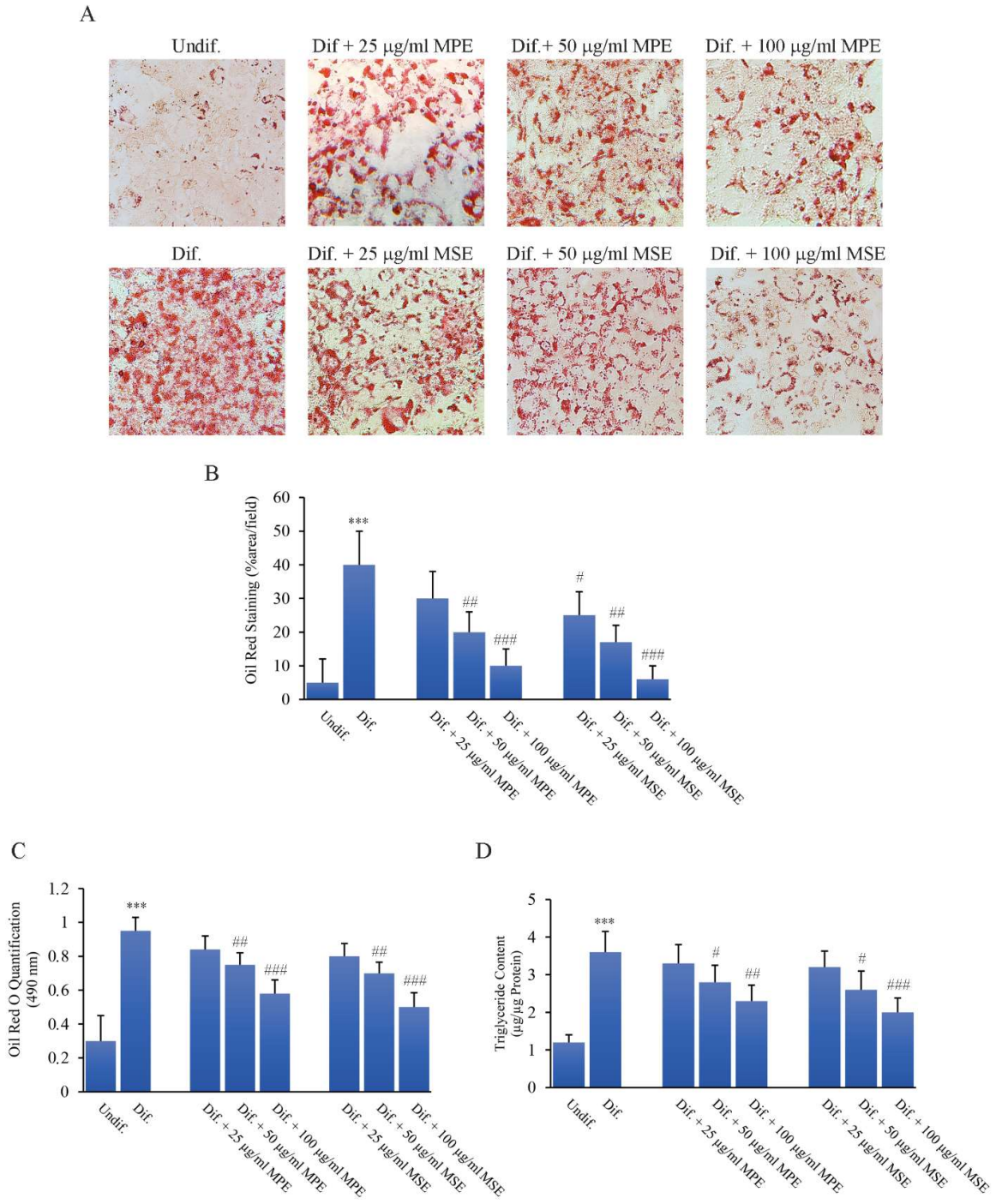

Figure 13. MPE and MSE reduce lipid content in 3T3-L1 adipocytes. 3T3-L1 cells were treated with pro-differentiative agents for 8 days in the presence or absence of different concentrations (25, 50 and 100 µg/mL) MPE or MSE. Representative photographs showing LDs reduction by Oil red O staining after MPE and MSE treatment (200× original magnification) (**A**). LDs content was ascertained by analysing the percentage area of Oil Red O stained by Image J (**B**) Quantitative Oil Red O staining measured by spectrophotometer at 490 nm reading (**C**). Cellular TAGs content quantified by spectrophotometer at 546 nm reading (**D**). The results are the mean of three independent experiments ± SD. *** $p < 0.001$ with respect to the undifferentiated cells (Undif.). # $p < 0.05$, ## $p < 0.01$ and ### $p < 0.001$ with respect to the differentiated untreated cells (Dif.).

5. MPE and MSE Reduced the Expression of Key Factors of Adipogenic Differentiation and Lipid Accumulation

Peroxisome proliferator activated receptor γ (PPARγ) is a member of the nuclear hormone receptor superfamily. In the form of heterodimer with retinoid X receptor, PPARγ binds to the PPAR response element and modulate the expression of adipogenic and lipogenic genes (*Mota et al., 2017*). PPARγ activation during adipocyte differentiation has been reported to be sufficient for adipogenesis *in vitro* and *in vivo* (*Xiaoru et al., 2016*). We observed that the level of PPARγ at differentiation day 8 markedly increased in differentiated 3T3-L1 cells respect to undifferentiated control cells (Figure 14). Notably, consistent with the decrease in lipid accumulation, lower levels of PPARγ were found in 3T3-L1 cells grown with adipogenic medium and treated with MPE or MSE (44% and 66%, respectively, in comparison with differentiated 3T3-L1 cells). Moreover, treatment with MPE or MSE resulted in a reduced expression of PPARγ downstream target genes. In fact, as evidenced in the same Figure 14, both MPE and MSE lowered in adipocytes the adipocyte fatty-acid binding protein (FABP4/aP2), a lipid-chaperone of adipose tissue whose level is greatly increased during the last stage of differentiation of adipocytes (*Amri et al., 1991; Prentice et al., 2019*); the glucose transporter 4 (GLUT4), a member of glucose transporter in adipose tissue involved in the insulin-stimulated glucose uptake (*Govers, 2014*); and the Complement Factor D/Adipsin, an adipokine which promotes adipocyte differentiation and lipid accumulation (*Song et al., 2016*).

We further examined the effects of mango extracts on the expression level of Sterol-regulatory element-binding protein-1c (SREBP-1c). SREBP-1c is a transcription factor upregulated under adipocyte differentiation which regulates the expression of genes involved in de novo lipogenesis and TAGs synthesis, including ATP-citrate lyase (ACL), Acetil-Coa Carboxylase (ACC), Fatty acid synthase (FAS), Stearoyl-CoA desaturase (SCD1) and Glycerol-3-phosphate acyltransferase (GPAT) (*Magaña et al., 1997; Tabor et al., 1998; Shimomura et al., 1998; Horton et al., 2002*). We demonstrated that the level of SREBP-1c increased by 50% in differentiated 3T3-L1 cells in comparison with undifferentiated cells. Interestingly, the addition MPE or MSE in the differentiation medium lowered the level of this factor (33% and 67%, respectively, in comparison with 3T3-L1 differentiated cells (Figure 14).

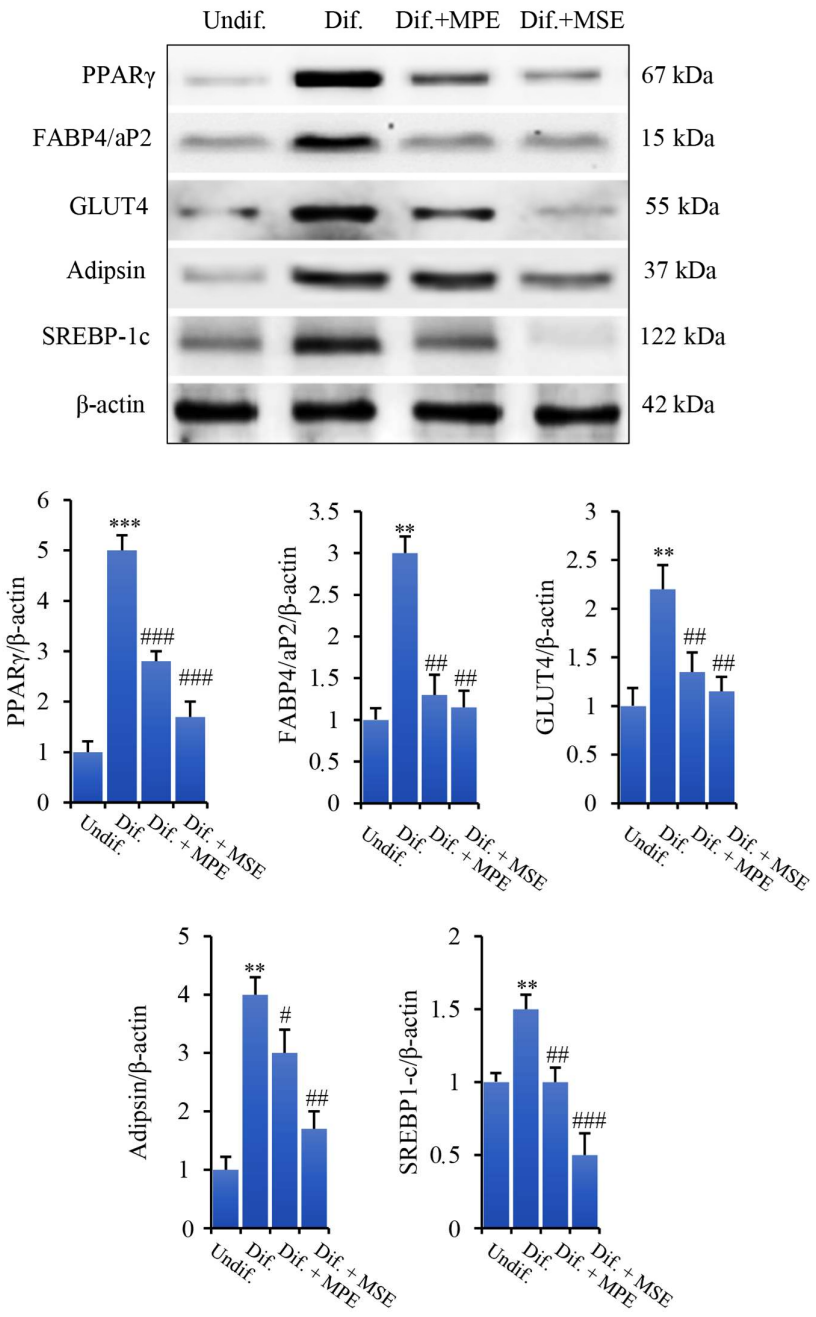

Figure 14. MPE and MSE down-regulate the expression of adipogenic differentiation and lipid accumulation markers in 3T3-L1 adipocytes. 3T3-L1 cells were treated with pro-differentiative agents for 8 days in the presence or absence of 100 µg/mL MPE or MSE. Then, cell lysates were analysed by Western blotting using specific primary antibodies directed against PPARγ, FABP4/aP2, GLUT4, Adipsin and SREBP1-c. Equal loading of proteins was verified by immunoblotting for β-actin and showed values were assigned in relation to undifferentiated cells (Undif.). The bar graphs represent the mean of three independent experiments ± SD. ** $p < 0.01$ and *** $p < 0.001$ with respect to undifferentiated 3T3-L1 cells (Undif). # $p < 0.05$, ## $p < 0.01$ and ### $p < 0.001$ with respect to the differentiated untreated 3T3-L1 cells (Dif.).

6. MPE and MSE Increase the Levels of Lipolytic Factors

We further examined the ability of MPE and MSE to activate factors promoting lipolysis in adipocytes, such as PPARα and AMPK. Peroxisome proliferator-activated receptor-α (PPARα) is another member of PPAR family expressed mostly in tissues with high rates of fatty acid oxidation, such as the liver, brown fat and muscle (*Pyper et al., 2010*). It has been shown to up-regulate the expression of genes involved in fatty acid oxidation, particularly when co-activated by PPAR coactivator 1 α (PGC-1α) (*Haemmerle et al., 2011*). Our data, shown in Figure 15, demonstrated that the addition of MPE or MSE in the differentiation medium enhanced the expression level of PPARα (40% and 70%, respectively).

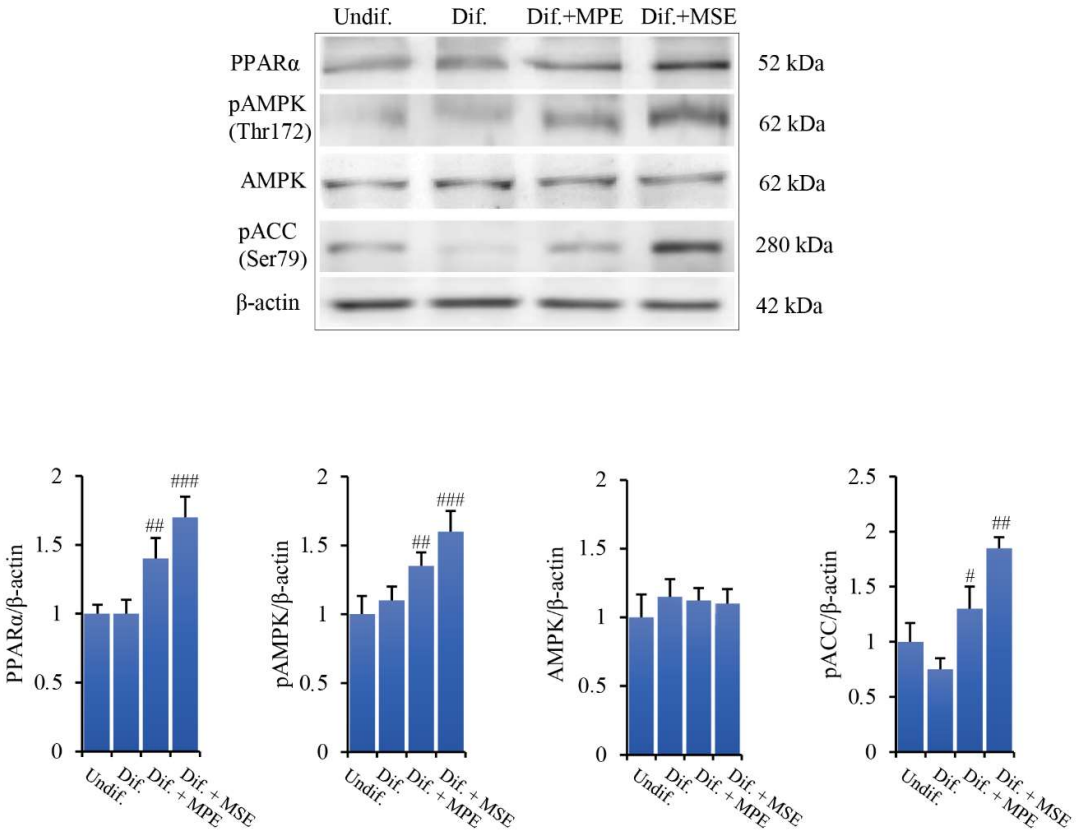

Figure 15. MPE and MSE up-regulate PPARα and activate AMPK in 3T3-L1 adipocytes. 3T3-L1 cells were treated with pro-differentiative agents for 8 days in the presence or absence of 100 µg/mL MPE or MSE. Then, cell lysates were analysed by Western blotting using specific primary antibodies directed against PPARα, AMPK, phospho-AMPK and phospho-ACC. Equal loading of proteins was verified by immunoblotting for β-actin and showed values were assigned in relation to undifferentiated 3T3-L1 cells (Undif). The bar graphs represent the mean of three independent experiments ± SD. # $p < 0.05$, ## $p < 0.01$ and ### $p < 0.001$ with respect to differentiated untreated cells (Dif.).

AMP-activated kinase (AMPK) is an energy sensor regulating glucose and lipid metabolism (*Herzig and Shaw, 2018*). Upon activation in the phosphorylated form, AMPK reduces lipid

synthesis by inhibiting the activity of the key enzymes of fatty acid de novo synthesis, such as Acetyl-CoA carboxylase (ACC) (*Herzig and Shaw, 2018*). To investigate whether MPE and MSE are capable of activating AMPK, we examined by Western blotting analysis the levels of AMPK and its phosphorylated form. As shown in Figure 15, compared to differentiated 3T3-L1 cells, the presence of MPE or MSE in the differentiation medium enhanced the phosphorylation of AMPK by 23% and 45%, respectively. The results also showed that MPE or MSE did not significantly modify the basal levels of AMPK (Figure 15), thus supporting a role of mango extracts on AMPK activation. Concomitantly, the expression of the phosphorylated and inactive form of ACC increased following MPE and MSE treatment by 44% and 110%, respectively.

To ascertain whether mango extracts act via AMPK, confluent 3T3-L1 pre-adipocytes were pre-treated for 4 h with Compound C (10 µM, CC), a highly selective inhibitor of AMPK (*Zhou et al., 2001*). Then, the cells were treated for 24 h in the presence of 100 µg/mL MPE or MSE. Notably, CC counteracted the effects of MSE and MPE on AMPK and ACC phosphorylation, while did not affect the basal level of AMPK (Figure 16). These results demonstrate that MPE and MSE are capable of activating AMPK with consequent inhibition of ACC, suggesting a role of this factor in reducing lipogenesis.

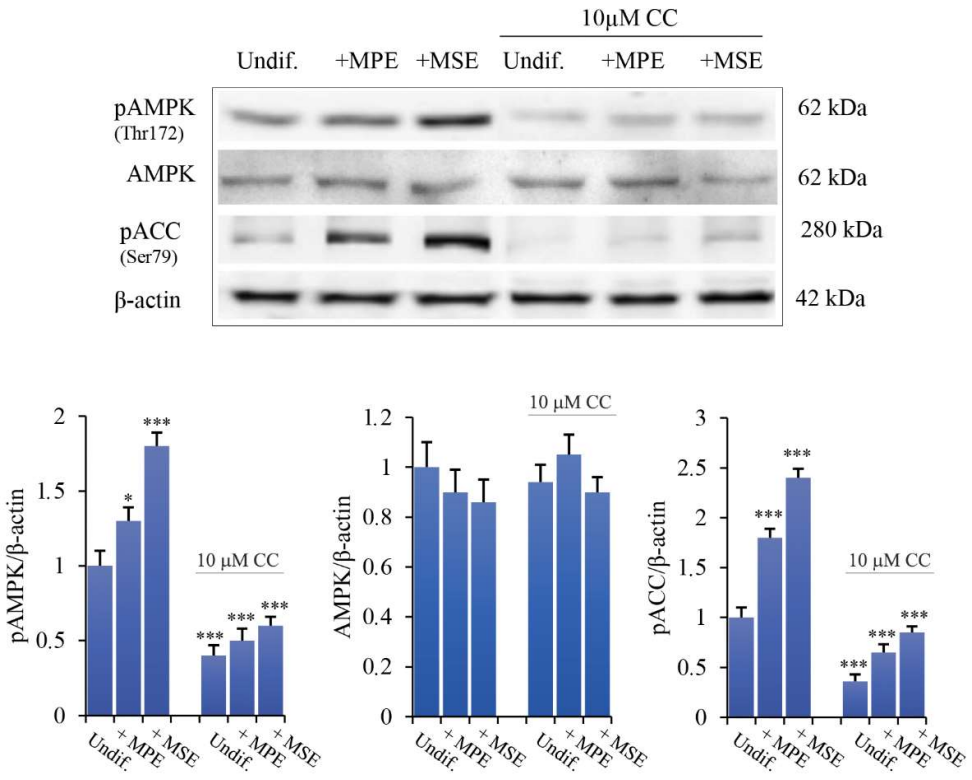

Figure 16. Compound C counteracts the effects of MPE and MSE on AMPK activation and ACC phosphorylation. Confluent 3T3-L1 cells were pre-treated for 4 h with 10 µM AMPK inhibitor, compound C (CC), and for another 24 h

in the presence or absence of 100 µg/mL MPE or MSE. Cell extracts were then prepared and immunoblotted with antibodies to AMPK, phospho-AMPK, or phospho-ACC. Equal loading of proteins was verified by immunoblotting for β-actin and showed values were assigned in relation to undifferentiated 3T3-L1 cells (Undif). The bar graphs represent the mean of three independent experiments ± SD. * $p < 0.05$ and *** $p < 0.001$ with respect to the undifferentiated untreated 3T3-L1 cells.

7. MPE and MSE Reduce ROS Production in Adipocytes

It has been reported that reactive oxygen species (ROS) generation favours adipogenesis by regulating clonal expansion during adipocyte differentiation (*Pyper et al., 2010*). To ascertain ROS involvement in our model system, we performed fluorescence microscopy analysis by employing the fluorochrome H_2DCFDA, a dye employed as a general indicator of intracellular ROS levels. As evidenced in Figure 17A, differentiated 3T3-L1 cells exhibited a pronounced green fluorescence detectable using fluorescence microscopy which is indicative of intracellular ROS production. Such an effect was consistently attenuated by 100 µg/mL MPE and counteracted by 100 µg/mL MSE.

In the next phase of our experiments, studies were carried out to ascertain the mechanism responsible for the anti-oxidant effect of MPE and MSE. In this regard, the analyses were focused on Nrf2, one of the major transcription factors that promotes cellular defence against oxidative stress (*Horton et al., 2002*). Our data show that Nrf2 level is enhanced in adipocytes differentiated in the presence of MPE or MSE. In fact, in comparison with differentiated control cells the level of Nrf2 protein increases with MPE or MSE by about 1,1-fold and 2,8-fold, respectively (Figure 17B).

Superoxide dismutase (MnSOD) and Heme oxygenase (HO-1) are ROS scavenger enzymes transcriptionally regulated by Nrf2 (*Cernigliaro et al., 2019*). We demonstrated that the levels of these proteins markedly increased after treatment with MPE or MSE (Figure 17B). Taken together, these results seem to indicate that the activation of Nrf2 plays a role in the antioxidant behaviour of MPE and MSE.

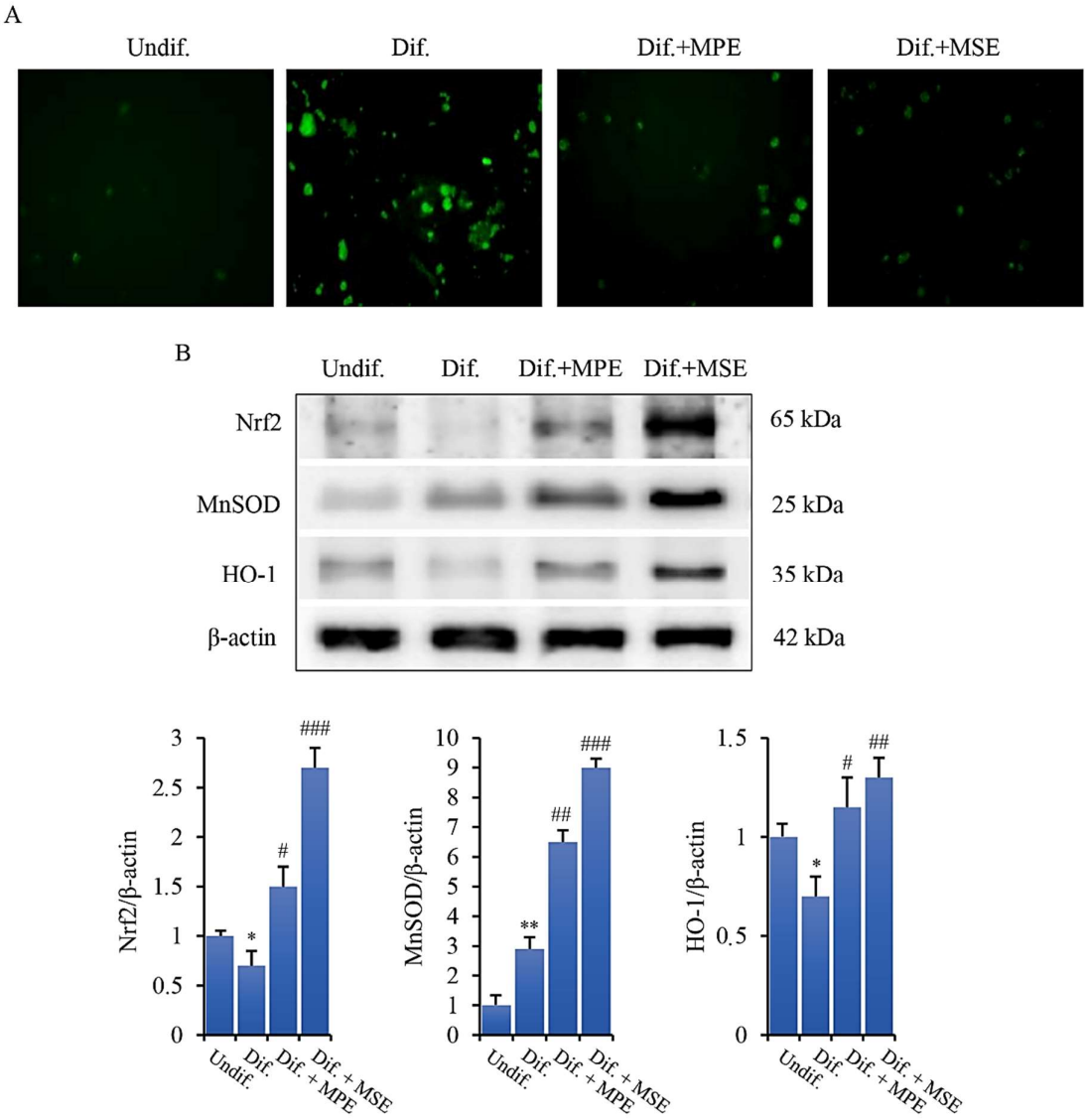

Figure 17. MPE and MSE exert anti-oxidant effects in 3T3-L1 adipocytes. 3T3-L1 cells were treated with pro-differentiative agents for 8 days in the presence or absence of 100 µg/mL MPE or MSE. (**A**) Intracellular ROS were detected using the redox-sensitive fluorochrome H_2DCFDA. After differentiation, the medium was replaced with 10 µM H_2DCFDA solution and the incubation was protracted for 30 min at 37 °C. The oxidation of the fluorochrome generates green fluorescence, which was visualized by a Leica microscope equipped with a DC300F camera using a FITC filter. Representative micrographs of fluorescence microscopy were taken at 200× magnification. (**B**) Western blotting analysis of Nrf2, MnSOD and HO-1 in 3T3-L1 cells differentiated without or with 100 µg/mL MPE or MSE. Equal loading of proteins was verified by immunoblotting for β-actin and showed values were assigned in relation to undifferentiated cells (Undif.). The bar graphs represent the mean of three independent experiments ± SD. * $p < 0.05$, ** $p < 0.01$ with respect to the undifferentiated 3T3-L1 cells, # $p < 0.05$, ## $p < 0.01$ and ### $p < 0.001$ with respect to the differentiated untreated 3T3-L1 cells.

8. MPE and MSE Reduce Palmitate (PA)-Induced Toxicity in 3T3-L1 Adipocytes

This research project also aimed at investigating whether MPE and MSE were capable of reducing lipotoxicity exerted by high doses of palmitate on differentiated 3T3-L1 adipocytes. Palmitate (PA) is the main saturated long fatty acids present in the diet Notably, a diet rich in PA has been show to favors fat accumulation and obesity (*Palomer et al., 2018*). Thus, differentiated 3T3-L1 adipocytes were treated with high doses of PA to generate artificially hypertrophied mature adipocytes (*Baldini et al., 2021*). Firstly, 3T3-L1 pre-adipocyte cells were differentiated into adipocytes as reported in Materials and Methods and then treated for 48 h with different doses of PA (100–750 µM) to evaluate their effect on cell viability, in accordance with other authors (*Leroy et al., 2008*). Data obtained by MTT assay demonstrated that PA inhibited cell survival in a dose-dependent manner with a reduction of cell viability of 50% with 500 µM PA (Figure 18A).

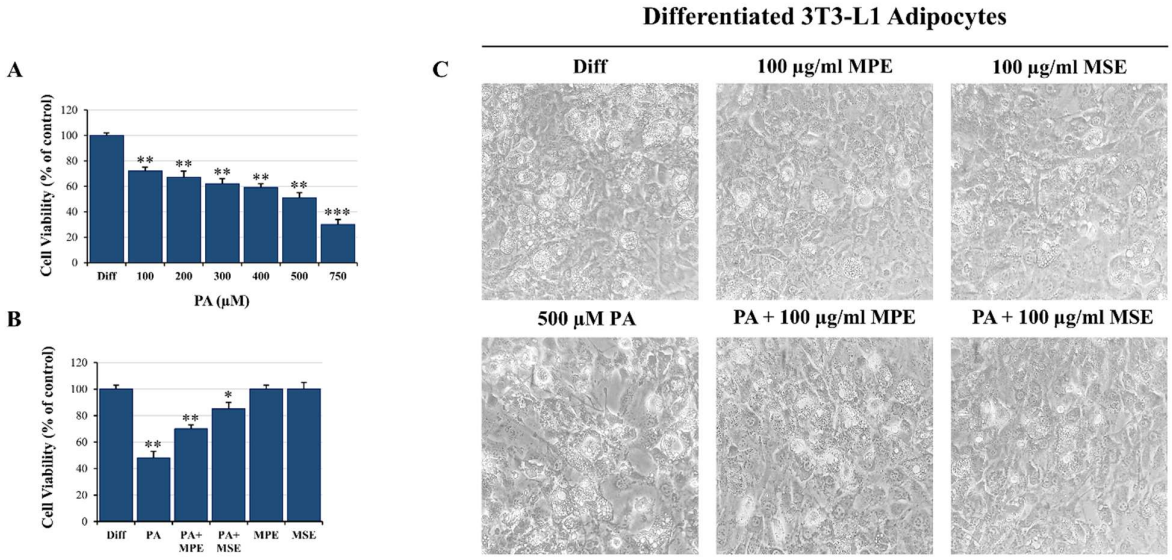

Figure 18. MPE and MSE counteract PA-induced toxicity in 3T3-L1 adipocytes. Differentiated 3T3-L1 adipocytes were exposed for 48 h to different doses of PA alone or in the presence of 100 µg/mL MPE and MSE. (**A**) MTT assays showing the reduction of cell viability induced in differentiated 3T3-L1 adipocytes by different doses of PA. (**B**) MTT assays showing the ability of 100 µg/mL of MPE or MSE to counteract the cytotoxic effect of 500 µM PA in differentiated 3T3-L1 adipocytes. (**C**) Representative phase contrast microscopy images showing the morphological changes induced by 500 µM PA alone or in the presence of 100 µg/mL MPE or MSE in differentiated 3T3-L1 adipocytes. (A,B) The values reported are the mean ± SD of three independent experiments. * $p < 0.05$, ** $p < 0.01$ and *** $p < 0.001$ were significant with respect to differentiated 3T3-L1 adipocytes treated with only vehicle BSA.

Notably, the addition of 100 µg/mL MPE or MSE increased cell viability by 46% and 77%, respectively, in comparison with PA-treated adipocytes (Figure 18B). Microscope images highlighted that the number of cells was reduced in PA-treated adipocyte cells with respect to

adipocytes co-treated with PA and MPE or MSE (Figure 18C). In addition, signs of toxicity were observed after PA treatment alone that disappeared after the addition of mango extracts (Figure 18C). Thus, in the following experiments, 100 µg/mL MPE or MSE was used to investigate the mechanism underlying the protective effects of mango extracts on lipotoxicity induced by 500 µM PA.

9. MPE and MSE Reduce Lipid Accumulation in Adipocytes Exposed to High Doses of PA

Excessive lipid availability has been related to adipose tissue hypertrophy (*Moseti et al., 2016*). To examine the anti-lipogenic effect of MPE and MSE, differentiated 3T3-L1 adipocytes were treated for 48 h with 500 µM PA in the absence or presence of 100 µg/mL MPE or MSE. Microscope images highlighted that the treatment of mature 3T3-L1 adipocytes with PA increased the content of lipids, as demonstrated by the presence of larger lipid vacuoles with respect to differentiated control 3T3-L1 adipocytes (Figure 18C). Notably, the content of these vacuoles was markedly reduced by MPE and MSE (Figure 18C). These observations were confirmed by staining the cells with Oil Red O (Figure 19A). In comparison with differentiated control adipocytes, 48 h treatment with 500 µM PA resulted in an increase in LDs in adipocytes. The addition of 100 µg/mL MPE or MSE to PA-treated adipocytes lowered lipid accumulation in comparison with PA-treated adipocytes. A modest reduction of LDs was also observed in adipocytes not exposed to PA and treated with the extracts alone (Figure 19A). These data were confirmed by microscopic quantification of the Oil Red O staining area (Figure 19B) as well as by measuring the absorbance of the solubilized Oil Red O at 490 nm (Figure 19C).

As shown in Figure 19B and 19C, the addition of 100 µg/mL MPE or MSE to PA-treated adipocytes reduced both the staining area and the absorbance of the stained cells by about 30% and 47%, respectively in comparison with PA-treated adipocytes alone. Such a reduction in lipid accumulation was also sustained by measuring the TAGs content (Figure 19D). The results showed that the intracellular TAG accumulation increased in PA-treated cells by 80% with respect to untreated differentiated adipocytes. Interestingly, the addition of MPE or MSE to PA-treated cells significantly decreased the TAGs content by 23% and 34%, respectively compared with PA-treated adipocytes (Figure 19D).

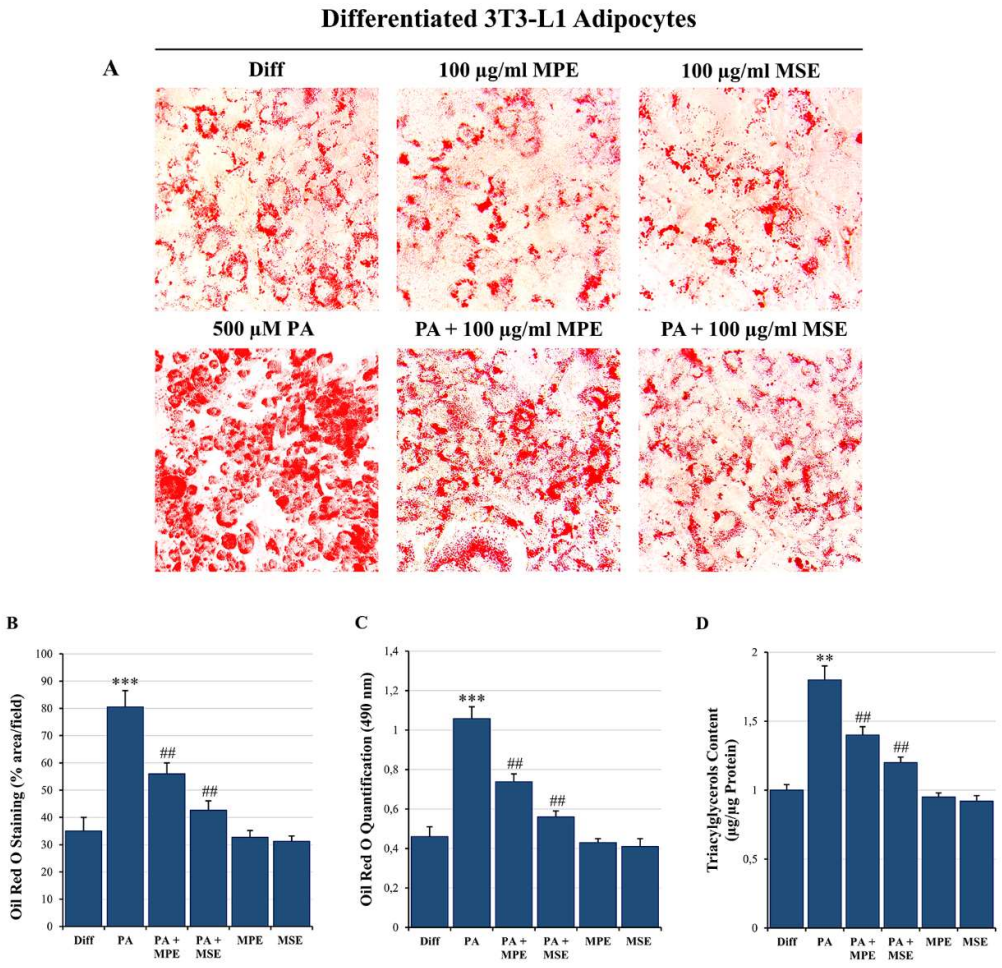

Figure 19. MPE and MSE reduce 3T3-L1 adipocyte hypertrophy induced by high concentrations of PA. 3T3-L1 differentiated adipocytes were treated for 48 h with 500 µM PA alone or in the presence of 100 µg/mL MPE or MSE. (**A**) Representative Oil red O staining microscopy images showing the increase in LDs after treatment with 500 µM PA alone and their reduction when 100 µg/mL MPE or MSE was added (200× original magnification). (**B**) LDs content was ascertained by analysing the percentage area of Oil Red O stained by ImageJ. (**C**) Quantitative Oil red O staining was measured by a spectrophotometer at 490 nm. (**D**) Cellular TAGs content was quantified by spectrophotometer at 546 nm. ** $p < 0.01$ and *** $p < 0.001$ were significant with respect to differentiated 3T3-L1 adipocytes and ## $p < 0.01$ with respect to PA-treated 3T3-L1 adipocytes.

10. MPE and MSE Inhibit PPARγ and Activate AMPK

To investigate the molecular basis for the anti-obesity effect of MPE and MSE, we first evaluated whether mango extracts are capable of reducing the level of PPARγ, the master regulator of adipogenesis and lipogenesis (*Ambele et al., 2020*). Our data supported the conclusion that PPARγ signaling sustained PA-induced hypertrophy in adipocytes. In fact, we observed an increase of 50% of PPARγ levels in adipocytes treated for 48 h with 500 µM PA, with respect to untreated adipocytes (Figure 20). A concomitant increase in the perilipin-2 levels (80%), a lipid droplet coating protein (*Sztalryd and Brasaemle, 2017*), was observed in PA-treated adipocytes (Figure 20).

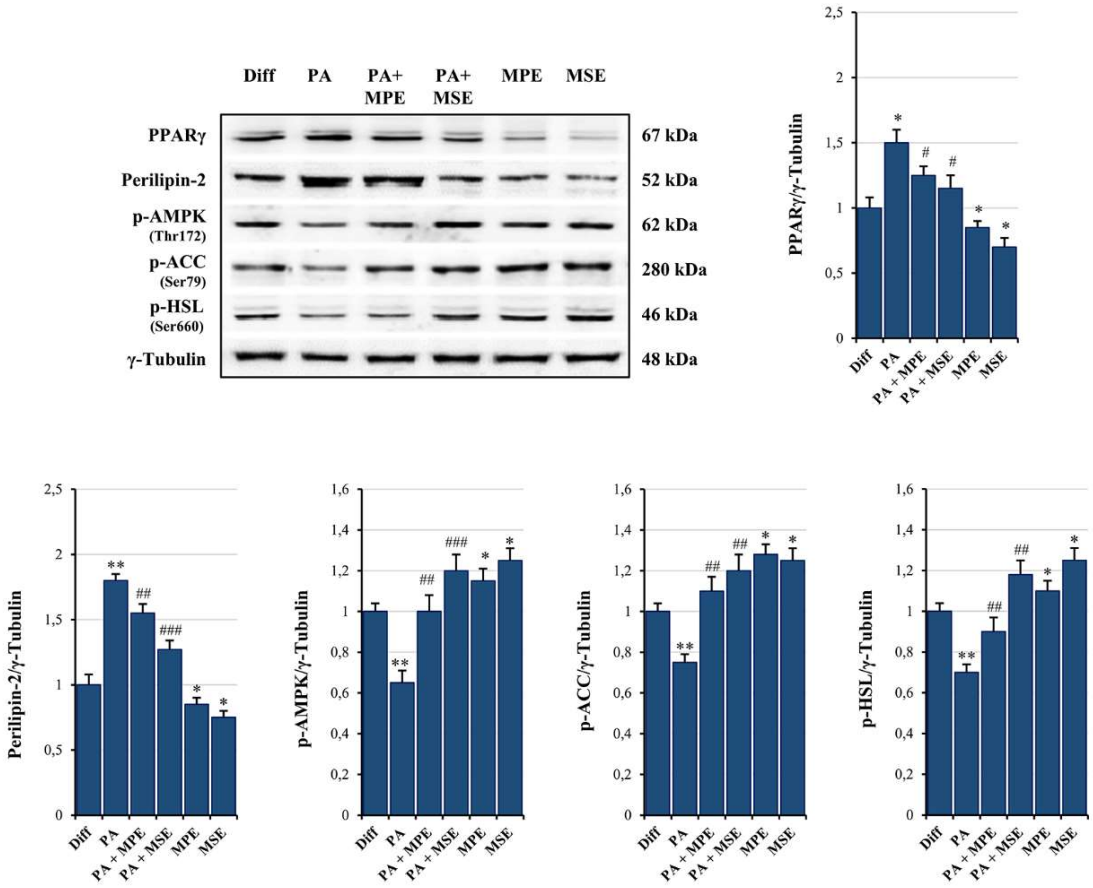

Figure 20. MPE and MSE reduce lipid accumulation, preventing lipogenesis and promoting lipolysis. Differentiated 3T3-L1 adipocytes were treated with 500 µM PA for 48 h in the presence or absence of 100 µg/mL MPE or MSE. Then, cell lysates were analysed by Western blotting using specific primary antibodies directed against PPARγ, Perilipin-2, phospho-AMPK, phospho-ACC and phospho-HSL. Equal amounts of proteins were loaded in each lane as normalized by γ-Tubulin detection. The bar graphs represent the means of three independent experiments ±SD. * $p < 0.05$, ** $p < 0.01$ were significant with respect to differentiated 3T3-L1 adipocytes. # $p < 0.05$, ## $p < 0.01$, ### $p < 0.001$ were significant with respect to PA-treated differentiated 3T3-L1 adipocytes.

Notably, the addition of MPE or MSE to PA-treated adipocytes reduced the increase in PPARγ to only 18% and 23%, respectively as well as that in perilipin-2 to only 15% and 30%, respectively, in comparison with PA-treated adipocytes (Figure 20). Next, we examined whether MPE and MSE affects AMPK activation, a kinase promoting catabolic pathways in adipocytes (*Fullerton et al., 2013*). As shown in Figure 20, the expression of the phosphorylated and active form of AMPK lowered in PA-treated differentiated 3T3-L1 adipocytes compared with control adipocytes. Interestingly, MPE or MSE alone and in the presence of PA significantly enhanced the phosphorylated form of AMPK (p-AMPK) (Figure 20). This is in line with our previous observation demonstrating that MPE and MSE activate AMPK during adipocyte differentiation. Moreover, the addition of MPE or MSE in control adipocytes as well as in PA-treated adipocytes increased the levels of the phosphorylated and inactive form of ACC (p-ACC) (Figure 20), the key enzyme of fatty acid synthesis, which is inactivated by phosphorylation by AMPK (*Fullerton et al., 2013*). Finally, our data also demonstrated that MPE and MSE markedly increased the phosphorylated and active form of hormone sensitive lipase (p-HSL), the enzyme activating lipolysis in adipocytes (*Holm, 2003*), by 30% and 65%, respectively (Figure 20).

11. MPE and MSE Reduce PA-Induced ER Stress in 3T3-L1 Adipocytes

Elevated levels of FAs, in particular SFAs such as PA, have been shown to produce endoplasmic reticulum (ER) stress in a number of cell types, including adipocytes (*Wei et al., 2006*). The activation of ER stress, in turn, represents a potential molecular mechanism of lipotoxicity (*Han and Kaufman, 2016*). We thus examined whether high doses of PA induce ER stress in mature adipocytes and the ability of MPE and MSE to counteract it. Interestingly, we observed an increase in ER stress protein markers, evidenced by an up-regulation in the expression of PERK, GRP78 and CHOP, as well as in JNK phosphorylation following the treatment of mature 3T3-L1 adipocytes with 500 μM PA for 48 h (Figure 21). These results suggest that the ER-associated unfolded protein response (UPR) pathway is activated by PA (*Ben-Dror and Birk, 2019*). Notably, the addition of 100 μg/mL MPE or MSE to PA-treated differentiated adipocytes reduced the levels of all ER stress protein markers (Figure 21), thus suggesting the ability of mango extracts to counteract ER stress.

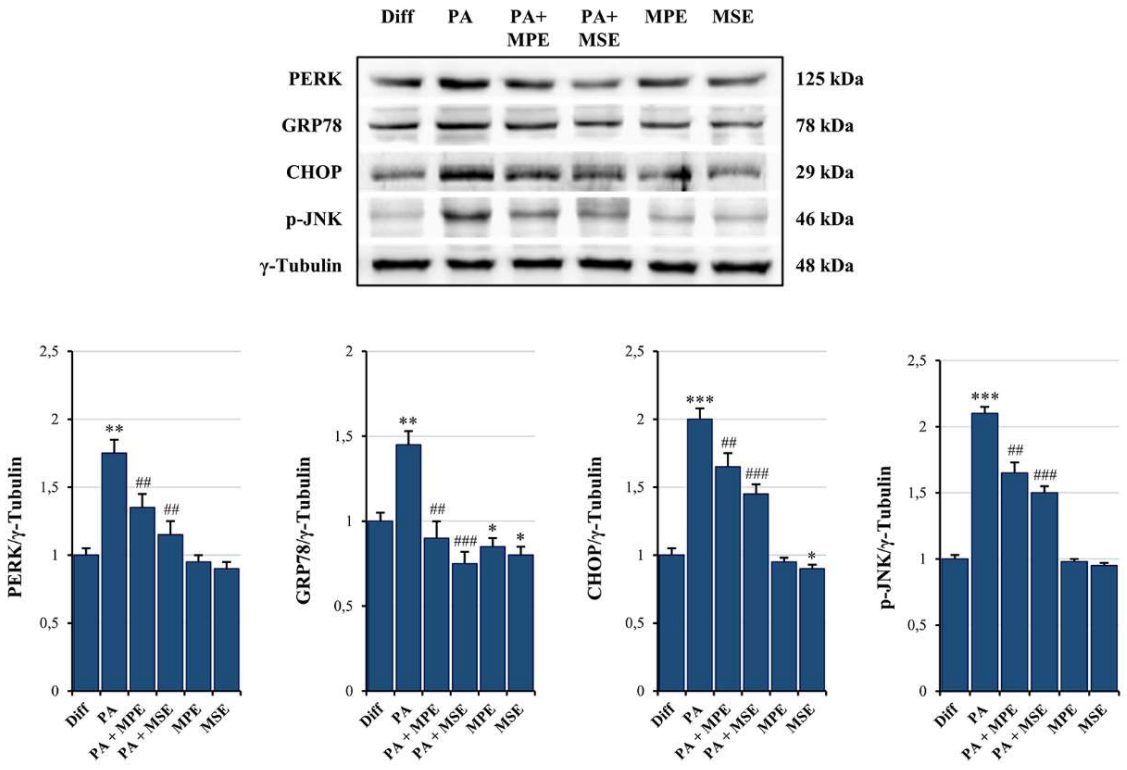

Figure 21. MPE and MSE reduce PA-induced ER stress in 3T3-L1 adipocytes. Differentiated 3T3-L1 adipocytes were treated with 500 µM PA for 48 h in the presence or absence of 100 µg/mL MPE or MSE. Cell lysates underwent Western blotting analysis for ER stress protein markers PERK, GRP78 and CHOP, as well as for phosphorylated JNK (p-JNK). Equal loading of protein was verified by immunoblotting for γ-Tubulin. The bar graphs represent the means of three independent experiments ± SD. * $p < 0.05$, ** $p < 0.01$ and *** $p < 0.001$ were significant with respect to differentiated 3T3-L1 adipocytes. ## $p < 0.01$, ### $p < 0.001$ were significant with respect to PA-treated differentiated 3T3-L1 adipocytes.

12. MPE and MSE Prevent PA-Induced ROS Production

It has been reported that lipids accumulation in WAT (hypertrophy) is associated to ROS generation increase (*Korbecki and Bajdak-Rusinek, 2019; Masschelin et al., 2019*). Thus, to evaluate whether PA increased intracellular ROS production, differentiated 3T3-L1 adipocytes were incubated with H_2DCFDA, a specific fluorescent probe that visualizes intracellular ROS (*Kaliuzhka, 2023*). H_2DCFDA-associated fluorescence was elevated by 65% after incubation with 500 µM PA for 48 h compared with untreated differentiated 3T3-L1 adipocytes (Figure 22A,B). Interestingly, the addition of 100 µg/mL MPE or MSE markedly reduced ROS content to 35% and 23% compared with adipocytes only treated with PA (Figure 22A,B), thus highlighting that mango extracts counteract ROS production and oxidative stress induced in adipocytes after PA treatment.

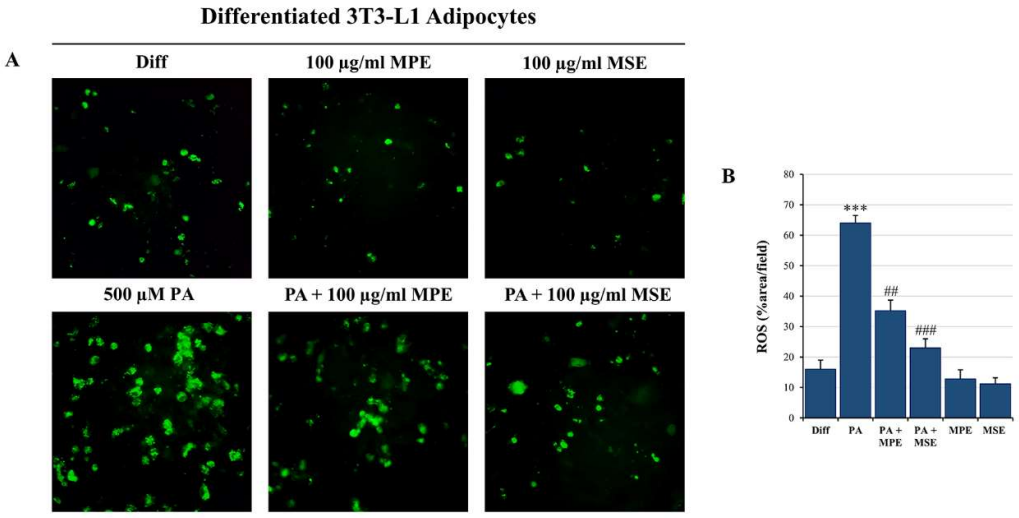

Figure 22. MPE and MSE reduce PA-induced oxidative stress in 3T3-L1 adipocytes, reducing ROS production. Intracellular ROS detection was performed by redox-sensitive fluorochrome H_2DCFDA. Differentiated 3T3-L1 adipocytes were treated with 500 µM PA for 48 h in the presence or absence of 100 µg/mL MPE or MSE. Then, cells were incubated with 10 µM H_2DCFDA solution for 30 min at 37 °C. The oxidation of the fluorochrome-generated green fluorescence was visualized by a Leica microscope equipped with a DC300F camera using a FITC filter. (**A**) Representative images of fluorescence microscopy were taken at 200× magnification. (**B**) ROS content was ascertained by analysing the percentage area with Image J. *** $p < 0.001$ was significant with respect to differentiated 3T3-L1 adipocytes, and ## $p < 0.01$, ### $p < 0.001$ were significant with respect to PA-treated 3T3-L1 adipocytes.

In addition, propidium iodide (PI) staining of cells confirmed the induction of cytotoxic effects in PA-treated differentiated adipocytes. PA treatment increased cell death by about 35% compared with control adipocyte cells (Figure 23A,B). These effects were counteracted by the addition of 100 µg/mL MPE or MSE that markedly reduced cell death by about 57% and 65%, respectively, with respect to PA-treated adipocytes. The cytotoxic effects induced by PA in adipocytes seem to be related to apoptosis induction. Pro-caspase-3 is a master apoptosis protein marker cleaved in active form during this process (*Kivinen et al., 2005*). PA treatment decreased the level of pro-caspase-3 by 43% (Figure 23C,D) and promoted the appearance of the cleaved active form of caspase-3. Notably, caspase activation was counteracted by the addition of MPE or MSE (Figure 23C,D).

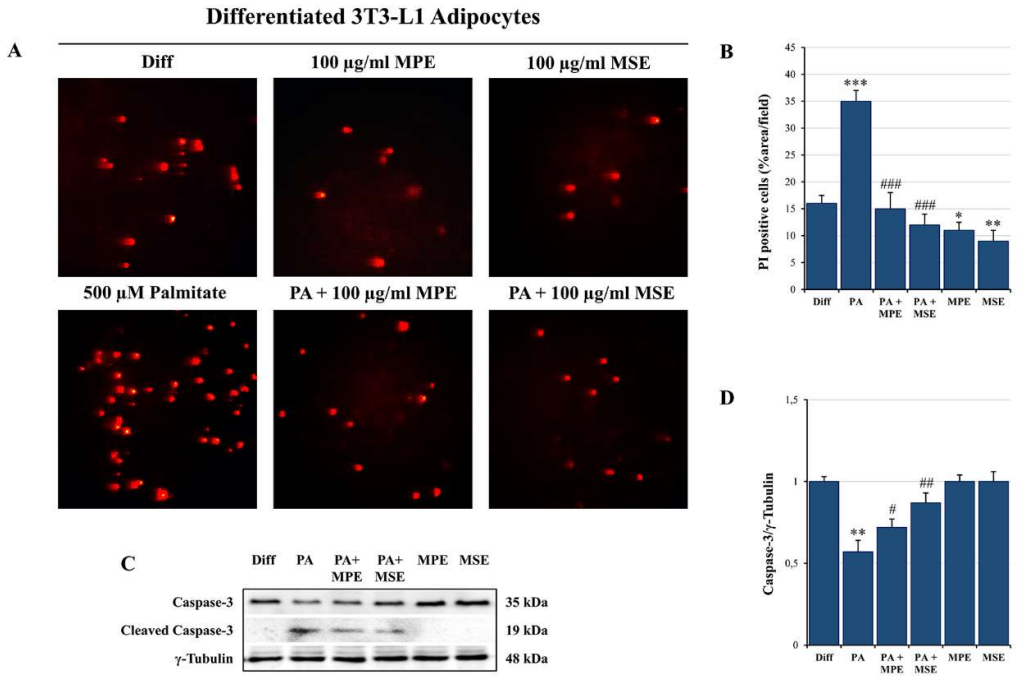

Figure 23. MPE and MSE reduce the cytotoxic effects of PA in 3T3-L1 adipocytes. Propidium iodide (PI) staining of differentiated 3T3-L1 adipocytes treated with 500 µM PA for 48 h in the presence or absence of 100 µg/mL MPE or MSE. (**A**) Representative fluorescence microscopy images were taken at 200× magnification by a Leica microscope equipped with a DC300F camera using a PE filter. (**B**) PI content was ascertained by analysing the percentage area with Image J. (**C**) Western blotting analysis of the procaspase-3 levels. An equal loading of protein was verified by immunoblotting for γ-Tubulin (**D**). The bar graphs represent the means of three independent experiments ± SD. * $p < 0.05$, ** $p < 0.01$ and *** $p < 0.001$ with respect to differentiated 3T3-L1 adipocytes. # $p < 0.05$, ## $p < 0.01$, ### $p < 0.001$ were significant with respect to PA-treated 3T3-L1 adipocytes.

Our data provided evidence that MPE and MSE contain factors capable of exerting ROS scavenger effects during 3T3-L1 adipocyte differentiation. These effects have been correlated with the ability of mango extracts to increase Nrf2, the main antioxidant transcription factor (*Emanuele et al., 2021*), during adipocyte differentiation. In accordance with our previous data, we demonstrated that in PA-treated adipocytes, MPE or MSE increased the level of Nrf2 by about 40% and 60%, respectively (Figure 24). Our data also showed that the levels of MnSOD and HO-1, two scavenger enzymes transcriptionally regulated by Nrf2 (*Li et al., 2019; Emanuele et al., 2021*), markedly increased after treatment with MPE or MSE. In particular, the increase in MnSOD in the presence of MPE or MSE was estimated to be 46% and 50%, while that of HO-1 was estimated to be 12% and 28%, respectively

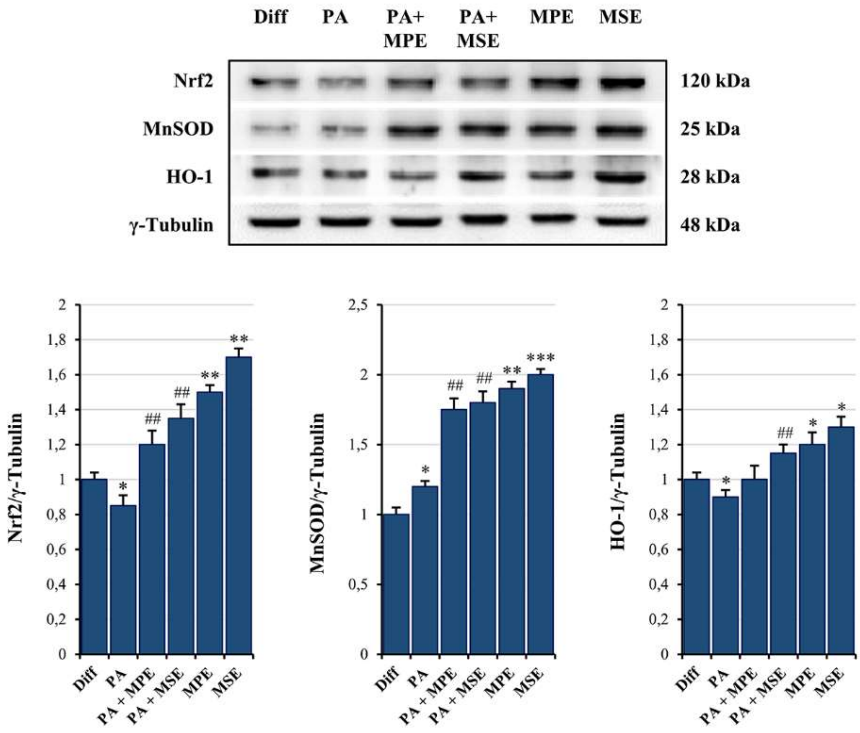

Figure 24. MPE and MSE increase the expression levels of the anti-oxidant molecules. Differentiated 3T3-L1 adipocytes were treated with 500 µM PA for 48 h in the presence or absence of 100 µg/mL MPE or MSE. Cell lysates underwent Western blotting analysis for Nrf2, MnSOD and HO-1. An equal loading (30 µg) of proteins was verified by immunoblotting for γ-Tubulin. The bar graphs represent the means of three independent experiments ±SD. * $p < 0.05$, ** $p < 0.01$ and *** $p < 0.001$ were significant with respect to differentiated 3T3-L1 adipocytes. ## $p < 0.01$ was significant with respect to PA-treated differentiated 3T3-L1 adipocytes.

DISCUSSION

This research project, carried out at the biochemistry section of the Department of Biomedicine, Neuroscience and Advanced Diagnostics (BIND) of the University of Palermo, aimed at investigating the anti-adipogenic and anti-lipogenic effects of peel and seed from mango (*Mangifera Indica* L) cultivated in Sicily in 3T3-L1 cell line.

Sicily is a region of the Southern Italy characterized by a favourable subtropical climate and adapted soils that favour mango cultivation conferring particular properties to the mango orchards (*Lauricella et al., 2017*).

It is worthwhile to mention that, although the chemical investigation of different phytocomponents of mango fruit has been already published by other researchers, in this study we focused on cultivars of mango grown in the Sicilian rural areas to provide an analysis of their specific composition. Indeed, many different factors can affect the plant phytochemical profile including environmental factors, mango variety, course of fruit ripeness (*Manach et al., 2004*). Such an aspect was also reported by Ajila et al. providing evidence that mango peel polyphenolic content strongly depends on fruit maturity stage at the time of harvest, favourable climatic conditions (*Ajila et al., 2007*) as well as growing location (*Lebaka et al., 2021*). In particular, we focused our attention on mango peel and seed, the main waste products of mango processing.

Interestingly, we characterized the polyphenolic profile of mango peel (MPE) and seed extracts (MSE) using HPLC-ESI-MS providing evidence that both these fractions of mango are rich in polyphenols (*Lauricella et al., 2019; Pratelli et al., 2022*). In particular, methyl digallate, methyl gallate, gallic acid and glucosyl gallate were the principal phenolic compounds in MPE. The polyphenols profile of MSE is similar to MPE, with methyl digallate and methyl gallate representing the main components. Notably, these polyphenols are at higher concentration in MSE than MPE. Gallic acid and its derivatives methyl gallate, methyl digallate and glucosyl gallate are plant secondary polyphenolic metabolites which possess strong anti-oxidant effects, due to their ability to act as ROS scavenger (*Daglia et al., 2014*). Interestingly, gallic acid exerts protective effects against obesity-related inflammation by reducing adipocyte size and the inflammation markers, as IL-6, NOS and COX2 (*Tanaka et al., 2020*). Notably, methy gallate has been shown to exert anti-adipogenic effects in 3T3-L1 cells and human subcutaneous adipocytes, by reducing TAGs content and down-regulating adipocyte differentiation markers as C/EBPα, PPARγ and FABP4 (*Rahman et al., 2016*).

On the basis of these observations, our aim was to evaluate the effects of Sicilian mango extracts both on the ability to prevent adipogenesis and on the reduction of toxic effects induced by high doses of palmitate (PA), the main long-chain saturated fatty acid present in the diet (*Murru et al.,*

2022). It is important to note that an accumulation of fat mass in white adipose tissue (WAT) that leads to obesity can result both from an increased differentiation of pre-adipocytes into adipocytes (hyperplasia) and from lipid accumulation in pre-existing adipocytes (hypertrophy) (*Cristancho and Lazar, 2011; Berry et al., 2014*).

Interestingly, our data demonstrated that accumulation of lipid droplets (LDs) and triacylglycerols (TAGs) induced by adipocyte differentiation was largely reduced by treatment of MPE and MSE compared with untreated differentiated 3T3-L1 cells, thus indicating the ability of MPE and MSE to counteract adipogenesis and the consequent lipid accumulation. Notably, the highest dose of MPE and MSE (100 μg/mL) which exerts anti-adipogenic effects did not show toxic effects on both pre-adipocyte and differentiated 3T3-L1 cells. Therefore, inhibition of TAGs accumulation by mango extracts seems to be related to reduction in adipogenesis without cytotoxicity.

To understand the molecular mechanism underlying the anti-adipogenic effect of MPE and MSE, we then focused our attention on some key factors involved in both adipocyte differentiation and lipid metabolism. Adipogenesis is a complex process which is tightly regulated by sequential activation of various transcriptional factors (*Ambele et al., 2020*). PPARγ is a member of the nuclear hormone receptor family expressed in adipose tissue. Its level increases at an early stage of this differentiation process to stimulate the expression of many adipocyte-specific genes which control fatty acid metabolism (*Mota de Sá et al., 2017*). Induction of PPARγ has been shown to be necessary for adipogenesis both *in vitro* and *in vivo* and in many cases sufficient to convert non-adipose cells to adipocyte-like cells (*Rosen et al., 1999; Xiaoru et al., 2016*). Notably, both MPE and MSE significantly reduced the expression level of PPARγ consistent with the decrease in lipid accumulation compared with untreated adipocytes. In addition, the presence of mango extracts during adipogenic differentiation led to a reduction in the levels of FABP4 and GLUT4, two markers of late adipogenesis which are transcriptionally regulated by PPARγ (*Thompson et al., 2004*). In addition, we found that MPE and MSE significantly lowered SREBP-1c, a member of the basic helix-loop-helix-leucine zipper family of transcription factors, which has been shown to have an important role in adipogenesis (*Horton et al., 2002*). Taken together, our data suggest that mango extracts could counteract adipogenesis by down-regulating the expression of PPARγ and SREBP-1c.

In addition to downregulate transcription factors involved in the stimulation of adipogenesis, our results demonstrated that MPE and MSE also up-regulated factors promoting catabolic process in adipocytes. PPARα is another member of PPAR family mainly expressed in liver and muscle cells (*Pyper et al., 2010*) which promotes fatty acid oxidation (*Haemmerle et al., 2011*). Its level is low

in WAT suggesting a limited role for this isotype during adipogenesis (*Pyper et al., 2010*). Of note however, pharmacologic PPARα activators reduced adiposity in mouse models of obesity (*Osinski et al., 2020*). Our data demonstrated that MPE and MSE up-regulated PPARα levels, thus supporting a role of this transcription factor in reducing lipid accumulation in 3T3-L1 adipocytes.

Interestingly, we also demonstrate that MPE and MSE increased the phosphorylated and active form of AMP-activated protein Kinase (AMPK). AMPK is an important regulator of lipid metabolism (*Marin et al., 2017*). Activation of AMPK by phosphorylation increases lipolysis and fatty acid oxidation, while inhibits lipogenesis (*Ahmad et al., 2020*). Our results are in line with the observation that many polyphenols derived from plants and fruits, such as resveratrol, quercetin, genistein and epigallocatechin gallate, effects are able to activate AMPK exerting anti-obesity (*Kim et al., 2016*; *Marin et al., 2017*). This activation seems to be mediated by the increase in AMP levels as a consequence of inhibition of mitochondrial ATP production (*Kim et al., 2016*). Notably, AMPK activation could favors the inhibition of adipogenesis induced by MPE and MSE. This conclusion is in accordance with observation that AMPK negatively regulates white adipocyte differentiation (*Wang et al., 2015*). To this end, 5-Aminoimidazole-4-carboxamide-1-β-D-ribofuranoside (AICAR), an activator of AMPK, led to the inhibition of differentiation in 3T3-L1 pre-adipocytes and such an effect was accompanied by decreased PPARγ and C/EBPα (*Lee et al., 2011*). Moreover, the anti-adipogenic effects of several natural compounds seem to be mediated by AMPK activation (*Choi et al., 2015; Wang et al., 2017; Han et al., 2018*).

In concomitance with activation of AMPK, we observed an increase in the phosphorylated and inactive form of Acetyl-CoA C arboxylase (ACC). ACC is the key rate-limiting enzyme in the first stage of fatty acid synthesis and it is inactivated via phosphorylation by AMPK (*Cho et al., 2010*; *Fullerton et al., 2013*) leading to the reduction of fatty acid synthesis (*Galic et al., 2018*). Notably, we observed that the addition of compound C, a specific AMPK inhibitor, counteracted the effects of MPE and MSE on phosphorylation of both AMPK and ACC, thus demonstrating the ability of mango extracts to activate AMPK and suggesting a role of this factor in inhibiting lipogenesis and adipogenesis in 3T3-L1 cells.

Both in rodents and in humans, excessive fat consumption in the diet is associated with fat accumulation and overweight, representing an important health risk (*Hill et al., 2000; Raatz et al., 2017; Hu et al., 2018*). However, evidences shown that the quality of dietary fats induces differential lipid storage. In fact, a high consumption of saturated long-chain fatty acids (SLFAs), such as PA, is associated with obesity (*Palomer et al., 2018*), conversely a diet rich in monounsaturated (MUFAs) and polyunsaturated fatty acids (PUFA), as oleic or linoleic acid, or

medium-chain fatty acids (MFAs), including caprylic acid, capric acid and lauric acid, may have beneficial effects on body weight and obesity (*Ibrahim et al., 2021*). This can be explained considering that certain fatty acids (FAs) are more likely to be stored in (AT) versus being oxidate for energy. In particular, SLFAs have lower oxidation rate than MUFAs, PUFAs and MFAs, leading to increased fat storage in WAT (*DiNicolantonio and O'Keefe, 2017*). Fat accumulation into AT due to high consume of SLFAs produces hypertrophic and dysfunctional adipocytes, leading to a state of chronic low-grade inflammation (*Calder, 2011*) that contributes to the development of obesity-related diseases (*Russo et al., 2021*).

In our study we also aimed at investigating whether MPE and MSE could ameliorate lipotoxicity induced in mature 3T3-L1 adipocytes by high doses of PA. Here, we provided evidence that MPE and MSE are capable of lowering adipocyte hypertrophy induced by PA treatment demonstrating that MPE and MSE reduced PA-induced fat accumulation, as evidenced by the decrease in LDs and TAGs content in differentiated 3T3-L1 adipocytes co-treated with PA and MPE or MSE.

The ability of MPE and MSE to reduce lipid content in PA-treated adipocytes results from both stimulation of lipolysis and inhibition of lipogenesis. PPARγ has been also reported to play a critical role in adipocyte hypertrophy under high fat diets (*Guo et al., 2020*). We provided evidence that the PPARγ level increased under PA-treatment in differentiated 3T3-L1 adipocytes. Notably, this effect was markedly counteracted by the addition of MPE or MSE to PA-treated adipocytes. These results are in line with our previous data demonstrating that MPE and MSE counteract 3T3-L1 adipocyte differentiation by reducing the level of PPARγ and its target FABP4.

Furthermore, as demonstrated during adipocyte differentiation, our data showed that MPE and MSE significantly enhanced the phosphorylation of AMPK and its substrate ACC in both controls and PA-treated adipocytes, thus suggesting an effective role of AMPK activation in reducing lipogenesis induced by MPE and MSE. As previously reported, HPLC-ESI-MS characterization of MPE and MSE demonstrated the presence of different polyphenols, among which methyl digallate and methyl gallate are the most represented components *(Lauricella et al., 2019; Pratelli et al., 2022).* These compounds could be responsible for the anti-lipogenic effects of the mango extracts. In line with this conclusion, Fang et al. demonstrated that gallotannin derivatives from mango counteract adipogenesis by activating AMPK (*Fang et al., 2018*). In addition, Lu, et al. showed that gallic acid reduced lipogenesis and improved liver steatosis by activating AMPK. This effect could result by a direct interaction of gallic acid with AMPKα/β subunits, as evidenced by computational docking analysis (*Lu et al., 2022*). Finally, mangiferin, a polyphenol derived from Mangifera indica promotes browning of adipocytes by activating AMPK (*Rahman and Kim, 2020*).

In this study, we also provided evidence that MPE and MSE increased the level of the phosphorylated and active forms of hormone-sensitive lipase (HSL), the key lipase activating lipolysis of TAGs in adipocytes, in PA-treated adipocytes (*Grabner at al., 2021*). Different lipolytic agents activate HSL by increasing cAMP levels, with the consequent activation of cAMP-dependent protein kinase (protein kinase A; PKA). This enzyme in turn phosphorylates and activates HSL (*Braun et al., 2018*). MSE and MPE could activate HSL because of their content of polyphenols. In line of this conclusion, it has been shown that different polyphenols are able to increase cAMP by inhibiting phosphodiesterase, the enzyme that degrades cAMP (*Rouse et al., 2014; Rauf et al., 2017*).

A high content of SLFAs has been associated with lipotoxicity in adipocytes as a consequence of endoplasmic reticulum (ER) stress induction (*Fernandes-da-Silva et al., 2021*). Notably, when present at a high level, PA is metabolized into saturated diacylglycerols (DAGs) and saturated lysophosphatidylcholine. These PA-derived metabolites accumulate in the ER, causing destructive changes in its structure and the activation of ER stress sensors (*Korbecki and Bajdak-Rusinek, 2019*). In line with these observations, we demonstrated that PA treatment enhanced the ER stress markers GRP78, PERK and CHOP as well as activated JNK by increasing its phosphorylated form in differentiated 3T3-L1 adipocytes. ER stress is a protective cellular mechanism that initiates the unfolded protein response (UPR) to restore cellular homeostasis; however, in severe ER stress, the adaptive response fails and apoptotic cell death is induced (*Tabas and Ron, 2011*). In obese animals, elevated ER stress is present in different organs (*Kawasaki et al., 2012; Yilmaz, 2017*). In this condition, ER stress-induced UPR activates JNK, which in turn promotes apoptosis by inhibiting the mitochondrial respiratory chain and activating caspases (*Win et al., 2014*). Our data confirmed that PA causes lipotoxicity in differentiated adipocytes, as evidenced by cell viability reduction, increased PI-positive cells and caspase-3 activation. Interestingly, MPE and MSE counteracted PA-induced ER stress by lowering all ER stress markers, GRP78, PERK and CHOP, as well as p-JNK. Concomitantly, mango extracts restored cell viability, reduced PI-positive cells and the activation of caspase-3 induced by PA treatment, thus suggesting their protective effects against lipotoxicity induced by high levels of SFAs in adipocytes.

Reactive oxygen species (ROS) generation has been observed during adipogenesis and seems to promote adipocyte differentiation (*De Villiers et al., 2018*). In particular, it has been shown that ROS increased PPARγ in early pre-adipocyte differentiation and promotes mitotic clonal expansion of pre-adipocytes (*Lee et al., 2009*). In addition, ROS production has been correlated with enhanced mitochondrial biogenesis and metabolism during adipogenesis (*Wang et al., 2015*). To support this

conclusion, it has been shown that mitochondrial-targeted antioxidants inhibited adipocyte differentiation, while the addition of hydrogen peroxide restored it (*Tormos et al., 2011*). Notably, our results showed that both MPE and MSE are capable of counteracting ROS production during 3T3-L1 adipocyte differentiation. This is in line with the observation that mango extracts possess a strong scavenger activity, as demonstrated by the ability of MPE and MSE to significantly inhibit DPPH activity.

Furthermore, we demonstrated that PA treatment increased in 3T3-L1 adipocytes the level of ROS, as evidenced by staining adipocytes with H_2DCFDA. This finding is in line with previous reports demonstrating that high levels of FAs increase oxidative stress in adipocytes (*Wang et al., 2017*). It has been reported that ceramide and DAG, which are fatty acid-derived lipid metabolites, activate NADPH oxidase (NOX), enhancing the ROS level in adipocytes (*Brookheart et al., 2009*). In addition, dysfunction of the mitochondrial respiratory chain in obesity can amplify oxidative stress and inflammation (*de Mello et al., 2018*). ROS production has been shown to activate JNK, which mediates activation of NF-κB and AP-1 (*Nakano et al., 2006*) with the consequent enhanced expression of pro-inflammatory cytokines, such as IL-6 and TNFα. Notably, we showed that the production of ROS in PA-treated adipocytes was markedly reduced by the addition of MPE and MSE. This effect could be a consequence of the high content of polyphenols in mango extracts. This is in line with the observation that methyl-gallate, the main component of MPE and MSE, protects the cells against oxidative damage through its ROS scavenger ability (*Crispo et al., 2010*).

Nrf2 is the master regulator of the cellular antioxidant response, regulating the expression of a battery of genes encoding for antioxidant and detoxifying factors (*Dovinova et al., 2020; Emanuele et al., 2021; Ngo and Duennwald, 2022*). Under normal condition, kelch-like ECH-associated protein 1 (Keap1) binds Nrf2 in an inactive complex, leading to its ubiquitin-proteasomal degradation. Under oxidative stress condition, ROS promote oxidation of Keap1 in a critical cysteine residue, promoting its dissociation from Nrf2 (*Wang et al., 2017*). Thus, Nrf2 traslocates into the nucleus where up-regulate a panel of antioxidant genes, including superoxide dismutase (MnSOD) and Heme Oxygenase 1 (HO-1). Our data showed that during adipocyte differentiation MPE or MSE upregulated Nrf2 and its transcriptional targets MnSOD and HO-1. Moreover, MPE and MSE increase Nrf2 and its targets MnSOD and HO-1 also in adipocytes co-treated with PA and MSE or MPE. Thus, the induction of these anti-oxidant enzymes could explain MPE- and MSE-induced ROS reduction in adipocytes. Several reports suggest that different natural compounds exert anti-oxidant effects by activating Nrf2 through different mechanisms including interaction with cysteine residues on Keap1, disruption of Nrf2/Keap1 interaction or Nrf2 phosphorylation.

Indeed, the activation of Nrf2 also has been reported in different dietary polyphenols, including resveratrol, gallic acid and caffeic acid (*Ooi et al., 2018; Zhou et al., 2019*).

Notably, Nrf2 and AMPK has been shown to be functionally connected and collaborate to reduce oxidative stress. Induction of AMPK by natural compounds (*Chen et al., 2018*) or chemical activators (*Kong et al., 2021*) leads in turn to activation via phosphorylation of Nrf2. This has been correlated with a reduction in inflammation in several cell types, as adipocytes, macrophages and pancreatic cells (*Vasileva et al., 2020; Kong et al., 2021*). Thus, MPE and MSE could explain antioxidant effects by promoting activation of both AMPK and Nrf2 in 3T3-L1 adipocytes.

In fact, the lowering in ROS content induced by MPE and MSE, not only could be a consequence of the up-regulation of Nrf2 and its transcriptional targets MnSOD and HO-1 (*Lauricella et al., 2019; Pratelli et al., 2022*), but also MPE and MSE could reduce ROS levels and oxidative stress in adipocytes by activating AMPK. In line with this hypothesis, the deregulated activity of AMPK has been associated with an inflammatory state in *in vivo* models of obesity and obese patients (*Gauthier et al., 2011*). The activation of AMPK signaling also has been shown to protect against oxidative stress by suppressing NOX (*Huang et al., 2019*) and mitochondrial dysfunction (*Wang et al., 2010*).

CONCLUSIONS

In conclusion, our results demonstrated that MPE and MSE exert anti-adipogenic and anti-lipogenic effects in 3T3-L1 cells. In particular, mango extracts are capable of counteracting the differentiation of 3T3-L1 pre-adipocytes, by down-regulating adipogenic markers such as PPARγ, FABP4, GLUT4, Adipsin, and SREBP-1c. Furthermore, MPE and MSE increased the phosphorylated and active form of AMPK resulting in inhibition of ACC, the key enzyme of fatty acid synthesis (Figure 25).

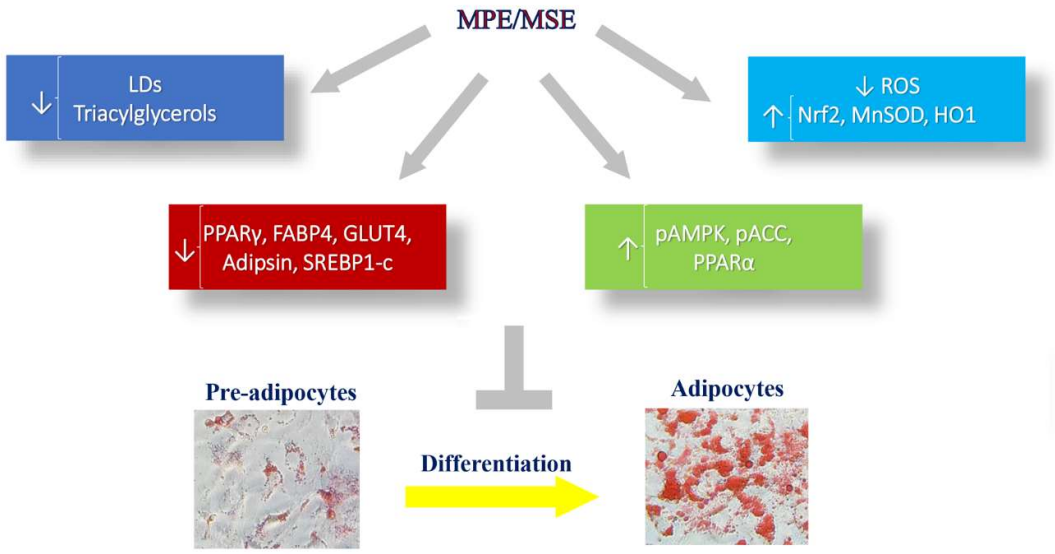

Figure 25. The addition of MPE and MSE to the differentiation medium reduced 3T3-L1 adipocytes differentiation, as demonstrated by the loss of LDs and TGs. The anti-adipogenic and anti-lipogenic effects of MPE and MSE seem to be correlated with the ability of mango extracts to reduce PPARγ and SREBP-1c and their targets, as well as to increase AMPK and PPARα. MPE and MSE also reduce ROS content produced during adipocyte differentiation, by activating Nrf2 and its downstream targets.

Notably, MPE and MSE were also capable of reducing hypertrophy induced in mature 3T3-L1 adipocytes by high levels of PA. The decrease in LDs and TAGs levels in adipocytes co-treated with PA and MPE or MSE, seems to be a consequence of inhibition of lipogenic factors as PPARγ and ACC, and activation of lipolytic factors as AMPK and HSL. MPE and MSE also counteract PA-induced lipotoxicity in mature adipocytes. This effect resulted from a reduction of PA-induced ER-stress as well as ROS production (Figure 26).

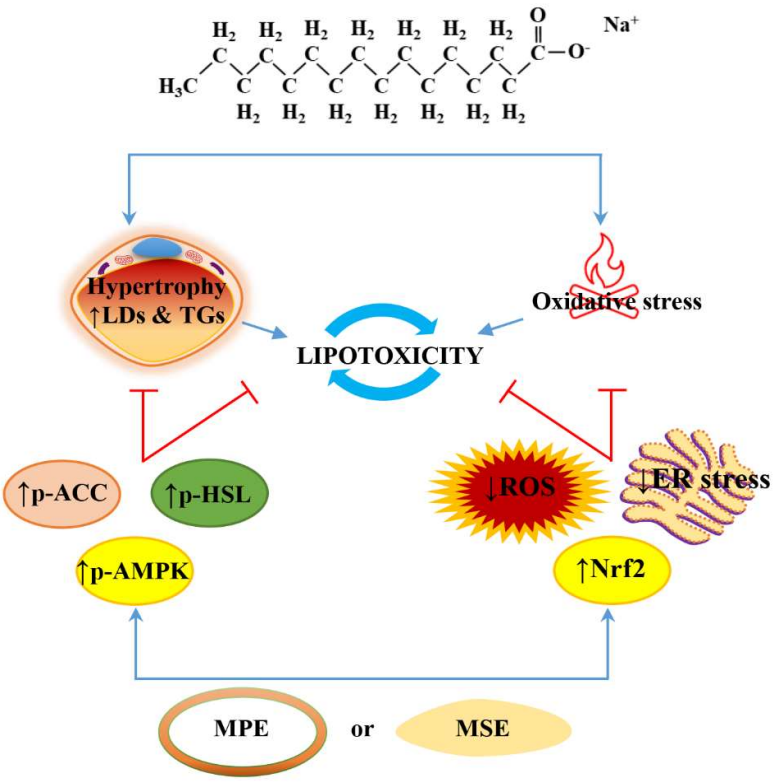

Figure 26. MPE and MSE counteracted lipotoxicity induced by PA in differentiated adipocytes. MPE and MSE lowered fat accumulation induced by high doses of PA in differentiated 3T3-L1 adipocytes, as demonstrated by the reduction of LDs and TAGs contents. These anti-lipogenic effects seem to be mediated by the activation of HSL and inhibition of ACC as a result of AMPK activation. MPE and MSE also counteracted PA-induced ER stress and ROS increase in adipocytes. The anti-oxidative effects could be ascribed to the activation of the Nrf2/OH-1/MnSOD pathway. Reduced fat content and oxidative stress production could protect the cells from PA-induced cytotoxicity.

HPLC-ESI-MS characterization of the polyphenolic profile of MPE and MSE provided evidence that both mango extracts are a good source of polyphenols which can explain the anti-oxidant and anti-adipogenic effect of these mango fractions. In light of the chemical data, we wondered about the putative phytochemicals responsible for the effect observed in 3T3-L1 adipocytes exposed to MPE or MSE treatment. A possible candidate seems to be methyl gallate. This is a phenolic compound that is the most represented phytochemical in our tested mango extracts. Our hypothesis is also sustained by experimental evidence reported by Roh et al. demonstrating that methyl gallate is able to counteract the lipid accumulation in 3T3-L1 cells and could represent a good candidate as an anti-obesity agent (*Roh et al., 2012*). However, we cannot exclude that the ability of MPE and MSE to counteract PA lipotoxicity, as well as hypertrophy and ER stress induced by PA exposure could be ascribed to a combined or synergistic effect among the different phytochemicals identified in mango. To better elucidate this aspect, in our future studies we will test mango phytochemicals as compounds alone and their combinations on 3T3-L1 cells. These data offer novel perspectives

suggesting that MPE and MSE may be associated with the reduced metabolic dysfunction of adipose tissue induced by high levels of SLFAs. Thus, bio-waste products from mango, such as peel and seed, could be used as a potential supplement to improve the nutritional value of food with health benefits in the prevention of overweight, obesity and related diseases.

ACKNOWLEDGMENTS

I thank my Tutor, Prof.ssa Marianna Lauricella, and my co-Tutor, Prof.ssa Daniela Carlisi, for loving-kindness and the precious support in carrying out this research project. Thanks also to all the members of the Biochemistry laboratory, for the great affection shown to me in these years of PhD course, and not only.

Thanks to all the members of the Prof. Martin Gericke's research group of the University of Leipzig, for the helpfulness and friendship shown to me throughout my period of stay in Leipzig. Thanks for making me feel at home.

A special and immense thanks to my Family and Friends, for their love and for having always believed in me.

……. to My Grandmother Gina …….

REFERENCES

Aaseth, J.; Ellefsen, S.; Alehagen, U.; Sundfør, T.M.; Alexander, J. Diets and drugs for weight loss and health in obesity - An update. Biomed Pharmacother. **2021**, 140, 111789.

Ahmad, B.; Serpell, C.J.; Fong, I.L.; Wong, E.H. Molecular Mechanisms of Adipogenesis: The Anti-adipogenic Role of AMP-Activated Protein Kinase. Front Mol Biosci. **2020**, 7, 76.

Ajila, C.M.; Bhat, S.G.; Prasada Rao, U.J.S. Valuable Components of Raw and Ripe Peels from Two Indian Mango Varieties. Food Chem. **2007**, 102, 1006-1011.

Ambele, M.A.; Dhanraj, P.; Giles, R.; Pepper, M.S. Adipogenesis: A Complex Interplay of Multiple Molecular Determinants and Pathways. Int. J. Mol. Sci. **2020**, 21, 4283.

Amri, E.; Bertrand, B.; Ailhaud, G.; Grimaldi, P. Regulation of Adipose Cell Differentiation. I. Fatty Acids Are Inducers of the AP2 Gene Expression. J. Lipid Res. **1991**, 32, 1449-1456.

Angelidi, A.M.; Belanger, M.J.; Kokkinos, A.; Koliaki, C.C.; Mantzoros, C.S. Novel Noninvasive Approaches to the Treatment of Obesity: From Pharmacotherapy to Gene Therapy. Endocr Rev. **2022**, 43. 507-557.

Ansary, J.; Forbes-Hernández, T.Y.; Gil, E.; Cianciosi, D.; Zhang, J.; Elexpuru-Zabaleta, M.; Simal-Gandara, J.; Giampieri, F.; Battino, M. Potential Health Benefit of Garlic Based on Human Intervention Studies: A Brief Overview. Antioxidants **2020**, 9, 619.

Apovian, C.M. Obesity: definition, comorbidities, causes, and burden. Am J Manag Care. **2016**, 22, s176-85.

Arshad, F.; Umbreen, H.; Aslam, I.; Hameed, A.; Aftab, K.; Al-Qahtani, W.H.; Aslam, N.; Noreen, R. Therapeutic Role of Mango Peels in Management of Dyslipidemia and Oxidative Stress in Obese Females. Biomed. Res. Int. **2021**, 2021, 3094571.

Avgerinos, K.I.; Spyrou, N.; Mantzoros, C.S.; Dalamaga, M. Obesity and cancer risk: Emerging biological mechanisms and perspectives. Metabolism **2019**, 92, 121-135.

Bahmad, H.F.; Daouk, R.; Azar, J.; Sapudom, J.; Teo, J.C.M.; Abou-Kheir, W.; Al-Sayegh, M. Modeling Adipogenesis: Current and Future Perspective. Cells. **2020**, 9, 2326.

Baldini, F.; Fabbri, R.; Eberhagen, C.; Voci, A.; Portincasa, P.; Zischka, H.; Vergani, L. Adipocyte hypertrophy parallels alterations of mitochondrial status in a cell model for adipose tissue dysfunction in obesity. Life Sci. **2021**, 265, 118812.

Barnes, A.S. The epidemic of obesity and diabetes: Trends and treatments. Tex. Heart Inst. J. **2011**, 38, 142-144.

Batsis, J.A.; Huyck, K.L.; Bartels, S.J. Challenges with the Medicare obesity benefit: practical concerns & proposed solutions. J Gen Intern Med. **2015**, 30, 118-22.

Ben-Dror, K.; Birk, R. Oleic acid ameliorates palmitic acid-induced ER stress and inflammation markers in naive and cerulein-treated exocrine pancreas cells. Biosci. Rep. **2019**, 39, BSR20190054.

Berry, D.C.; Stenesen, D.; Zeve, D.; Graff, J.M. The developmental origins of adipose tissue. Development. **2013**, 140, 3939-3949.

Berry, R.; Jeffery, E.; Rodeheffer, M.S. Weighing in on Adipocyte Precursors. Cell Metab. **2014**, 19, 8-20.

Blüher, M. Obesity: global epidemiology and pathogenesis. Nat Rev Endocrinol. **2019**, 15, 288-298.

Booth, A.; Magnuson, A.; Fouts, J.; Foster, M.T. Adipose tissue: an endocrine organ playing a role in metabolic regulation. Horm Mol Biol Clin Investig. **2016**, 26, 25-42.

Braun, K.; Oeckl, J.; Westermeier, J.; Li, Y.; Klingenspor, M. Non-adrenergic control of lipolysis and thermogenesis in adipose tissues. J Exp Biol. **2018**, 221, jeb165381.

Brookheart, R.T.; Michel, C.I.; Schaffer, J.E. As a matter of fat. Cell Metab. **2009**, 10, 9-12.

Bu, S.; Yuan, C.Y.; Xue, Q.; Chen, Y.; Cao, F. Bilobalide Suppresses Adipogenesis in 3T3-L1 Adipocytes via the AMPK Signaling Pathway. Molecules **2019**, 24, 3503.

Calder, P.C. Fatty acids and inflammation: The cutting edge between food and pharma. Eur. J. Pharmacol. **2011**, 668 (Suppl. S1), S50-S58.

Celesia, A.; Morana, O.; Fiore, T.; Pellerito, C.; D'Anneo, A.; Lauricella, M.; Carlisi, D.; De Blasio, A.; Calvaruso, G.; Giuliano, M.; Emanuele, S. ROS-Dependent ER Stress and Autophagy Mediate the Anti-Tumor Effects of Tributyltin (IV) Ferulate in Colon Cancer Cells. Int. J. Mol. Sci. **2020**, 21, 8135.

Cernigliaro, C.; D'Anneo, A.; Carlisi, D.; Giuliano, M.; Marino Gammazza, A.; Barone, R.; Longhitano, L.; Cappello, F.; Emanuele, S.; Distefano, A.; et al. Ethanol-Mediated Stress Promotes Autophagic Survival and Aggressiveness of Colon Cancer Cells via Activation of Nrf2/HO-1 Pathway. Cancers **2019**, 11, 505.

Chait, A.; den Hartigh, L.J. Adipose Tissue Distribution, Inflammation and Its Metabolic Consequences, Including Diabetes and Cardiovascular Disease. Front Cardiovasc Med. **2020**, 7, 22.

Chen, X.; Jiang, Z.; Zhou, C.; Chen, K.; Li, X.; Wang, Z.; Wu, Z.; Ma, J.; Ma, Q.; Duan, W. Activation of Nrf2 by Sulforaphane Inhibits High Glucose-Induced Progression of Pancreatic Cancer via AMPK Dependent Signaling. Cell. Physiol. Biochem. **2018**, 50, 1201-1215.

Cho, Y.S.; Lee, J.I.; Shin, D.; Kim, H.T.; Jung, H.Y.; Lee, T.G.; Kang, L.W.; Ahn, Y.J.; Cho, H.S.; Heo, Y.S. Molecular mechanism for the regulation of human ACC2 through phosphorylation by AMPK. Biochem. Biophys. Res. Commun. **2010**, 391, 187-192.

Choe, S.S.; Huh, J.Y.; Hwang, I.J.; Kim, J.I.; Kim, J.B. Adipose Tissue Remodeling: Its Role in Energy Metabolism and Metabolic Disorders. Front Endocrinol (Lausanne). **2016**, 7, 30.

Choi, H.-S.; Jeon, H.-J.; Lee, O.-H.; Lee, B.-Y. Dieckol, a Major Phlorotannin in Ecklonia Cava, Suppresses Lipid Accumulation in the Adipocytes of High-Fat Diet-Fed Zebrafish and Mice: Inhibition of Early Adipogenesis via Cell-Cycle Arrest and AMPK Activation. Mol. Nutr. Food Res. **2015**, 59, 1458-1471.

Choi, S.-S.; Park, J.; Choi, J.H. Revisiting PPARγ as a Target for the Treatment of Metabolic Disorders. BMB Rep. **2014**, 47, 599-608.

Chooi, Y.C.; Ding, C.; Magkos, F. The Epidemiology of Obesity. Metab. Clin. Exp. **2019**, 92, 6-10.

Chouchani, E.T.; Kajimura, S. Metabolic adaptation and maladaptation in adipose tissue. Nat Metab. **2019**, 1, 189-200.

Cinti, S. Pink Adipocytes. Trends Endocrinol Metab. **2018**, 29, 651-666.

Cinti, S. The adipose organ at a glance. Dis Model Mech. **2012**, 5, 588-594.

Coelho, M.; Oliveira, T.; Fernandes, R. Biochemistry of adipose tissue: an endocrine organ. Arch Med Sci. **2013**, 9, 191-200.

Colquitt, J. L.; Pickett, K.; Loveman, E.; Frampton, G. K. Surgery for weight loss in adults. Cochrane Database of Systematic Reviews. **2014**, 8, CD003641.

Conway, B.; Rene, A. Obesity as a Disease: No Lightweight Matter. Obes. Rev. **2004**, 5, 145-151.

Crewe, C.; Zhu, Y.; Paschoal, V.A.; Joffin, N.; Ghaben, A.L.; Gordillo, R.; Oh, D.Y.; Liang, G.; Horton, J.D.; Scherer, P.E. SREBP-regulated adipocyte lipogenesis is dependent on substrate availability and redox modulation of mTORC1. JCI Insight. **2019**, 5, e129397.

Crispo, J.A.; Piche, M.; Ansell, D.R.; Eibl, J.K.; Tai, I.T.; Kumar, A.; Ross, G.M.; Tai, T.C. Protective effects of methyl gallate on H2O2-induced apoptosis in PC12 cells. Biochem. Biophys. Res. Commun. **2010**, 393, 773-778.

Cristancho, A.G.; Lazar, M.A. Forming Functional Fat: A Growing Understanding of Adipocyte Differentiation. Nat. Rev. Mol. Cell Biol. **2011**, 12, 722-734.

Czech, M.P. Mechanisms of insulin resistance related to white, beige, and brown adipocytes. Mol Metab. **2020**, 34, 27-42.

Daglia, M.; Lorenzo, A.D.; Nabavi, S.F.; Talas, Z.S.; Nabavi, S.M. Polyphenols: Well Beyond The Antioxidant Capacity: Gallic Acid and Related Compounds as Neuroprotective Agents: You Are What You Eat! Curr. Pharm. Biotechnol. **2014**, 15, 362-372.

De Blasio, A.; D'Anneo, A.; Lauricella, M.; Emanuele, S.; Giuliano, M.; Pratelli, G.; Calvaruso, G.; Carlisi, D. The Beneficial Effects of Essential Oils in Anti-Obesity Treatment. Int. J. Mol. Sci. **2021**, 22, 11832.

de Mello, A.H.; Costa, A.B.; Engel, J.D.G.; Rezin, G.T. Mitochondrial dysfunction in obesity. Life Sci. **2018**, 192, 26-32.

De Villiers, D.; Potgieter, M.; Ambele, M.A.; Adam, L.; Durandt, C.; Pepper, M.S. The Role of Reactive Oxygen Species in Adipogenic Differentiation. Adv. Exp. Med. Biol. **2018**, 1083, 125-144.

DiNicolantonio, J.J.; O'Keefe, J.H. Good Fats versus Bad Fats: A Comparison of Fatty Acids in the Promotion of Insulin Resistance, Inflammation, and Obesity. Mo Med. **2017**, 114, 303-307.

Dovinova, I.; Kvandova, M.; Balis, P.; Gresova, L.; Majzunova, M.; Horakova, L.; Chan, J.Y.; Barancik, M. The role of Nrf2 and PPARgamma in the improvement of oxidative stress in hypertension and cardiovascular diseases. Physiol. Res. **2020**, 69 (Suppl.S4), S541-S553.

Driskell, R.R.; Jahoda, C.A.; Chuong, C.M.; Watt, F.M.; Horsley, V. Defining dermal adipose tissue. Exp Dermatol. **2014**, 23, 629-631.

Emanuele, S.; Celesia, A.; D'Anneo, A.; Lauricella, M.; Carlisi, D.; De Blasio, A.; Giuliano, M. The Good and Bad of Nrf2: An Update in Cancer and New Perspectives in COVID-19. Int. J. Mol. Sci. **2021**, 22, 7963.

Engin, A.B. What Is Lipotoxicity? Adv. Exp. Med. Biol. **2017**, 960, 197-220.

Fang, C.; Kim, H.; Barnes, R.C.; Talcott, S.T.; Mertens-Talcott, S.U. Obesity-Associated Diseases Biomarkers Are Differently Modulated in Lean and Obese Individuals and Inversely Correlated to Plasma Polyphenolic Metabolites After 6 Weeks of Mango (*Mangifera indica* L.) Consumption. Mol. Nutr. Food Res. **2018**, 62, 1800129.

Fang, C.; Kim, H.; Noratto, G.; Sun, H.; Talcott, S.T.; Mertens-Talcott, S.U. Gallotannin derivatives from mango (*Mangifera indica* L.) suppress adipogenesis and increase thermogenesis in 3T3-L1 adipocytes in part through the AMPK pathway. J. Funct. Foods **2018**, 46, 101-109.

Fernandes-da-Silva, A.; Miranda, C.S.; Santana-Oliveira, D.A.; Oliveira-Cordeiro, B.; Rangel-Azevedo, C.; Silva-Veiga, F.M.; Martins, F.F.; Souza-Mello, V. Endoplasmic reticulum stress as the basis of obesity and metabolic diseases: Focus on adipose tissue, liver, and pancreas. Eur. J. Nutr. **2021**, 60, 2949-2960.

Fratianni, A.; Adiletta, G.; Di Matteo, M.; Panfili, G.; Niro, S.; Gentile, C.; Farina, V.; Cinquanta, L.; Corona, O. Evolution of Carotenoid Content, Antioxidant Activity and Volatiles Compounds in Dried Mango Fruits (*Mangifera Indica* L.). Foods. **2020**, 9, 1424;

Fritsche, K.L. The science of fatty acids and inflammation. Adv. Nutr. **2015**, 6, 293S-301S.

Fullerton, M.D.; Galic, S.; Marcinko, K.; Sikkema, S.; Pulinilkunnil, T.; Chen, Z.P.; O'Neill, H.M.; Ford, R.J.; Palanivel, R.; O'Brien, M.; et al. Single phosphorylation sites in Acc1 and Acc2 regulate lipid homeostasis and the insulin-sensitizing effects of metformin. Nat. Med. **2013**, 19, 1649-1654.

Fullerton, M.D.; Galic, S.; Marcinko, K.; Sikkema, S.; Pulinilkunnil, T.; Chen, Z.; O'Neill, H.M.; Ford, R.J.; Palanivel, R.; O'Brien, M.; et al. Single Phosphorylation Sites in Acc1 and Acc2 Regulate Lipid Homeostasis and the Insulin–Sensitizing Effects of Metformin. Nat. Med. **2013**, 19, 1649-1654.

Furukawa, S.; Fujita, T.; Shimabukuro, M.; Iwaki, M.; Yamada, Y.; Nakajima, Y.; Nakayama, O.; Makishima, M.; Matsuda, M.; Shimomura, I. Increased oxidative stress in obesity and its impact on metabolic syndrome. J. Clin. Investig. **2004**, 114, 1752-1761.

Galic, S.; Loh, K.; Murray-Segal, L.; Steinberg, G.R.; Andrews, Z.B.; Kemp, B.E. AMPK signaling to acetyl-CoA carboxylase is required for fasting- and cold-induced appetite but not thermogenesis. eLife **2018**, 7, e32656.

Galic, S.; Oakhill, J.S.; Steinberg, G.R. Adipose tissue as an endocrine organ. Mol. Cell Endocrinol. **2010**, 316, 129-139.

Gallagher, E.J.; LeRoith, D. Obesity and Diabetes: The Increased Risk of Cancer and Cancer-Related Mortality. Physiol Rev. **2015**, 95, 727-48.

García-Rivera, D.; Delgado, R.; Bougarne, N.; Haegeman, G.; Vanden Berghe, W. Gallic Acid Indanone and Mangiferin Xanthone Are Strong Determinants of Immunosuppressive Anti-Tumour Effects of Mangifera Indica L. Bark in MDA-MB231 Breast Cancer Cells. Cancer Lett. **2011**, 305, 21–31.

Gauthier, M.S.; O'Brien, E.L.; Bigornia, S.; Mott, M.; Cacicedo, J.M.; Xu, X.J.; Gokce, N.; Apovian, C.; Ruderman, N. Decreased AMP-activated protein kinase activity is associated with increased inflammation in visceral adipose tissue and with whole-body insulin resistance in morbidly obese humans. Biochem. Biophys. Res. Commun. **2011**, 404, 382-387.

GBD 2017 Diet Collaborators. Health effects of dietary risks in 195 countries, 1990-2017: a systematic analysis for the Global Burden of Disease Study 2017. Lancet. **2019**, 393, 1958-1972.

Gentile, C.; Di Gregorio, E.; Di Stefano, V.; Mannino, G.; Perrone, A.; Avellone, G.; Sortino, G.; Inglese, P.; Farina, V. Food quality and nutraceutical value of nine cultivars of mango (*Mangifera indica* L.) fruits grown in Mediterranean subtropical environment. Food Chem. **2019**, 277, 471-479.

Ghesmaty Sangachin M, Cavuoto LA, Wang Y. Use of various obesity measurement and classification methods in occupational safety and health research: a systematic review of the literature. BMC Obes. 2018 Nov 1;5:28.

Giordano, A.; Smorlesi, A.; Frontini, A.; Barbatelli, G.; Cinti, S. MECHANISMS IN ENDOCRINOLOGY: White, brown and pink adipocytes: the extraordinary plasticity of the adipose organ. Eur. J. Endocrinol. **2014**, 170, 159-171.

Gomes Natal, D.I.; de Castro Moreira, M.E.; Soares Miliao, M.; Dos Anjos Benjamin, L.; de Souza Dantas, M.I.; Machado Rocha Ribeiro, S.; Stampini Duarte Martino, H. Uba mango juices intake decreases adiposity and inflammation in high-fat diet-induced obese Wistar rats. Nutrition **2016**, 32, 1011-1018.

Gómez-Caravaca, A.M.; López-Cobo, A.; Verardo, V.; Segura-Carretero, A.; Fernández-Gutiérrez, A. HPLC-DAD-q-TOF-MS as a powerful platform for the determination of phenolic and other polar compounds in the edible part of mango and its by-products (peel, seed, and seed husk): Liquid phase separations. ELECTROPHORESIS **2016**, 37, 1072-1084.

Gondi, M.; Prasada Rao, U.J.S. Ethanol extract of mango (*Mangifera indica* L.) peel inhibits α-amylase and α-glucosidase activities, and ameliorates diabetes related biochemical parameters in streptozotocin (STZ)-induced diabetic rats. J. Food Sci. Technol. **2015**, 52, 7883-7889.

Govers, R. Molecular Mechanisms of GLUT4 Regulation in Adipocytes. Diabetes Metab. **2014**, 40, 400-410.

Grabner, G.F.; Xie, H.; Schweiger, M.; Zechner, R. Lipolysis: cellular mechanisms for lipid mobilization from fat stores. Nat Metab. **2021**, 3, 1445-1465.

Green, H.; Meuth, M. An Established Pre-Adipose Cell Line and Its Differentiation in Culture. Cell **1974**, 3, 127-133.

Guo, F.; Xu, S.; Zhu, Y.; Zheng, X.; Lu, Y.; Tu, J.; He, Y.; Jin, L.; Li, Y. PPARgamma Transcription Deficiency Exacerbates High-Fat Diet-Induced Adipocyte Hypertrophy and Insulin Resistance in Mice. Front Pharmacol. **2020**, 11, 1285.

Habinowski, S.A.; Witters, L.A. The Effects of AICAR on Adipocyte Differentiation of 3T3-L1 Cells. Biochem. Biophys. Res. Commun. **2001**, 286, 852-856.

Haemmerle, G.; Moustafa, T.; Woelkart, G.; Büttner, S.; Schmidt, A.; van de Weijer, T.; Hesselink, M.; Jaeger, D.; Kienesberger, P.C.; Zierler, K.; et al. ATGL-Mediated Fat Catabolism Regulates Cardiac Mitochondrial Function via PPAR-α and PGC-1. Nat. Med. **2011**, 17, 1076-1085.

Han, J.; Kaufman, R.J. The role of ER stress in lipid metabolism and lipotoxicity. J. Lipid Res. **2016**, 57, 1329-1338.

Han, M.H.; Kim, H.J.; Jeong, J.-W.; Park, C.; Kim, B.W.; Choi, Y.H. Inhibition of Adipocyte Differentiation by Anthocyanins Isolated from the Fruit of Vitis Coignetiae Pulliat Is Associated with the Activation of AMPK Signaling Pathway. Toxicol. Res. **2018**, 34, 13-21.

Harms, M.; Seale, P. Brown and beige fat: development, function and therapeutic potential. Nat Med. **2013**, 19, 1252-1263.

Harvey, I.; Boudreau, A.; Stephens, J.M. Adipose tissue in health and disease. Open Biol. **2020**, 10, 200291.

Heeren, J.; Scheja, L. Brown adipose tissue and lipid metabolism. Curr Opin Lipidol. **2018**, 29, 180-185.

Herzig, S.; Shaw, R.J. AMPK: Guardian of Metabolism and Mitochondrial Homeostasis. Nat. Rev. Mol. Cell Biol. **2018**, 19, 121-135.

Hill, J.O.; Melanson, E.L.;Wyatt, H.T. Dietary fat intake and regulation of energy balance: Implications for obesity. J. Nutr. **2000**, 130 (Suppl. S2), 284S-288S.

Hofer, P.; Taschler, U.; Schreiber, R.; Kotzbeck, P.; Schoiswohl, G. The Lipolysome-A Highly Complex and Dynamic Protein Network Orchestrating Cytoplasmic Triacylglycerol Degradation. Metabolites. **2020**, 10, 147.

Holm, C. Molecular mechanisms regulating hormone-sensitive lipase and lipolysis. Biochem. Soc. Trans. **2003**, 31 Pt 6, 1120-1124.

Horton, J.D.; Goldstein, J.L.; Brown, M.S. SREBPs: Activators of the Complete Program of Cholesterol and Fatty Acid Synthesis in the Liver. J. Clin. Investig. **2002**, 109, 1125-1131.

Hotamisligil, G.S. Inflammation, metaflammation and immunometabolic disorders. Nature. **2017**, 542, 177-185.

Hu, S.; Wang, L.; Yang, D.; Li, L.; Togo, J.; Wu, Y.; Liu, Q.; Li, B.; Li, M.; Wang, G.; et al. Dietary Fat, but Not Protein or Carbohydrate, Regulates Energy Intake and Causes Adiposity in Mice. Cell Metab. **2018**, 28, 415-431.e4.

Huang, Y.; Zhu, X.; Chen, K.; Lang, H.; Zhang, Y.; Hou, P.; Ran, L.; Zhou, M.; Zheng, J.; Yi, L.; et al. Resveratrol preventssarcopenic obesity by reversing mitochondrial dysfunction and oxidative stress via the PKA/LKB1/AMPK pathway. Aging **2019**, 11, 2217-2240.

Ibrahim, K.S.; El-Sayed, E.M. Dietary conjugated linoleic acid and medium-chain triglycerides for obesity management. J. Biosci. **2021**, 46, 12.

Idrees, Z.; Cancarevic, I.; Huang, L. FDA-Approved Pharmacotherapy for Weight Loss Over the Last Decade. Cureus. **2022**, 14, e29262.

Ishaq, A.; Tchkonia, T.; Kirkland, J.L.; Siervo, M.; Saretzki, G. Palmitate induces DNA damage and senescence in human adipocytes in vitro that can be alleviated by oleic acid but not inorganic nitrate. Exp. Gerontol. **2022**, 163, 111798.

Ismail, A.M.; Cirvilleri, G.; Lombard, L.; Crous, P.W.; Groenewald, J.Z.; Polizzi, G. Characterisation of neofusicoccum species causing mango dieback in Italy. J. Plant Pathol. **2013**, 95, 549–557.

Kakouri A, Kanti G, Kapantais E, Kokkinos A, Lanaras L, Farajian P, Galanakis C, Georgantopoulos G, Vlahos NF, Mastorakos G, Bargiota A, Valsamakis G. New Incretin Combination Treatments under Investigation in Obesity and Metabolism: A Systematic Review. Pharmaceuticals (Basel). **2021**, 14, 869.

Kaliuzhka, V.; Tkachenko, A.; Myasoedov, V.; Markevych, M.; Onishchenko, A.; Babalyan, I.; Piatykop, V. The Prognostic Value of Eryptosis Parameters in the Cerebrospinal Fluid for Cerebralvasospasm and Delayed Cerebral Ischemia Formation. World Neurosurg. **2023**.

Kawai, T.; Autieri, M.V.; Scalia, R. Adipose tissue inflammation and metabolic dysfunction in obesity. Am J Physiol Cell Physiol. **2021**, 320, C375-C391.

Kawasaki, N.; Asada, R.; Saito, A.; Kanemoto, S.; Imaizumi, K. Obesity-induced endoplasmic reticulum stress causes chronic inflammation in adipose tissue. Sci. Rep. **2012**, 2, 799.

Kershaw, E.E.; Flier, J.S. Adipose tissue as an endocrine organ. J Clin Endocrinol Metab. **2004**, 89, 2548-56.

Kim, B.Y.; Kang, S.M.; Kang, J.H.; Kim, K.K.; Kim, B.; Kim, S.J.; Kim, Y.H.; Kim, J.H.; Kim, J.H.; Nam, G.E.; Park, J.Y.; Son, J.W.; Shin, H.J.; Oh, T.J.; Lee, H.; Jeon, E.J.; Chung, S.; Hong, Y.H.; Kim, C.H.; Committee of Clinical Practice Guidelines, Korean Society for the Study of Obesity (KSSO). Current Long-Term Pharmacotherapies for the Management of Obesity. J Obes Metab Syndr. **2020**, 29, 99-109.

Kim, H.; Castellon-Chicas, M.J.; Arbizu, S.; Talcott, S.T.; Drury, N.L.; Smith, S.; Mertens-Talcott, S.U. Mango (*Mangifera indica* L.) Polyphenols: Anti-Inflammatory Intestinal Microbial Health Benefits, and Associated Mechanisms of Actions. Molecules. **2021**, 26, 2732.

Kim, J.; Yang, G.; Kim, Y.; Kim, J.; Ha, J. AMPK Activators: Mechanisms of Action and Physiological Activities. Exp. Mol. Med. **2016**, 48, e224.

Kivinen, K.; Kallajoki, M.; Taimen, P. Caspase-3 is required in the apoptotic disintegration of the nuclear matrix. Exp. Cell Res. **2005**, 311, 62-73.

Koenen, M.; Hill, M.A,; Cohen, P.; Sowers, J.R. Obesity, Adipose Tissue and Vascular Dysfunction. Circ Res. **2021**, 128, 951-968.

Kong, L.; Zhang, H.; Lu, C.; Shi, K.; Huang, H.; Zheng, Y.; Wang, Y.; Wang, D.; Wang, H.; Huang, W. AICAR, an AMP-Activated Protein Kinase Activator, Ameliorates Acute Pancreatitis-Associated Liver Injury Partially Through Nrf2-Mediated Antioxidant Effects and Inhibition of NLRP3 Inflammasome Activation. Front. Pharmacol. **2021**, 12, 724514.

Korbecki, J.; Bajdak-Rusinek, K. The effect of palmitic acid on inflammatory response in macrophages: An overview of molecular mechanisms. Inflamm. Res. **2019**, 68, 915-932.

Lauricella, M.; Carlisi, D.; Giuliano, M.; Calvaruso, G.; Cernigliaro, C.; Vento, R.; D'Anneo, A. The analysis of estrogen receptoralpha positive breast cancer stem-like cells unveils a high expression of the serpin proteinase inhibitor PI-9: Possible regulatory mechanisms. Int. J. Oncol. **2016**, 49, 352-360.

Lauricella, M.; Emanuele, S.; Calvaruso, G.; Giuliano, M.; D'Anneo, A. Multifaceted Health Benefits of *Mangifera Indica* L. (Mango): The Inestimable Value of Orchards Recently Planted in Sicilian Rural Areas. Nutrients **2017**, 9, 525.

Lauricella, M.; Lo Galbo, V.; Cernigliaro, C.; Maggio, A.; Palumbo Piccionello, A.; Calvaruso, G.; Carlisi, D.; Emanuele, S.; Giuliano, M.; D'Anneo, A. The Anti-Cancer Effect of *Mangifera Indica* L. Peel Extract Is Associated to GH2AX-Mediated Apoptosis in Colon Cancer Cells. Antioxidants **2019**, 8, 422.

Lebaka, V.R.; Wee, Y.J.; Ye, W.; Korivi, M. Nutritional Composition and Bioactive Compounds in Three Different Parts of Mango Fruit. Int J Environ Res Public Health. **2021**, 18, 741.

Lee, H.; Kang, R.; Bae, S.; Yoon, Y. AICAR, an Activator of AMPK, Inhibits Adipogenesis via the WNT/β-Catenin Pathway in 3T3-L1 Adipocytes. Int. J. Mol. Med. **2011**, 28, 65-71.

Lee, H.; Lee, Y.J.; Choi, H.; Ko, E.H.; Kim, J. Reactive Oxygen Species Facilitate Adipocyte Differentiation by Accelerating Mitotic Clonal Expansion. J. Biol. Chem. **2009**, 284, 10601-10609.

Lenucci, M.S.; Tornese, R.; Mita, G.; Durante, M. Bioactive Compounds and Antioxidant Activities in Different Fractions of Mango Fruits (*Mangifera indica* L., Cultivar Tommy Atkins and Keitt). Antioxidants (Basel). **2022**, 11, 484.

Leroy, C.; Tricot, S.; Lacour, B.; Grynberg, A. Protective effect of eicosapentaenoic acid on palmitate-induced apoptosis in neonatal cardiomyocytes. Biochim. Biophys. Acta **2008**, 1781, 685-693.

Li, H.; Zhang, Q.; Li, W.; Li, H.; Bao, J.; Yang, C.; Wang, A.; Wei, J.; Chen, S.; Jin, H. Role of Nrf2 in the antioxidation and oxidative stress induced developmental toxicity of honokiol in zebrafish. Toxicol. Appl. Pharmacol. **2019**, 373, 48-61.

Li, Y.; Li, Z.; Ngandiri, D.A.; Llerins Perez, M.; Wolf, A.; Wang, Y. The Molecular Brakes of Adipose Tissue Lipolysis. Front Physiol. **2022**, 13, 826314.

Liu, F.; He, J.; Wang, H.; Zhu, D.; Bi, Y. Adipose Morphology: a Critical Factor in Regulation of Human Metabolic Diseases and Adipose Tissue Dysfunction. Obes Surg. **2020**, 30, 5086-5100.

Liu, Y.; Douglas, P.S.; Lip, G.Y.H.; Thabane, L.; Li, L.; Ye, Z.; Li, G. Relationship between obesity severity, metabolic status and cardiovascular disease in obese adults. Eur. J. Clin. Investig. **2022**, 53, e13912.

Lo Galbo, V.; Lauricella, M.; Giuliano, M.; Emanuele, S.; Carlisi, D.; Calvaruso, G.; De Blasio, A.; Di Liberto, D.; D'Anneo, A. Redox Imbalance and Mitochondrial Release of Apoptogenic Factors at the Forefront of the Antitumor Action of Mango Peel Extract. Molecules. **2021**, 26, 4328.

Longo, M.; Zatterale, F.; Naderi, J.; Parrillo, L.; Formisano, P.; Raciti, G.A.; Beguinot, F.; Miele, C. Adipose Tissue Dysfunction as Determinant of Obesity-Associated Metabolic Complications. Int J Mol Sci. **2019**, 20, 2358.

Loos, R.J.F.; Yeo, G.S.H. The genetics of obesity: from discovery to biology. Nat Rev Genet. **2022**, 23, 120-133.

Lu, Y.; Zhang, C.; Song, Y.; Chen, L.; Chen, X.; Zheng, G.; Yang, Y.; Cao, P.; Qiu, Z. Gallic acid impairs fructose-driven de novo lipogenesis and ameliorates hepatic steatosis via AMPK-dependent suppression of SREBP-1/ACC/FASN cascade. Eur. J. Pharmacol. **2022**, 940, 175457.

Luo, L.; Liu, M. Adipose tissue in control of metabolism. J Endocrinol. **2016**, 23, R77-R99.

Magaña, M.M.; Lin, S.S.; Dooley, K.A.; Osborne, T.F. Sterol Regulation of Acetyl Coenzyme A Carboxylase Promoter Requires Two Interdependent Binding Sites for Sterol Regulatory Element Binding Proteins. J. Lipid Res. **1997**, 38, 1630-1638.

Maggio, B.; Raimondi, M.V.; Raffa, D.; Plescia, F.; Scherrmann, M.-C.; Prosa, N.; Lauricella, M.; D'Anneo, A.; Daidone, G. Synthesis and Antiproliferative Activity of a Natural like Glycoconjugate Polycyclic Compound. Eur. J. Med. Chem. **2016**, 122, 247-256.

Maldonado-Celis, M.E.; Yahia, E.M.; Bedoya, R.; Landázuri, P.; Loango, N.; Aguillòn, J.; Restrepo, B.; Ospina, J.C.G. Chemical composition of mango (*Mangifera indica* L.) fruit: Nutritional and phytochemical compounds. Front. Plant. Sci. **2019**, 10, 1073.

Manach, C.; Scalbert, A.; Morand, C.; Rémésy, C.; Jiménez, L. Polyphenols: Food Sources and Bioavailability. Am. J. Clin. Nutr. **2004**, 79, 727-747.

Marin, T.L.; Gongol, B.; Zhang, F.; Martin, M.; Johnson, D.A.; Xiao, H.;Wang, Y.; Subramaniam, S.; Chien, S.; Shyy, J.Y. AMPK promotes mitochondrial biogenesis and function by phosphorylating the epigenetic factors DNMT1, RBBP7, and HAT1. Sci. Signal **2017**, 10, eaaf7478.

Masschelin, P.M.; Cox, A.R.; Chernis, N.; Hartig, S.M. The Impact of Oxidative Stress on Adipose Tissue Energy Balance. Front Physiol **2019**, 10, 1638.

Menendez, A.; Wanczyk, H.; Walker, J.; Zhou, B.; Santos, M.; Finck, C. Obesity and Adipose Tissue Dysfunction: From Pediatrics to Adults. Genes (Basel). **2022**, 13, 1866.

Mirza, B.; Croley, C.R.; Ahmad, M.; Pumarol, J.; Das, N.; Sethi, G.; Bishayee, A. Mango (*Mangifera indica* L.): a magnificent plant with cancer preventive and anticancer therapeutic potential. Crit Rev Food Sci Nutr. **2021**, 61, 2125-2151.

Mohan, C.; Deepak, M.; Viswanatha, G.; Savinay, G.; Hanumantharaju, V.; Rajendra, C.; Halemani, P.D. Anti-Oxidant and Anti-Inflammatory Activity of Leaf Extracts and Fractions of *Mangifera Indica*. Asian Pac. J. Trop. Med. **2013**, 6, 311-314.

Moltrer, M.; Pala, L.; Cosentino, C.; Mannucci, E.; Rotella, C.M.; Cresci, B. Body mass index (BMI), waist circumference (WC), waist-to-height ratio (WHtR) e waist body mass index (wBMI): Which is better? Endocrine. **2022**, 76, 578-583.

Morales, M.; Zapata, K.; Sagaste, C.A.; Angulo, A.A.; Rojano, B. Optimization of the Ultrasound-Assisted Extraction of Polyphenol, Mangiferin, and Its Antioxidant Expression in Mango Peel (*Mangifera Indica*) Using Response Surface Methodology. Acta Sci. Pol. Technol. Aliment. **2020**, 19, 5-14.

Moseti, D.; Regassa, A.; Kim,W.K. Molecular Regulation of Adipogenesis and Potential Anti-Adipogenic Bioactive Molecules. Int. J. Mol. Sci. **2016**, 17, 124.

Mota de Sá, P.; Richard, A.J.; Hang, H.; Stephens, J.M. Transcriptional Regulation of Adipogenesis. Compr Physiol. **2017**, 7, 635-674.

Muir, L.A.; Neeley, C.K.; Meyer, K.A.; Baker, N.A.; Brosius, A.M.; Washabaugh, A.R.; Varban, O.A.; Finks, J.F.; Zamarron, B.F.; Flesher, C.G.; Chang, J.S.; DelProposto, J.B.; Geletka, L.; Martinez-Santibanez, G.; Kaciroti, N.; Lumeng, C.N.; O'Rourke, R.W. Adipose tissue fibrosis, hypertrophy, and hyperplasia: Correlations with diabetes in human obesity. Obesity (Silver Spring). **2016**, 24, 597-605.

Murru, E.; Manca, C.; Carta, G.; Banni, S. Impact of Dietary Palmitic Acid on Lipid Metabolism. Front Nutr. **2022**, 9, 861664.

Mwaurah, P.W.; Kumar, S.; Kumar, N.; Panghal, A.; Attkan, A.K.; Singh, V.K.; Garg, M.K. Physicochemical characteristics, bioactive compounds and industrial applications of mango kernel and its products: A review. Compr Rev Food Sci Food Saf. **2020**, 19, 2421-2446.

Nakano, H.; Nakajima, A.; Sakon-Komazawa, S.; Piao, J.H.; Xue, X.; Okumura, K. Reactive oxygen species mediate crosstalk between NF-kappaB and JNK. Cell Death Differ. **2006**, 13, 730–737.

Ngo, V.; Duennwald, M.L. Nrf2 and Oxidative Stress: A General Overview of Mechanisms and Implications in Human Disease. Antioxidants **2022**, 11, 2345.

Nunn, E.R.; Shinde, A.B.; Zaganjor, E. Weighing in on Adipogenesis. Front Physiol. **2022**, 13, 821278.

Ojulari, O.V.; Lee, S.G.; Nam, J.-O. Beneficial Effects of Natural Bioactive Compounds from *Hibiscus Sabdariffa* L. on Obesity. Molecules **2019**, 24, 210.

Ooi, B.K.; Chan, K.-G.; Goh, B.H.; Yap,W.H. The Role of Natural Products in Targeting Cardiovascular Diseases via Nrf2 Pathway: Novel Molecular Mechanisms and Therapeutic Approaches. Front. Pharmacol. **2018**, 9, 1308.

Osinski, V.; Bauknight, D.K.; Dasa, S.S.K.; Harms, M.J.; Kroon, T.; Marshall, M.A.; Garmey, J.C.; Nguyen, A.T.; Hartman, J.; Upadhye, A.; et al. In Vivo Liposomal Delivery of PPARα/γ Dual

Agonist Tesaglitazar in a Model of Obesity Enriches Macrophage Targeting and Limits Liver and Kidney Drug Effects. Theranostics **2020**, 10, 585-601.

Palomer, X.; Pizarro-Delgado, J.; Barroso, E.; Vazquez-Carrera, M. Palmitic and Oleic Acid: The Yin and Yang of Fatty Acids in Type 2 Diabetes Mellitus. Trends Endocrinol. Metab. **2018**, 29, 178-190.

Pant, R.; Firmal, P.; Shah, V.K.; Alam, A.; Chattopadhyay, S. Epigenetic Regulation of Adipogenesis in Development of Metabolic Syndrome. Front Cell Dev Biol. **2021**, 8, 619888.

Piché, M.E.; Tchernof, A.; Després, J.P. Obesity Phenotypes, Diabetes, and Cardiovascular Diseases. Circ Res. **2020**, 126, 1477-1500.

Pinneo, S.; O'Mealy, C.; Rosas, M., Jr.; Tsang, M.; Liu, C.; Kern, M.; Hooshmand, S.; Hong, M.Y. Fresh Mango Consumption Promotes Greater Satiety and Improves Postprandial Glucose and Insulin Responses in Healthy Overweight and Obese Adults. J. Med. Food **2022**, 25, 381-388.

Polizzi, G.; Di Pietro, C.; Gusella, G.; Ismail, A.M.; Aiello, D. First report of seedling stem blight of mango caused by Neofusicoccum parvum in Italy. Plant Dis. **2022**.

Pratelli, G.; Carlisi, D.; D'Anneo, A.; Maggio, A.; Emanuele, S.; Palumbo Piccionello, A.; Giuliano, M.; De Blasio, A.; Calvaruso, G.; Lauricella, M. Bio-Waste Products of Mangifera indica L. Reduce Adipogenesis and Exert Antioxidant Effects on 3T3-L1 Cells. Antioxidants **2022**, 11, 363.

Prentice, K.J.; Saksi, J.; Hotamisligil, G.S. Adipokine FABP4 Integrates Energy Stores and Counterregulatory Metabolic Responses. J. Lipid Res. **2019**, 60, 734-740.

Pyper, S.R.; Viswakarma, N.; Yu, S.; Reddy, J.K. PPARα: Energy Combustion, Hypolipidemia, Inflammation and Cancer. Nucl. Recept. Signal. **2010**, 8, nrs.08002.

Raatz, S.K.; Conrad, Z.; Johnson, L.K.; Picklo, M.J.; Jahns, L. Relationship of the Reported Intakes of Fat and Fatty Acids to Body Weight in US Adults. Nutrients **2017**, 9, 438.

Rahman, M.S.; Kim, Y.S. Mangiferin induces the expression of a thermogenic signature via AMPK signaling during brown-adipocyte differentiation. Food Chem. Toxicol. **2020**, 141, 111415.

Rahman, N.; Jeon, M.; Kim, Y.-S. Methyl Gallate, a Potent Antioxidant Inhibits Mouse and Human Adipocyte Differentiation and Oxidative Stress in Adipocytes through Impairment of Mitotic Clonal Expansion. BioFactors **2016**, 42, 716-726.

Rauf, A.; Orhan, I.E.; Ertas, A.; Temel, H.; Hadda, T.B.; Saleem, M.; Raza, M.; Khan, H. Elucidation of Phosphodiesterase-1 Inhibitory Effect of Some Selected Natural Polyphenolics Using In Vitro and In Silico Methods. Curr. Top. Med. Chem. 2017, 17, 412-417.

Richard, A.J.; White, U.; Elks, C.M.; Stephens, J.M. Adipose Tissue: Physiology to Metabolic Dysfunction. In: Feingold KR, Anawalt B, Blackman MR, et al., eds. *Endotext*. South Dartmouth (MA): MDText.com, Inc.; **2020**.

Rodríguez Pleguezuelo, C.R.; Durán Zuazo, V.H.; Muriel Fernández, J.L.; Franco Tarifa, D. Physico-chemical Quality Parameters of Mango (*Mangifera indica* L.) Fruits Grown in a Mediterranean Subtropical Climate (SE Spain). J. Agric. Sci. Technol. **2012**, 14, 365–374.

Rodriguez-Casado, A. The Health Potential of Fruits and Vegetables Phytochemicals: Notable Examples. Crit Rev Food Sci Nutr. **2016**, 56, 1097-107.

Roh, C.; Jung, U. Screening of Crude Plant Extracts with Anti-Obesity Activity. Int. J. Mol. Sci. **2012**, 13, 1710-1719.

Roh, C.; Jung, U.; Jo, S.K. Screening of anti-obesity agent from herbal mixtures. Molecules **2012**, 17, 3630-3638.

Rohm, T.V.; Meier, D.T.; Olefsky, J.M.; Donath, M.Y. Inflammation in obesity, diabetes, and related disorders. Immunity. **2022**, 55, 31-55.

Rosen, E.D.; Sarraf, P.; Troy, A.E.; Bradwin, G.; Moore, K.; Milstone, D.S.; Spiegelman, B.M.; Mortensen, R.M. PPARγ Is Required for the Differentiation of Adipose Tissue In Vivo and In Vitro. Mol. Cell **1999**, 4, 611-617.

Rouse, M.; Younes, A.; Egan, J.M. Resveratrol and curcumin enhance pancreatic beta-cell function by inhibiting phosphodiesterase activity. J. Endocrinol. **2014**, 223, 107-117.

Rui, L. Brown and Beige Adipose Tissues in Health and Disease. Compr Physiol. **2017**, 7, 1281-1306.

Russo, S.; Kwiatkowski, M.; Govorukhina, N.; Bischoff, R.; Melgert, B.N. Meta-Inflammation and Metabolic Reprogramming of Macrophages in Diabetes and Obesity: The Importance of Metabolites. Front Immunol. **2021**, 12, 746151.

Sabater, A.G.; Ribot, J.; Priego, T.; Vazquez, I.; Frank, S.; Palou, A.; Buchwald-Werner, S. Consumption of a Mango Fruit Powder Protects Mice from High-Fat Induced Insulin Resistance and Hepatic Fat Accumulation. Cell Physiol. Biochem. **2017**, 42, 564-578.

Salari, N.; Jafari, S.; Darvishi, N.; Valipour, E.; Mohammadi, M.; Mansouri, K.; Shohaimi, S. The best drug supplement for obesity treatment: a systematic review and network meta-analysis. Diabetol Metab Syndr. **2021**, 13, 110.

Sarwar, R.; Pierce, N.; Koppe, S. Obesity and nonalcoholic fatty liver disease: current perspectives. Diabetes Metab Syndr Obes. **2018**, 11, 533-542.

Scheele, C.; Wolfrum, C. Brown Adipose Crosstalk in Tissue Plasticity and Human Metabolism. Endocr Rev. **2020**, 41, 53-65.

Schoettl, T.; Fischer, I.P.; Ussar, S. Heterogeneity of adipose tissue in development and metabolic function. J Exp Biol. **2018**, 221.

Sferrazzo, G.; Palmeri, R.; Restuccia, C.; Parafati, L.; Siracusa, L.; Spampinato, M.; Carota, G.; Distefano, A.; Di Rosa, M.; Tomasello, B.; Costantino, A.; Gulisano, M.; Li Volti, G.; Barbagallo, I. *Mangifera indica* L. Leaves as a Potential Food Source of Phenolic Compounds with Biological Activity. Antioxidants. **2022**, 11, 1313.

Sferrazzo, G.; Palmeri, R.; Vanella, L.; Parafati, L.; Ronsisvalle, S.; Biondi, A.; Basile, F.; Li Volti, G.; Barbagallo, I. *Mangifera Indica* L. Leaf Extract Induces Adiponectin and Regulates Adipogenesis. Int. J. Mol. Sci. **2019**, 20, 3211.

Shimomura, I.; Shimano, H.; Korn, B.S.; Bashmakov, Y.; Horton, J.D. Nuclear Sterol Regulatory Element-Binding Proteins Activate Genes Responsible for the Entire Program of Unsaturated Fatty Acid Biosynthesis in Transgenic Mouse Liver. J. Biol. Chem. **1998**, 273, 35299-35306.

Song, N.-J.; Kim, S.; Jang, B.-H.; Chang, S.-H.; Yun, U.J.; Park, K.-M.;Waki, H.; Li, D.Y.; Tontonoz, P.; Park, K.W. Small Molecule-Induced Complement Factor D (Adipsin) Promotes Lipid Accumulation and Adipocyte Differentiation. PLoS ONE **2016**, 11, e0162228.

Song, Z.; Xiaoli, A.M.; Yang, F. Regulation and Metabolic Significance of De Novo Lipogenesis in Adipose Tissues. Nutrients. **2018**, 10, 1383.

Sztalryd, C.; Brasaemle, D.L. The perilipin family of lipid droplet proteins: Gatekeepers of intracellular lipolysis. Biochim Biophys. Acta Mol. Cell Biol. Lipids **2017**, 1862 Pt 10, 1221-1232.

Tabas, I.; Ron, D. Integrating the mechanisms of apoptosis induced by endoplasmic reticulum stress. Nat. Cell. Biol. **2011**, 13, 184-190.

Tabor, D.E.; Kim, J.B.; Spiegelman, B.M.; Edwards, P.A. Transcriptional Activation of the Stearoyl-CoA Desaturase 2 Gene by Sterol Regulatory Element-Binding Protein/Adipocyte Determination and Differentiation Factor 1. J. Biol. Chem. **1998**, 273, 22052-22058.

Taing, M.-W.; Pierson, J.-T.; Shaw, P.N.; Dietzgen, R.G.; Roberts-Thomson, S.J.; Gidley, M.J.; Monteith, G.R. Mango (*Mangifera indica* L.) Peel Extract Fractions from Different Cultivars Differentially Affect Lipid Accumulation in 3T3-L1 Adipocyte Cells. Food Funct. **2013**, 4, 481-491.

Tak, Y.J.; Lee, S.Y. Long-Term Efficacy and Safety of Anti-Obesity Treatment: Where Do We Stand? Curr Obes Rep. **2021**, 10, 14-30.

Tanaka, M.; Sugama, A.; Sumi, K.; Shimizu, K.; Kishimoto, Y.; Kondo, K.; Iida, K. Gallic Acid Regulates Adipocyte Hypertrophy and Suppresses Inflammatory Gene Expression Induced by the Paracrine Interaction between Adipocytes and Macrophages in Vitro and in Vivo. Nutr. Res. **2020**, 73, 58-66.

Tchang, BG.; Aras, M.; Kumar, R.B.; et al. Pharmacologic Treatment of Overweight and Obesity in Adults. [Updated **2021** Aug 2]. In: Feingold KR, Anawalt B, Blackman MR, et al., editors. Endotext [Internet]. South Dartmouth (MA): MDText.com, Inc.; 2000-2023.

Thompson, G.M.; Trainor, D.; Biswas, C.; LaCerte, C.; Berger, J.P.; Kelly, L.J. A High-Capacity Assay for PPAR Ligand Regulation of Endogenous AP2 Expression in 3T3-L1 Cells. Anal. Biochem. **2004**, 330, 21-28.

Tormos, K.V.; Anso, E.; Hamanaka, R.B.; Eisenbart, J.; Joseph, J.; Kalyanaraman, B.; Chandel, N.S. Mitochondrial Complex III ROS Regulate Adipocyte Differentiation. Cell Metab. **2011**, 14, 537-544.

van Breda, S.G.J.; de Kok, T.M.C.M. Smart Combinations of Bioactive Compounds in Fruits and Vegetables May Guide New Strategies for Personalized Prevention of Chronic Diseases. Mol Nutr Food Res. **2018**, 62.

van der Valk ES, van den Akker ELT, Savas M, Kleinendorst L, Visser JA, Van Haelst MM, Sharma AM, van Rossum EFC. A comprehensive diagnostic approach to detect underlying causes of obesity in adults. Obes Rev. 2019 Jun;20(6):795-804.

Vasileva, L.V.; Savova, M.S.; Amirova, K.M.; Dinkova-Kostova, A.T.; Georgiev, M.I. Obesity and NRF2-Mediated Cytoprotection: Where Is the Missing Link? Pharmacol. Res. **2020**, 156, 104760.

Vinesh, D.; Neeru, V.; Sunil, S.; Ashok, K.; David, R. Lead Anti-Obesity Compounds from Nature. Endocr. Metab. Immune Disord. Drug Targets **2020**, 20, 1637-1653.

Wang, M.; Chen, Y.; Xiong, Z.; Yu, S.; Zhou, B.; Ling, Y.; Zheng, Z.; Shi, G.;Wu, Y.; Qian, X. Ginsenoside Rb1 inhibits free fatty acids-induced oxidative stress and inflammation in 3T3-L1 adipocytes. Mol. Med. Rep. **2017**, 16, 9165-9172.

Wang, S.; Liang, X.; Yang, Q.; Fu, X.; Rogers, C.J.; Zhu, M.; Rodgers, B.D.; Jiang, Q.; Dodson, M.V.; Du, M. Resveratrol Induces Brown-like Adipocyte Formation in White Fat through Activation of AMP-Activated Protein Kinase (AMPK) A1. Int. J. Obes. **2015**, 39, 967-976.

Wang, S.; Liang, X.; Yang, Q.; Fu, X.; Zhu, M.; Rodgers, B.D.; Jiang, Q.; Dodson, M.V.; Du, M. Resveratrol Enhances Brown Adipocyte Formation and Function by Activating AMP-Activated Protein Kinase (AMPK) A1 in Mice Fed High-Fat Diet. Mol. Nutr. Food Res. **2017**, 61, 1600746.

Wang, S.; Zhang, M.; Liang, B.; Xu, J.; Xie, Z.; Liu, C.; Viollet, B.; Yan, D.; Zou, M.H. AMPKalpha2 deletion causes aberrant expression and activation of NAD(P)H oxidase and consequent endothelial dysfunction in vivo: Role of 26S proteasomes. Circ. Res. **2010**, 106, 1117-1128.

Wang, W.; Seale, P. Control of brown and beige fat development. Nature Reviews Molecular Cell Biology. **2016**, 17, 691-702.

Wang, W.; Zhang, Y.; Lu, W.; Liu, K. Mitochondrial Reactive Oxygen Species Regulate Adipocyte Differentiation of Mesenchymal Stem Cells in Hematopoietic Stress Induced by Arabinosylcytosine. PLoS ONE **2015**, 10, e0120629.

Wei, Y.; Wang, D.; Topczewski, F.; Pagliassotti, M.J. Saturated fatty acids induce endoplasmic reticulum stress and apoptosis independently of ceramide in liver cells. Am. J. Physiol. Endocrinol. Metab. **2006**, 291, E275–E281.

Wiechert, M.; Holzapfel, C. Nutrition Concepts for the Treatment of Obesity in Adults. Nutrients. **2021**, 14, 169.

Win, S.; Than, T.A.; Fernandez-Checa, J.C.; Kaplowitz, N. JNK interaction with Sab mediates ER stress induced inhibition of mitochondrial respiration and cell death. Cell Death Dis. **2014**, 5, e989.

Xiaoru, S.; Meiqi, W.; Xueqin, W.; Shuwen, D.; Na, F.; Qiang, P.; Yan, J.; Ling, Y.; Jiamin, X.; Yunfeng, L. Peroxisome Proliferator-Activated Receptor-γ: Master Regulator of Adipogenesis and Obesity. Curr. Stem Cell Res. Ther. **2016**, 11, 282-289.

Yang, A.; Mottillo, E.P. Adipocyte lipolysis: from molecular mechanisms of regulation to disease and therapeutics. Biochem J. **2020**, 477, 985-1008.

Yanovski, S. Z.; Yanovski, J. A. Long-term drug treatment for obesity: a systematic and clinical review. JAMA. **2014**, 311, 74-86.

Yen, C.L.; Stone, S.J.; Koliwad, S.; Harris, C.; Farese, R.V. Jr. Thematic review series: glycerolipids. DGAT enzymes and triacylglycerol biosynthesis. J Lipid Res. **2008**, 49, 2283-301.

Yilmaz, E. Endoplasmic Reticulum Stress and Obesity. Adv. Exp. Med. Biol. **2017**, 960, 261–276.

Zechner, R.; Zimmermann, R.; Eichmann, T.O.; Kohlwein, S.D.; Haemmerle, G.; Lass, A.; Madeo, F. FAT SIGNALS-lipases and lipolysis in lipid metabolism and signaling. Cell Metab. **2012**, 15, 279-291.

Zhao, J.; Zhou, A.; Qi, W. The Potential to Fight Obesity with Adipogenesis Modulating Compounds. Int J Mol Sci. **2022**, 23, 2299.

Zhao, S.; Kusminski, C.M.; Scherer, P.E. Adiponectin, Leptin and Cardiovascular Disorders. Circ Res. **2021**, 128, 136-149.

Zhou, G.; Myers, R.; Li, Y.; Chen, Y.; Shen, X.; Fenyk-Melody, J.; Wu, M.; Ventre, J.; Doebber, T.; Fujii, N.; et al. Role of AMP-Activated Protein Kinase in Mechanism of Metformin Action. J. Clin. Investig. **2001**, 108, 1167-1174.

Zhou, Y.; Jiang, Z.; Lu, H.; Xu, Z.; Tong, R.; Shi, J.; Jia, G. Recent Advances of Natural Polyphenols Activators for Keap1-Nrf2 Signaling Pathway. Chem. Biodivers. **2019**, 16, e1900400.

Zinngrebe, J.; Debatin, K.M.; Fischer-Posovszky, P. Adipocytes in hematopoiesis and acute leukemia: friends, enemies, or innocent bystanders? Leukemia. **2020**, 34, 2305-2316.

Zwick, R.K.; Guerrero-Juarez, C.F.; Horsley, V.; Plikus, M.V. Anatomical, Physiological, and Functional Diversity of Adipose Tissue. Cell Metab. **2018**, 27, 68-83.

FIGURES AND TABLES RFERENCES

Table 1. Iqbal, A.; Rehman, A. Obesity Brain Gut Adipocyte Interaction. [Updated 2022 Jul 4]. In: StatPearls [Internet]. Treasure Island (FL): StatPearls Publishing; **2023** Jan.

Table 2. Maldonado-Celis, M.E.; Yahia, E.M.; Bedoya, R.; Landázuri, P.; Loango, N.; Aguilllòn, J.; Restrepo, B.; Ospina, J.C.G. Chemical composition of mango (*Mangifera indica* L.) fruit: Nutritional and phytochemical compounds. Front. Plant. Sci. **2019**, 10, 1073.

Table 3. Lauricella, M.; Lo Galbo, V.; Cernigliaro, C.; Maggio, A.; Palumbo Piccionello, A.; Calvaruso, G.; Carlisi, D.; Emanuele, S.; Giuliano, M.; D'Anneo, A. The Anti-Cancer Effect of *Mangifera Indica* L. Peel Extract Is Associated to GH2AX-Mediated Apoptosis in Colon Cancer Cells. Antioxidants **2019**, 8, 422.

Table 4. Pratelli, G.; Carlisi, D.; D'Anneo, A.; Maggio, A.; Emanuele, S.; Palumbo Piccionello, A.; Giuliano, M.; De Blasio, A.; Calvaruso, G.; Lauricella, M. Bio-Waste Products of Mangifera indica L. Reduce Adipogenesis and Exert Antioxidant Effects on 3T3-L1 Cells. Antioxidants **2022**, 11, 363.

Figure 1. Keipert, S.; Jastroch, M. Brite/beige fat and UCP1 - is it thermogenesis? Biochim Biophys Acta. **2014**, 1837, 1075-82.

Figure 2. Zinngrebe, J.; Debatin, K.M.; Fischer-Posovszky, P. Adipocytes in hematopoiesis and acute leukemia: friends, enemies, or innocent bystanders? Leukemia. **2020**, 34, 2305-2316.

Figure 3. Ahmad, B.; Serpell, C.J.; Fong, I.L.; Wong, E.H. Molecular Mechanisms of Adipogenesis: The Anti-adipogenic Role of AMP-Activated Protein Kinase. Front Mol Biosci. **2020**, 7, 76.

Figure 4. Rodríguez, A.; Becerril, S.; Hernández-Pardos, A.W.; Frühbeck, G. Adipose tissue depot differences in adipokines and effects on skeletal and cardiac muscle. Curr Opin Pharmacol. **2020**, 52, 1-8.

Figure 5. Song, Z.; Xiaoli, A.M.; Yang, F. Regulation and Metabolic Significance of De Novo Lipogenesis in Adipose Tissues. Nutrients. **2018**, 10, 1383.

Figure 6. Li, Y.; Li, Z.; Ngandiri, D.A.; Llerins Perez, M.; Wolf, A.; Wang, Y. The Molecular Brakes of Adipose Tissue Lipolysis. Front Physiol. **2022**, 13, 826314.

Figure 7. Braun, K.; Oeckl, J.; Westermeier, J.; Li, Y.; Klingenspor, M. Non-adrenergic control of lipolysis and thermogenesis in adipose tissues. J Exp Biol. **2018**, 221, jeb165381.

Figure 8. Luo, L.; Liu, M. Adipose tissue in control of metabolism. J Endocrinol. **2016**, 23, R77-R99.

Figure 9. Liu, F.; He, J.; Wang, H.; Zhu, D.; Bi, Y. Adipose Morphology: a Critical Factor in Regulation of Human Metabolic Diseases and Adipose Tissue Dysfunction. Obes Surg. **2020**, 30, 5086-5100.

Figure 10. Lenucci, M.S.; Tornese, R.; Mita, G.; Durante, M. Bioactive Compounds and Antioxidant Activities in Different Fractions of Mango Fruits (*Mangifera indica* L., Cultivar Tommy Atkins and Keitt). Antioxidants (Basel). **2022**, 11, 484.

Figures 11-17. Pratelli, G.; Carlisi, D.; D'Anneo, A.; Maggio, A.; Emanuele, S.; Palumbo Piccionello, A.; Giuliano, M.; De Blasio, A.; Calvaruso, G.; Lauricella, M. Bio-Waste Products of Mangifera indica L. Reduce Adipogenesis and Exert Antioxidant Effects on 3T3-L1 Cells. Antioxidants **2022**, 11, 363.

Figures 18-24. Pratelli, G.; Di Liberto, D.; Carlisi, D.; Emanuele, S.; Giuliano, M.; Notaro, A.; De Blasio, A.; Calvaruso, G.; D'Anneo, A.; Lauricella, M. Hypertrophy and ER Stress Induced by Palmitate Are Counteracted by Mango Peel and Seed Extracts in 3T3-L1 Adipocytes. Int J Mol Sci. **2023**, 24, 5419.

Figure 25. Pratelli, G.; Carlisi, D.; D'Anneo, A.; Maggio, A.; Emanuele, S.; Palumbo Piccionello, A.; Giuliano, M.; De Blasio, A.; Calvaruso, G.; Lauricella, M. Bio-Waste Products of Mangifera

indica L. Reduce Adipogenesis and Exert Antioxidant Effects on 3T3-L1 Cells. Antioxidants **2022**, 11, 363.

Figure 26. Pratelli, G.; Di Liberto, D.; Carlisi, D.; Emanuele, S.; Giuliano, M.; Notaro, A.; De Blasio, A.; Calvaruso, G.; D'Anneo, A.; Lauricella, M. Hypertrophy and ER Stress Induced by Palmitate Are Counteracted by Mango Peel and Seed Extracts in 3T3-L1 Adipocytes. Int J Mol Sci. **2023**, 24, 5419.